Emergent Dynamics of Slow and Fast Systems on Complex Networks

A thesis
Submitted in partial fulfillment of the requirements
of the degree of
Doctor of Philosophy

By

Kajari Gupta
20113143

INDIAN INSTITUTE OF SCIENCE EDUCATION AND RESEARCH PUNE

June 2018

I dedicate the thesis to my parents and sister

Certificate

I certify that the thesis entitled "Emergent Dynamics of Slow and Fast Systems on Complex Networks" presented by Ms. Kajari Gupta represents her original work which was carried out by her at IISER, Pune under my guidance and supervision. The work presented here or any part of it has not been included in any other thesis submitted previously for the award of any degree or diploma from any other University or institution.

Prof. G. Ambika
(Supervisor)

Date:

Declaration

I declare that this written submission represents my idea in my own words and where others' ideas have been included; I have adequately cited and referenced the original sources. I also declare that I have adhered to all principles of academic honesty and integrity and have not misrepresented or fabricated or falsified any idea/data/fact/source in my submission. I understand that violation of the above will be cause for disciplinary action by the Institute and can also evoke penal action from the sources which have thus not been properly cited or from whom proper permission has not been taken when needed.

Kajari Gupta
(20113143)

Date:

Acknowledgements

This thesis would have not been possible without the help and support of many people who has supported me in various forms. I would like to take this opportunity to thank each and every individual.

First of all, I would like to thank my supervisor Prof. G. Ambika for her continuous guidance and support throughout my Ph.D. I have learnt a lot from her regarding my research work and otherwise. In spite of having many ups and downs in research, her positive attitude has always kept me motivated. I would like to specially thank her for being so patient with me and trusting my abilities and pushing me towards it.

Apart from my supervisor, I must mention thanks to the RAC members, Prof. G. Rangarajan and Dr. M. S. Santhanam, for giving periodic reviews of my thesis progress and continuously suggesting to improve my work.

I thank IISER Pune for giving me all the facilities to do my research. I have seen IISER Pune growing from a grassroot level, where the institute did not have its own campus. Still IISER was at its best to give us the state of the art facilities starting from hostel to working environment.

I would like to acknowledge University Grant Commission for giving me fellowship to carry out the research for my Ph.D.

I thank Infosys foundation for funding me to present my work in "Complex Networks 2017" 29th Nov-1st Dec, Lyon, France.

I thank my past and present groupmates Resmi, Snehal, Sandip, Kashyap, Yamini, Sneha Kachhara, Kunal Mozumdar, Dinesh Choudhary, Harsh, Ameya, Saaransh for all the discussions about nonlinear dynamics and in general about physics that helped me in various forms. They were really helpful dealing with all the problems that one faces in their research, be it any programming related problem or any conceptual problem. It was nice to have a very close knit complex systems group.

No journey is complete without friends. I am very lucky that I had a bunch of really

good friends in this journey of Ph.D. I thank Sohini, Sneha Banerjee, Farhan, Mahendra, Sudeshna, Amruta, Sneha Kachhara, Sandip, Kunal Kothekar, Shweta, Arundhati, Vibishan, Anish, Vruta, Vrushali, Chaudhary, Yamini, Kapil, Turmoli, Saaransh, Priya, Sayan, Gokul, Wadikur and so many more people for being there. I also thank my seniors from previous batches, specially Resmi, Arun, Mayur, Vimal, Snehal for their friendship and guidance.

Hostel life in IISER was really enjoyable. Be it dinner parties after a long day or long music sessions with the fellow musicians. I would thank Farhan, Kapil, Vibishan, Harsha, Abhishek, Rutwik, Neelay for carrying out those days more musically. I specially thank Farhan for bringing me back to music after 9 long years break. I am thankfull to Dr. John Mathew and to all the members of 'IISER Choir' - Poornima, Alakananda, Nikita, Abhinaya, Lakshmi, Shivangi, Vibishan, Sandip, Akshay, Vishnu, Harsha, Kabir, Rohan and Sonu, for having such wonderfull choral practice sessions in my final days of IISER Pune. Life outside of IISER was equally enjoyable as natural beauties and photography spots like Pashan lake, Panchavati hills and Sus road hills were nearby. I thank Arun for being the great companion for all the photographic ventures and exploring the Pune city.

I would like to thank my teacher Dr. Rajsekhar Bhattacharyya for teaching me physics that helped me develop my understanding of the subject during my undergraduate studies.

My Ph.D would have definitely not been possible without the strong support of my family. I thank my parents, Ranjana Nandi and Subrata Gupta, my elder sister Manjari Gupta and my brother-in-law Yogeshwar Prasad for their guidance, support and encouragement throughout the time.

I am sure I have missed many important people to thank but this space may not be enough if I continue by name. Simply, I thank each and everyone who has supported me directly or indirectly in this journey.

Kajari

Abstract

Multiple-timescale phenomena occur frequently in real world systems and they most often add to the complexity of such systems, some of the examples being neuronal electrical activity, chemical reactions, turbulent flows, tropical atmospheric ocean systems etc. In all these cases, the variability and heterogeneity of the interacting systems are inevitable. Although there have been isolated studies addressing its various aspects, there are still many interesting and challenging questions to be addressed. There are many model systems proposed to understand multiple time scale phenomena in single systems, like dynamical model for neuronal dynamics. However studies on collective behavior of connected systems that differ in their intrinsic time scales, are very minimal. In this context the study reported in the present thesis is highly relevant and has resulted in many novel phenomena and promising approaches. The thesis is mainly on the study of the effect of heterogeneity in the natural frequencies on the emergent dynamics of connected systems. The study is exhaustive with at least three standard nonlinear systems, periodic and chaotic states as intrinsic dynamics, and fully connected, random and scale free topologies for connections or interactions on the networks with two types of coupling of diffusive and mean filed types. The main contributions from the study are the observation of onset of emergent phenomena like amplitude death, oscillation death, frequency synchronization, cluster synchronization and their characterization.

In chapter 1, we present a brief introduction to complex systems and their sources of complexity such as non linearity and complex pattern of interactions, dynamics of standard nonlinear systems used in the study as intrinsic dynamics, We also mention different types of complex networks which act as a framework to study such large complex systems.

The study presented in the thesis starts from Chapter 2, with the simple and basic model of dynamics of two interacting nonlinear systems with differing time scales. A parameter τ is introduced as time scale mismatch between the systems. We report the suppression of dynamics resulting in amplitude death (AD) when the parameters τ and coupling strength are changed. The transition curves to this state are studied analytically and confirmed by direct numerical simulations. We study the dynamics outside of AD and report frequency synchronization, frequency suppression, two frequency state etc for different time scale mismatch and coupling strength. As an important special case, we revisit the well-known model of coupled ocean atmosphere system used in climate studies for the interactive dynamics of a fast oscillating atmosphere and slowly changing ocean.

Our study in this context indicates occurrence of multi stable periodic states and steady states of convection coexisting in the system.

In the next chapter, we consider the case of a fully connected network, where all the nodes are connected to all other nodes and out of N nodes, m are slow. Here we identify the occurrence of AD with m/N ratio, τ and ϵ. In addition to AD we also observe synchronization in clusters, where slow systems evolve in a synchronized cluster and fast systems evolve in another, with frequency synchronization, two frequency states etc. depending upon the time scale mismatch, coupling strength and m. In this context, we observe an interesting cross over phenomenon, both in frequency and amplitudes of collective dynamics. In emergent frequency, the synchronized frequency of the coupled oscillators would go to frequency suppression for a critical m and the amplitudes of collective oscillations switches its nature as m is increased above a critical value. We study in detail all possible minimal configurations or motifs of networks with sizes N=3 and 4 for various kinds of connection topology. We analytically find the eigenvalues of the Jacobian of these network motifs about AD, and identify the boundary in the parameter plane for which at least one of the eigenvalue becomes positive. The transition curves are found to depend on the symmetry of connections.

In Chapter 4, we present the study on a random network of N systems where m are slow with probability of connection p. We take 100 realizations of this network to calculate how many of the realizations go to a full amplitude death state for a specific value of time scale mismatch and coupling strength. This fraction of realizations f, gives the transition curve with p and gives an optimum value of m where the transition to amplitude death occurs at the lowest possible p, or most sparse network. Using a data collapse, the scaling property of the universal transition curve is studied. This study is repeated by taking three types of probability of connections within the network. p_1 denoting the connectivity between slow to slow systems, p_2, within slow to fast systems and p_3, within fast to fast systems. We observe there can be amplitude death state for the bipartite network also even when $p_1 = p_3 = 0$

In the next chapter, our study on multi scale phenomena on scale free networks is presented. We generate scale-free network of N dynamical systems by Barabási-Albert algorithm. We mainly study the minimum number of slow hubs in the network that are required for the whole network to reach AD along with criteria for τ and ϵ for the same. We investigate the role of hubs as control nodes that can spread the effects of slowness over the network. For this, once the systems are synchronized, we make one of the nodes slow and study how soon the other nodes fall out of synchrony in time. This is characterized in terms of their degrees and shortest paths from the slow node. We discuss this for several starting slow nodes present in the network to quantify the importance of that node in the context of spread of slowness. In this context we also study self organization of the network where the whole system once perturbed from complete synchronization, organizes itself into a state of frequency synchronization.

We study the emergent dynamics with a distribution of time scales of the node where the time scale is inversely proportional to the degree of the node. This gives a more

realistic situation and brings out the relative importance of the nodes. In this case we find an interesting amplitude distribution of oscillations along with the amplitude death situation.

In the final chapter, we present the summary of work presented in the thesis, by giving the overview of the main results and their relevance. Our results have potential significance in biological, physical, and engineering networks consisting of heterogeneous oscillators and gives a new direction for further research on interacting time scales and the role of the same in complex systems. We discuss few of such possible future directions that can extend these studies further.

Publications

The work presented in this thesis has appeared in the following publications:

1. Kajari Gupta and G. Ambika, "Suppression of dynamics and frequency synchronization in coupled slow and fast dynamical systems", *Eur. Phys. J. B*,**89:147**,(2016).

2. Kajari Gupta and G. Ambika, "Dynamics of slow and fast systems on complex networks", *Indian Academy of Sciences Conference Series*, **1:1**,(2017).

3. Kajari Gupta and G. Ambika, "Role of time scales and topology on the dynamics of complex networks", *arXiv:1810.00687[nlin.AO]*, Communicated in AIP Chaos journal,(2018).

Contents

Chapter 1

Introduction

1.1 Complex systems

Most of the real world systems are complex, their complexity arising from large number of subunits or components with diverse and complex dynamics and different types of interactions. This makes the dynamics of the whole system often different from that of the interacting components. As examples of such complex systems, we can think of many biological systems like organisms, genes, brain, heart, living cell [1–13] etc their functions depending on a large number of neurons or cells with complex nature of connections among them. In a similar context, we can consider Earth's climate system, the ecosystem, human society, transportation system, stock market [14–25] also as examples of complex systems. In all these cases the nature of complexity and its role in deciding the emergent dynamics is a promising branch of study. In most of the complex systems, the individual dynamics itself can be complicated such as chaos, quasi-periodicity etc. and the emergent dynamics results in many interesting phenomena like synchronization, cluster formation, self organization etc. The complexity of emergent dynamics also can come from complicated pattern and nature of the interaction among sub components. Then most often the framework of complex networks is invoked to understand their complexity. We note that in the context of coupled systems, study of the emergent phenomena like synchronization, amplitude death etc are considered with interacting subsystems which evolve with the same time scale. However, many real world systems such as social networks, power transmission networks, transportation systems, global climate systems etc. have subsystems, which evolve with differing time scales. This motivates the present study on emergent dynamics when nonlinear systems of different time scales are coupled to form complex systems.

In the present study we focus on another aspect of complexity that can arise due to the heterogeneity in the dynamical time scales of interacting systems. The study is carried out in detail, starting from simple cases of two coupled systems, regular networks of systems to complex networks and we report many interesting phenomena like amplitude death, oscillation death, frequency synchronization, self organization etc. The transitions

and scaling behavior near such transitions as well as characterization of various possible emergent states make this study very extensive and relevant for understanding complex real world systems and developing possible control strategies in them.

1.2 Standard nonlinear systems

We start by considering the case of systems with intrinsic dynamics that is nonlinear and therefore has potential to exhibit different types of complicated dynamics. We present first a few such standard nonlinear systems that can have irregular dynamics called chaos. Historically the most interesting system in this context is the Lorenz system that arises in atmospheric dynamics. In 1963, in the paper called "deterministic non periodic flow", E. Lorenz has derived a set of nonlinear differential equations later known as the Lorenz system [26] as

$$\begin{aligned} \dot{x} &= a(y-x) \\ \dot{y} &= (x(b-z)-y) \\ \dot{z} &= (xy-cz) \end{aligned} \tag{1.1}$$

In the above equations, with three variables, x represents the rate of convection, y the horizontal temperature variation and z, the vertical temperature variation. The 3-d phase space representing the dynamical trajectory of the system is studied for various possible values of the parameters a, b and c. It is found that as typical of such nonlinear dynamical systems, the phase space dynamics depend on the values of the parameters and can undergo transitions from regular behaviour to chaotic state as they are varied [27, 28]. The various scenario through which a nonlinear system can reach chaos has been extensively studied in the early days itself [29]. For example for Lorenz system, the parameters a=10, b=28, c=8/3 results in a chaotic trajectory shown in Fig. 1.1. Since the system asymptotically settles to a stable chaotic trajectory shown, it is called the chaotic attractor of the system. One of the important characteristics of chaotic trajectory is its sensitivity to initial conditions. This means that two trajectories starting from very close initial conditions, diverge apart in time while being confined to the same attractor (Fig. 1.1) [26, 29].

In addition to chaotic states, nonlinear dynamical systems exhibit regular periodic dynamics called limit cycles and stationary or fixed points. The fixed point of the system is defined as the state where the system asymptotically goes to a stable static state. This state can be calculated by equating $\dot{x} = \dot{y} = \dot{z} = 0$. By solving these equations we can show that a pitchfork bifurcation occurs for fixed points at b=1. For b<1 there is only one fixed point at origin which corresponds to no convection and when b>1 there exit two fixed points; one is at $(\sqrt{c(b-1)}, \sqrt{c(b-1)}, b-1)$ and another at $(-\sqrt{c(b-1)}, -\sqrt{c(b-1)}, b-1)$ corresponding to steady convection. This pair of fixed points is stable for $b < a\frac{a+c+3}{a-c-1}$,

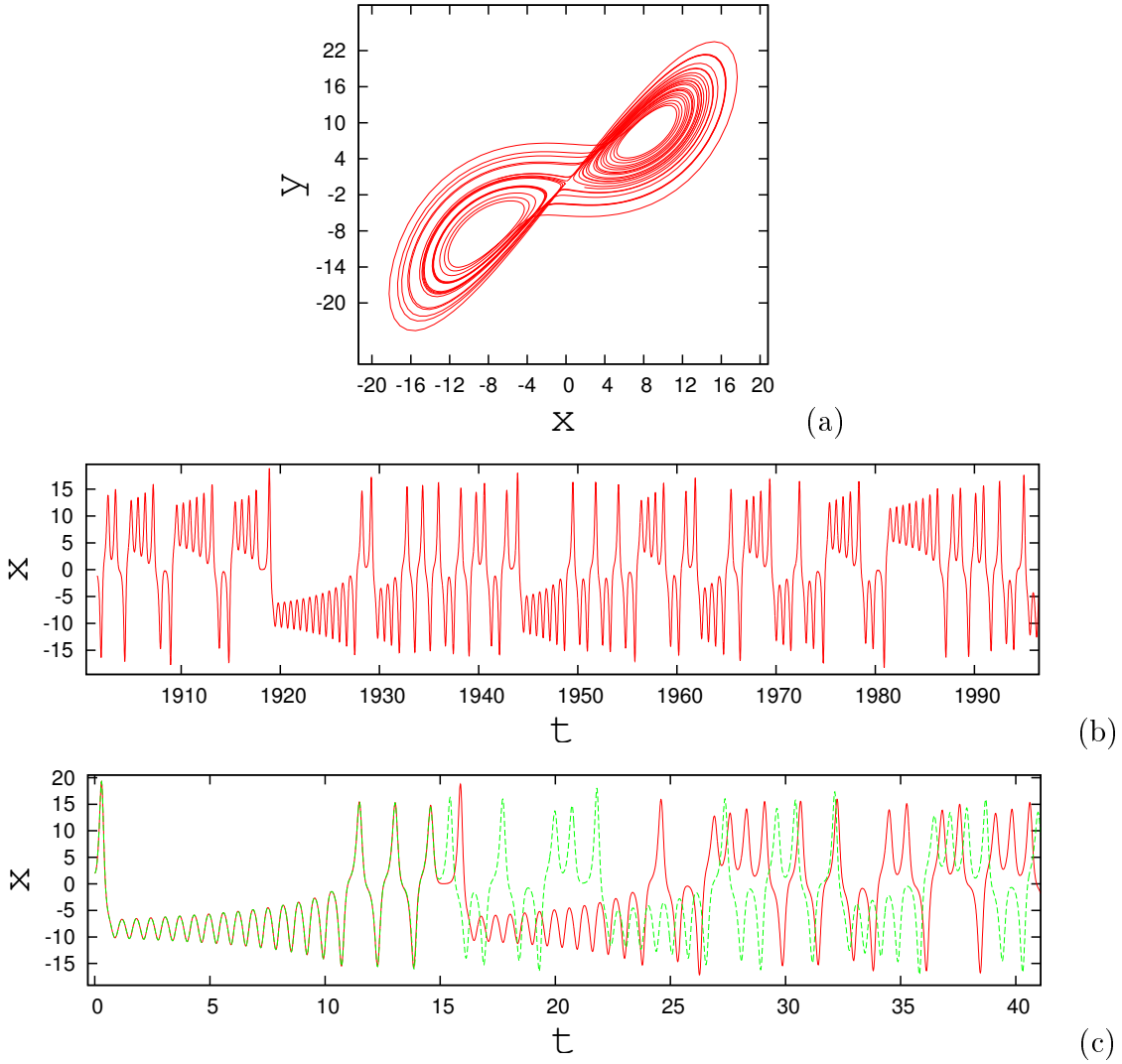

Figure 1.1: a)Phase plot of Lorenz system in X-Y plane showing chaotic trajectory for $a = 10, b = 28, c = 8/3$. b) time series of the x-variable c) time series starting from two nearby initial conditions, $x_1 = 2, y_1 = 2, z_1 = 2$ and $x_2 = 2.001, y = 2.001, z = 2.001$, indicating sensitivity to initial conditions

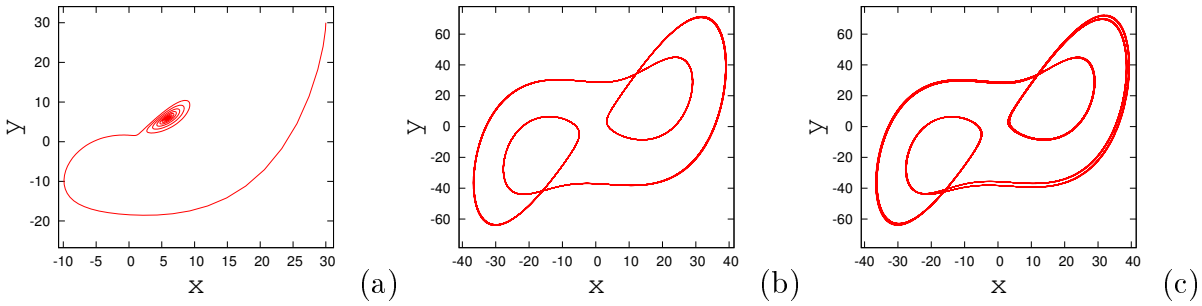

Figure 1.2: Phase plots of Lorenz system in X-Y plane a) Showing fixed point for $a = 10, b = 14, c = 8/3$ b) period 1 oscillation for $a = 10, b = 148.5, c = 8/3$ and c) period 2 oscillation for $a = 10, b = 147.5, c = 8/3$

provided $a > c + 1$. [28] In this case we find the system goes to one of the fixed point for $a = 10, b = 14, c = 8/3$ for initial conditions $x = 30, y = 30, z = 15$.

For larger values of the parameter b, Lorenz system has periodic orbits with periodicity depending on the parameters. For example period 1 oscillation is seen for b=148.5 and period 2 oscillation, for b=147.5. etc. [28] (Fig. 1.2).

1.2.1 Rössler system

Next we consider another standard nonlinear dynamical system in the context of chemical kinetics called Rössler system. Its dynamics is given by [30,31]

$$\begin{aligned} \dot{x} &= (-y - z) \\ \dot{y} &= (x + ay) \\ \dot{z} &= (b + z(x - c)) \end{aligned} \tag{1.2}$$

This system exhibits a period doubling route to chaos as shown in Fig. 1.4, as the values of parameters a, b and c are varied. Keeping b and c fixed, when a is changed, for $a \leq 0$ the system converges to fixed point. For a=0.1 it becomes periodic cycle of period 1. By further increasing of parameter a, the system goes to a chaotic attractor. Similarly for a=0.1, b=0.1, c=4 the system gives periodic orbits. In this case increasing c by keeping a and b fixed would also lead to a chaotic attractor (Fig. 1.3 [32]).

By setting $\dot{x} = \dot{y} = \dot{z} = 0$ in eqn.1.2, one can find out the fixed points of the system. The two fixed points in this case are $(\frac{c-\sqrt{c^2-4ab}}{2}, \frac{-c+\sqrt{c^2-4ab}}{2a}, \frac{c-\sqrt{c^2-4ab}}{2a})$ and $(\frac{c+\sqrt{c^2-4ab}}{2}, \frac{-c-\sqrt{c^2-4ab}}{2a}, \frac{c+\sqrt{c^2-4ab}}{2a})$

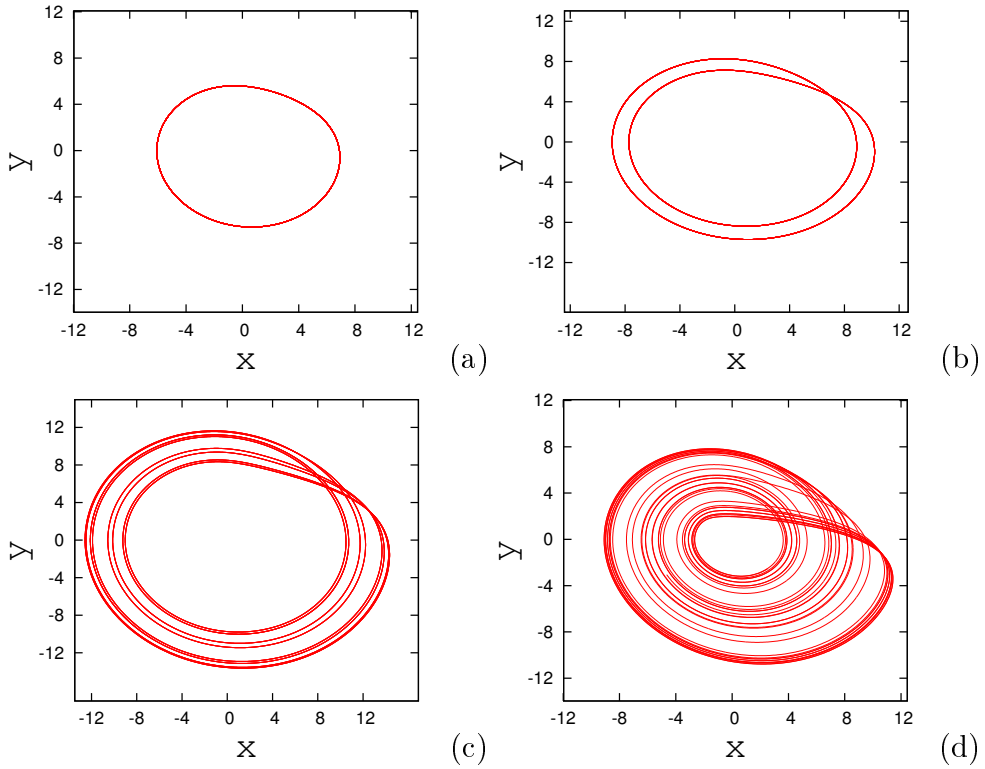

Figure 1.3: Phase plots of Rössler system in X-Y plane a) period 1 oscillation for $a = 0.1, b = 0.1, c = 4$ b) period 2 oscillation for $a = 0.1, b = 0.1, c = 6$ c) period 8 oscillation for $a = 0.1, b = 0.1, c = 8.7$ and d) chaotic trajectory for $a = 0.2, b = 0.2, c = 5.7$

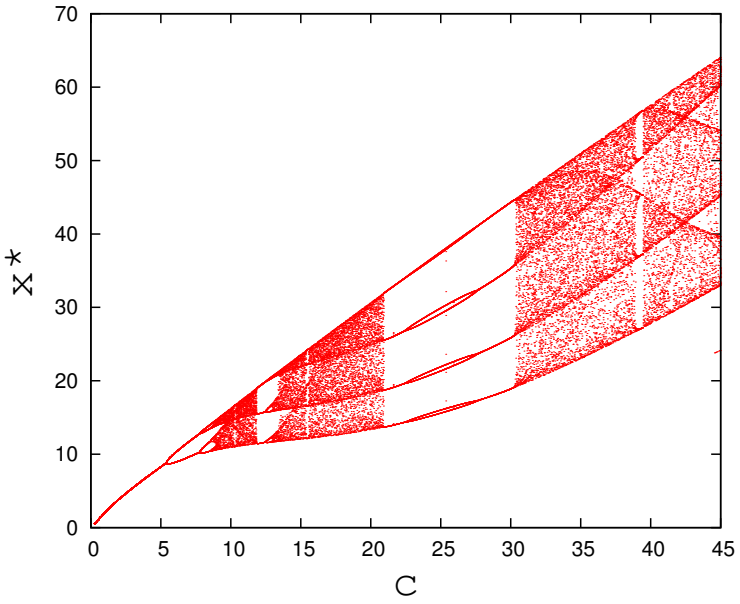

Figure 1.4: Period doubling bifurcation route to chaos for Rössler system with changing the parameter c for a=b=0.1.

1.2.2 Landau-Stuart oscillator

Landau-Stuart oscillator is a standard description of a nonlinear limit cycle oscillator. Its dynamics is given by [33]

$$\begin{aligned} \dot{x} &= (a - x^2 - y^2)x - \omega y \\ \dot{y} &= (a - x^2 - y^2)y + \omega x \end{aligned} \tag{1.3}$$

Or in polar coordinates

$$\begin{aligned} \dot{r} &= (a - r^2)r \\ \dot{\theta} &= \omega \end{aligned} \tag{1.4}$$

This equation has two stable solutions for equilibrium states.

- $r = 0$ or $(x, y) = (0, 0)$
- $r = \sqrt{a}$

The second solution gives a stable limit cycle attractor for all positive values of a with an amplitude of $\sqrt{a}$ with ω as the frequency of oscillations as shown in Fig. 1.5. The first solution is stable for $a < 0$ which means the system goes to fixed point (0,0) and the second solution is stable for $a > 0$ showing limit cycle behavior. The bifurcation at $a = 0$ is known as Hopf bifurcation [34].

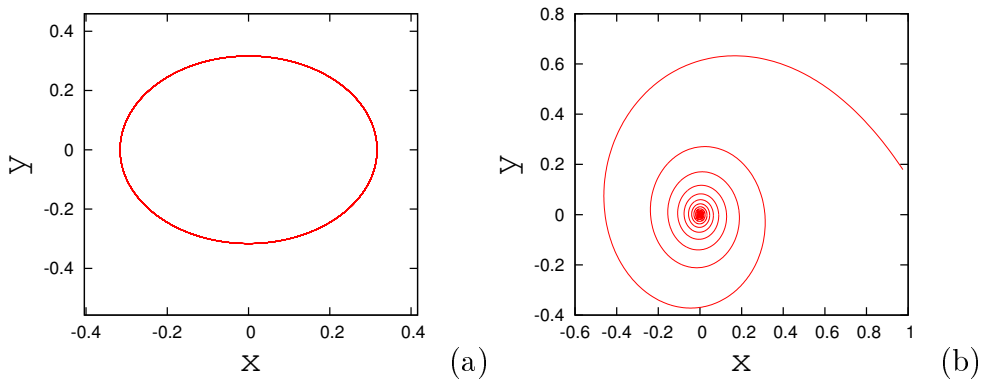

Figure 1.5: a)Phase plot of Landau-Stuart oscillator in X-Y plane showing limit cycle attractor. Here $a = 0.1$. b) fixed point in X-Y plane for a=-0.1

1.2.3 Stability of fixed points and basin of attraction

The stability of a fixed point is estimated by having a small perturbation on the variables around that fixed point state. It can be easily derived that the Jacobian of the system decides the rate of change of the small perturbation. A fixed point is hence stable in every direction when all the eigenvalues of the Jacobian have negative real parts [35].

Let us consider a general dynamical system in 3-dimension with dynamical equations

$$\begin{aligned} \dot{x} &= f_x(x, y, z) \\ \dot{y} &= f_y(x, y, z) \\ \dot{z} &= f_z(x, y, z) \end{aligned} \tag{1.5}$$

which has a fixed point at $x = x_0, y = y_0$ and $z = z_0$ so, $f_x(x_0, y_0, z_0) = 0$, $f_y(x_0, y_0, z_0) = 0$ and $f_z(x_0, y_0, z_0) = 0$. Now if we do Taylor's expansion for small perturbation around the fixed point x_0, y_0, z_0 in each direction and by discarding the higher order term since δx, δy and δz are very small we get

$$\begin{aligned} f(x_0 + \delta x, y_0, z_0) &= f_x(x_0, y_0, z_0) + \delta x \frac{\partial f_x(x_0, y_0, z_0)}{\partial x} + \delta y \frac{\partial f_x(x_0, y_0, z_0)}{\partial y} + \delta z \frac{\partial f_x(x_0, y_0, z_0)}{\partial z} \\ f(x_0, y_0 + \delta y, z_0) &= f_y(x_0, y_0, z_0) + \delta x \frac{\partial f_y(x_0, y_0, z_0)}{\partial x} + \delta y \frac{\partial f_y(x_0, y_0, z_0)}{\partial y} + \delta z \frac{\partial f_y(x_0, y_0, z_0)}{\partial z} \\ f(x_0, y_0, z_0 + \delta z) &= f_z(x_0, y_0, z_0) + \delta x \frac{\partial f_z(x_0, y_0, z_0)}{\partial x} + \delta y \frac{\partial f_z(x_0, y_0, z_0)}{\partial y} + \delta z \frac{\partial f_z(x_0, y_0, z_0)}{\partial z} \end{aligned} \tag{1.6}$$

Now from equation 1.5, rewriting equation 1.6

$$\begin{aligned} \frac{d(x_0 + \delta x, y_0, z_0)}{dt} &= f_x(x_0, y_0, z_0) + \delta x \frac{\partial f_x(x_0, y_0, z_0)}{\partial x} + \delta y \frac{\partial f_x(x_0, y_0, z_0)}{\partial y} + \delta z \frac{\partial f_x(x_0, y_0, z_0)}{\partial z} \\ \frac{d(x_0, y_0 + \delta y, z_0)}{dt} &= f_y(x_0, y_0, z_0) + \delta x \frac{\partial f_y(x_0, y_0, z_0)}{\partial x} + \delta y \frac{\partial f_y(x_0, y_0, z_0)}{\partial y} + \delta z \frac{\partial f_y(x_0, y_0, z_0)}{\partial z} \end{aligned}$$

$$\frac{d(x_0, y_0, z_0 + \delta z)}{dt} = f_z(x_0, y_0, z_0) + \delta x \frac{\partial f_z(x_0, y_0, z_0)}{\partial x} + \delta y \frac{\partial f_z(x_0, y_0, z_0)}{\partial y} + \delta z \frac{\partial f_z(x_0, y_0, z_0)}{\partial z} \tag{1.7}$$

or,

$$\begin{aligned}
(\dot{\delta x}) &= \delta x \frac{\partial f_x(x_0, y_0, z_0)}{\partial x} + \delta y \frac{\partial f_x(x_0, y_0, z_0)}{\partial y} + \delta z \frac{\partial f_x(x_0, y_0, z_0)}{\partial z} \\
(\dot{\delta y}) &= \delta x \frac{\partial f_y(x_0, y_0, z_0)}{\partial x} + \delta y \frac{\partial f_y(x_0, y_0, z_0)}{\partial y} + \delta z \frac{\partial f_y(x_0, y_0, z_0)}{\partial z} \\
(\dot{\delta z}) &= \delta x \frac{\partial f_z(x_0, y_0, z_0)}{\partial x} + \delta y \frac{\partial f_z(x_0, y_0, z_0)}{\partial y} + \delta z \frac{\partial f_z(x_0, y_0, z_0)}{\partial z}
\end{aligned} \tag{1.8}$$

or,

$$(\dot{\delta \mathbf{X}}) = \mathbf{J} \delta \mathbf{X} \tag{1.9}$$

where $\delta \mathbf{X}$ is column vector for $(\delta x, \delta y, \delta z)$ and $\mathbf{J}$ is the Jacobian for the system. The solution of $\delta \mathbf{X}$ is exponential in nature. So, in this case if all the eigenvalues of matrix J have negative real part, the solution converges with time giving the fixed point a stable solution. If at least one of the eigenvalues of J has positive real part, the fixed point becomes unstable.

From J, we can write the characteristic equation which holds the form of a polynomial. For a typical 4x4 Jacobian one can write

$$a_0 \lambda^4 + a_1 \lambda^3 + a_2 \lambda^2 + a_3 \lambda + a_4 = 0 \tag{1.10}$$

Now, Routh-Hurwitz stability criterion [36] states, the solutions for the eigenvalue λ will have negative real parts if $a_i > 0, \forall\ i$ and,

$$Det \begin{pmatrix} a_1 & a_0 \\ a_3 & a_2 \end{pmatrix} > 0, Det \begin{pmatrix} a_1 & a_0 & 0 \\ a_3 & a_2 & a_1 \\ 0 & a_4 & a_3 \end{pmatrix} > 0$$
$$Det \begin{pmatrix} a_1 & a_0 & 0 & 0 \\ a_3 & a_2 & a_1 & a_0 \\ 0 & a_4 & a_3 & a_2 \\ 0 & 0 & 0 & a_4 \end{pmatrix} > 0 \tag{1.11}$$

Basin of attraction of a fixed point or attractor represents the set of all initial conditions in the phase space which in time evolves towards that attractor or fixed point. When a system has multiple stable attractor in the phase space, the study of the structure of basins and their boundaries become important. For example Duffing oscillator given by equation

$$\begin{aligned}
\dot{x} &= y \\
\dot{y} &= -ay + bx - cx^3
\end{aligned} \tag{1.12}$$

has two stable fixed points at (-1,0) and (1,0) in the phase space and its basin structure is given in the Fig. 1.6

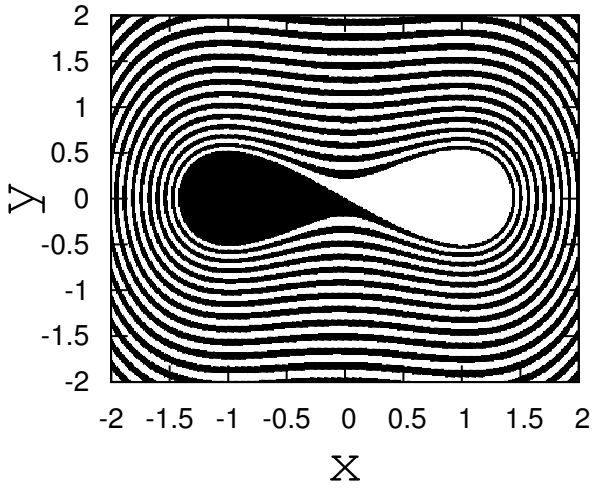

Figure 1.6: Basin structure of Duffing oscillator. Here black color represents the set of initial conditions that go to fixed point (-1,0) and white represents same for fixed point (1,0)

1.2.4 Interacting dynamical systems

Most of the real world systems are not isolated but interacting systems and hence the relevance in studying systems interacting or coupled with each other [37–40]. There are different types of coupling that are in general relevant depending upon the context of study, two of the most common ones among them are given below.

- Feedback coupling : when the variable is directly added as coupling.

$$\begin{aligned} \dot{\mathbf{X_1}} &= f(\mathbf{X_1}) + \epsilon \mathbf{G} \mathbf{X_2}, \\ \dot{\mathbf{X_2}} &= f(\mathbf{X_2}) - \epsilon \mathbf{G} \mathbf{X_1} \end{aligned}$$

- Diffusive coupling : when the difference in the variables is added as the coupling term.

$$\begin{aligned} \dot{\mathbf{X_1}} &= f(\mathbf{X_1}) + \epsilon \mathbf{G} (\mathbf{X_2} - \mathbf{X_1}), \\ \dot{\mathbf{X_2}} &= f(\mathbf{X_2}) - \epsilon \mathbf{G} (\mathbf{X_1} - \mathbf{X_2}) \end{aligned}$$

Where G is a diagonal matrix of the dimension of each system, having all diagonals as zero except i^{th} rows, which has entry 1, indicating that the i^{th} variable is coupled.

1.3 Complex networks

Complex network is the framework that is being used effectively to study complex dynamical systems in recent times. This formalism has nodes that can be considered as subsystems or

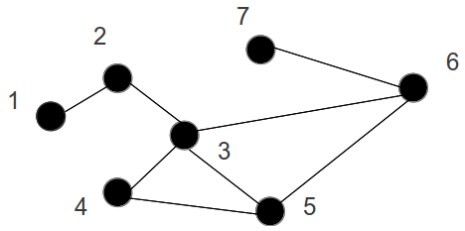

Figure 1.7: Typical complex network of 7 nodes and 8 links

units having intrinsic dynamical systems and links that connect those nodes as a graph that can model the pattern of interactions among them. The frequently used pattern of connections or links come from different types of networks such as regular, random and scale free networks. Their topology is characterized using measures that can be computed from the adjacency matrix of connections in the network [41–43].

- Adjacency matrix : This is a matrix A which has entries 1 or 0 that represents the connection topology. If in the network i^{th} and j^{th} nodes are connected then $A_{ij} = 1$ and otherwise $A_{ij} = 0$. For the undirected network this adjacency matrix is always a symmetric one. For example for a typical network shown in Fig. 1.7 the adjacency matrix would be

$$\begin{pmatrix} 0 & 1 & 0 & 0 & 0 & 0 & 0 \\ 1 & 0 & 1 & 0 & 0 & 0 & 0 \\ 0 & 1 & 0 & 1 & 1 & 1 & 0 \\ 0 & 0 & 1 & 0 & 1 & 0 & 0 \\ 0 & 0 & 1 & 1 & 0 & 1 & 0 \\ 0 & 0 & 1 & 0 & 1 & 0 & 1 \\ 0 & 0 & 0 & 0 & 0 & 1 & 0 \end{pmatrix}$$

- Degree distribution : Degree of i^{th} node k_i is defined as the number of nodes the i^{th} node is directly connected to. Hence it is clear that the sum of elements of i^{th} row gives the degree of i^{th} node.

$$k_i = \sum_{j=1}^{N} A_{ij} \tag{1.13}$$

  The degree distribution is the frequency of occurrence of degrees in the network. It is usually plotted with $p(k)$, the probability of finding a node with degree k i.e. number of nodes with degree k upon the total number of nodes, vs k.

- Characteristic path length : In the network, one can reach from one node to another along different paths, the shortest path among them being the one that requires the smallest number of connecting links between them. This is defined as the shortest path length, whose average over all possible pairs present in the network gives the characteristic path

length of the network [41]. If d(i,j) denotes the shortest path length between i and j, then characteristic path length L_c

$$L_c = \frac{1}{N(N-1)} \sum_{i \neq j} d(i,j) \tag{1.14}$$

- Clustering coefficient : Clustering coefficient is a measure of how much the network is clustered. Clustering coefficient of a network can be defined in two ways. When nodes are connected by links with each other there are cases when three of the nodes form a triangle or closed triplets. The local clustering coefficient defined for each node is the ratio of the number of triangles formed by i^{th} node to the number of all possible triangles that it can form. If i^{th} node has degree k and E_i is the actual number of present connections in neighbours of i^{th} node then local clustering coefficient c_i of i^{th} node is defined by [41]

$$c_i = E_i / \binom{k}{2} \tag{1.15}$$

We get the average clustering coefficient by averaging c_i over all nodes.

$$c_{avg} = \frac{1}{N} \sum_{i=1}^{N} c_i \tag{1.16}$$

If number of closed triplets is N_{closed} and number of connected triplets is $N_{connected}$ in the network then global clustering coefficient of the network is defined as [41]

$$c_g = \frac{N_{closed}}{N_{connected}} \tag{1.17}$$

- Assortativity and dissortativity : Assortativity or assortative mixing is the tendency of nodes to be connected to the nodes that are similar to them. The network is said to be assortative based on degree of the node, if nodes with similar degrees are connected to each other. Dissortativity on the other hand is tendency to attach with dissimilar nodes, for example high degree nodes are attached to low degree nodes in dissortative mixing.

Based on the characteristic measures of topology, networks can be classified into different types.

1.3.1 Regular network

Regular network is defined as the one where all the nodes have the same degree. For example, lattice, ring, tree etc. (Fig. 1.8) fall in the category of regular networks. A fully connected network is also regular network where each node is connected to all the other nodes. In this case all the elements in adjacency matrix is 1 other than the diagonals. The network is very densely connected and has clustering coefficient equal to 1.

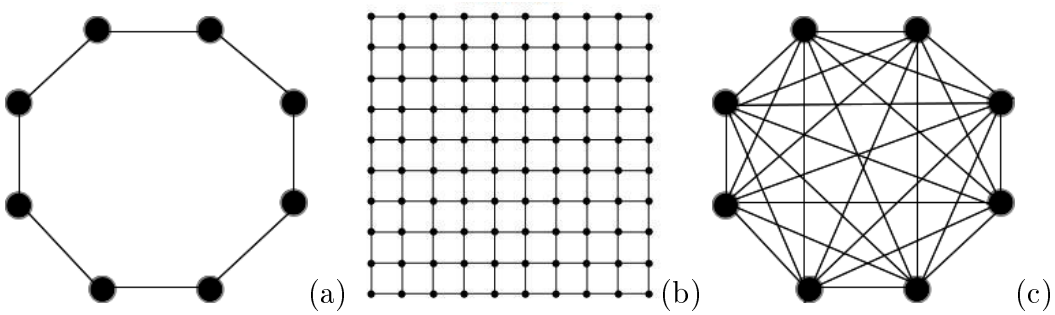

Figure 1.8: a)A ring b) a lattice c) an all to all connected network as examples of regular networks

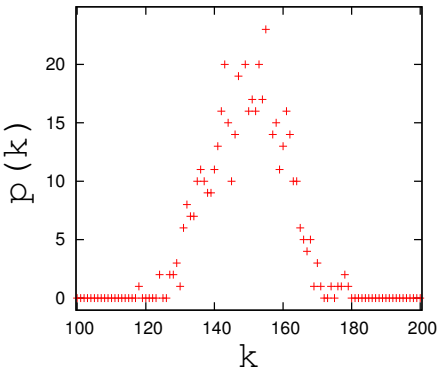

Figure 1.9: Degree distribution of random network

1.3.2 Random network

A random network is generated, by using a probability p such that the i^{th} and j^{th} node connect to each other with the probability p. If p is small the network is sparse and becomes more dense with increasing value of p. In this network the degree distribution shows a Poisson distribution (Fig. 1.9) where the mean value of degree is around pN, where N is the size of the network [41–43].

1.3.3 Scale free network

A scale free network has a degree distribution with a power law, i.e $p(k) = k^{-\gamma}$. The characteristic of this network is that there exist a large number of low degree nodes with very small number of high degree nodes known as hubs (Fig. 1.10).

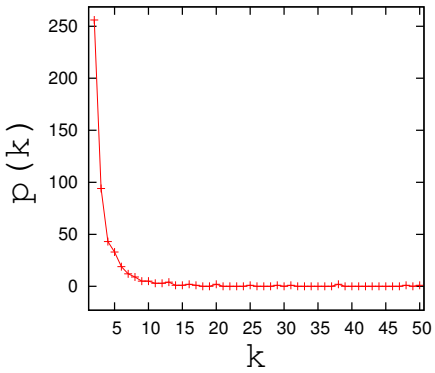

Figure 1.10: Degree distribution of scale free network

1.3.4 Interacting dynamical systems on network

Dynamical systems interacting with each other based on a network topology, can be modelled by the adjacency matrix and the nature of coupling. For example in a network of systems, when the difference between the variable of i^{th} node and the mean of the variables of its neighbours is coupled to the i^{th} node, the coupling is called mean field coupling and the equation of the i^{th} node is given by

$$\dot{x}_i = f(x_i) + \epsilon(\frac{1}{k_i}\sum_{j=1}^{N} A_{ij}x_j - x_i), \tag{1.18}$$

Similarly, when the difference between the variable of i^{th} node and the variables of its neighbours is summed up for all of them, and coupled to the i^{th} node the coupling is called diffusive coupling. In this case the equation of i^{th} node is given by

$$\dot{x}_i = f(x_i) + \epsilon\sum_{j=1}^{N} A_{ij}(x_j - x_i), \tag{1.19}$$

1.3.5 Emergent phenomena on networks

Now we consider the possible emergent dynamics when dynamical systems are connected to form a network. The most interesting dynamical phenomena observed in such coupled systems are given briefly below.

Synchronization

One of the most well studied emergent phenomena in coupled nonlinear systems is synchronization. This is a phenomenon where even though the individual chaotic systems are starting from different initial conditions and are evolving in different trajectories in time individually, when coupled, they come together and evolve together with a fixed relation with each other. Such synchronization phenomena in general, can be of different types [44–46].

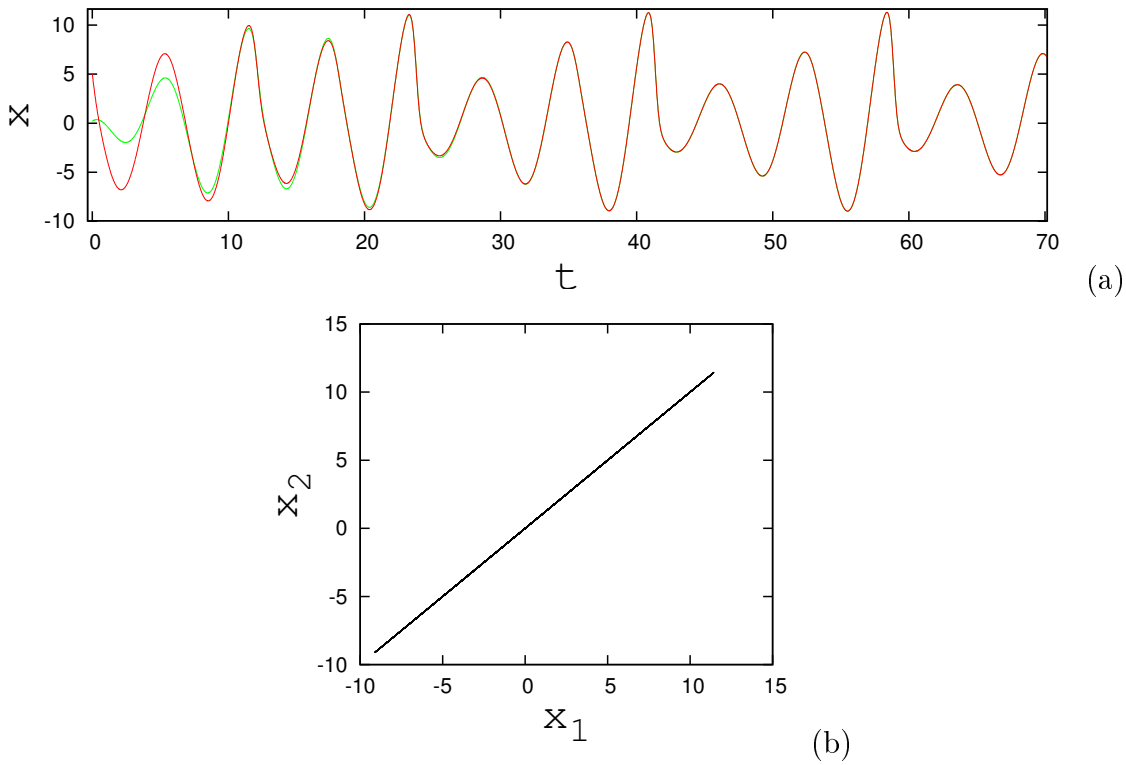

Figure 1.11: a)Time series showing complete synchronization of two coupled systems b) the functional relation between x_1 and x_2 as a straight line with slope 1 indicating complete synchronization.

- Complete(identical) synchronization : When the two or more dynamical systems, coupled diffusively, evolve on identical trajectories, they are said to be in identical or complete synchronization [44–50] (Fig. 1.11). In this case, the cross correlation coefficient r between the two systems serve as a quantifier or index to identify the state of synchronization.

$$r = \frac{\sum_{i=1}^{N}(x_i - \bar{x})(y_i - \bar{y})}{\sqrt{\sum_{i=1}^{N}(x_i - \bar{x})^2}\sqrt{\sum_{i=1}^{N}(y_i - \bar{y})^2}} \tag{1.20}$$

  For the case of complete synchronization r gives a value equal to 1. Another way of quantifying it is to take the variance of all systems involved.

$$r_1 = \frac{1}{N}\sum_{i=1}^{N}(x_i - \bar{x})^2 \tag{1.21}$$

  In equation 1.21 when $r_1 = 0$, all the systems are completely synchronized.

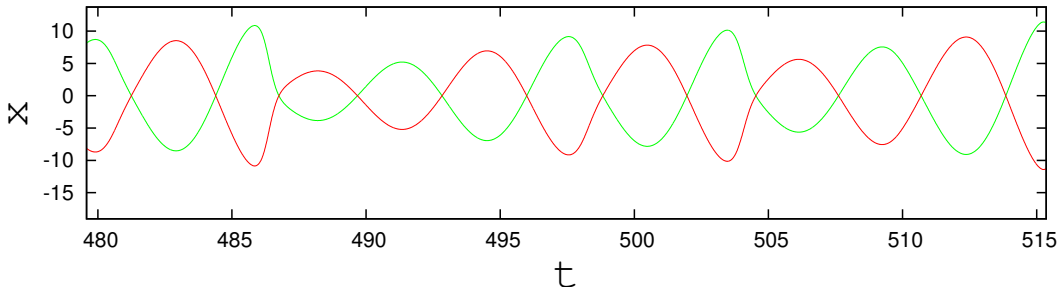

Figure 1.12: Time series showing anti synchronization in two coupled systems

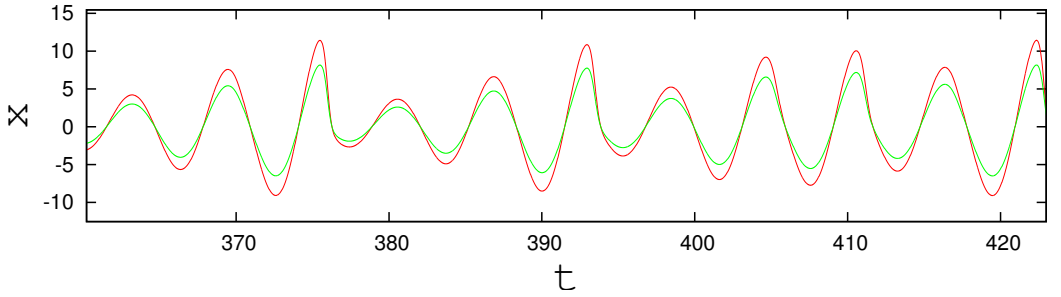

Figure 1.13: Time series showing phase synchronization in two coupled systems

- Anti synchronization : This corresponds to the case where two dynamical systems compensate each other such that the sum of their amplitudes at any given time is zero [51] (Fig. 1.12).
- Phase synchronization : In this case, the phase angle of two or more systems evolve simultaneously but their amplitudes might differ. This means if the zero crossing times for both the systems are calculated as t_i and t_j and $t_i - t_j$ is zero for all the zero crossings, the two oscillators are in phase synchronization. The phenomenon of phase synchronization usually occurs in coupled oscillators with small mismatch in their parameters [52–57] (Fig 1.13).
- Anti phase synchronization : In this state the phase difference between the two systems is π such that they are antiphase with each other. One example for anti phase synchronization is found in systems that are coupled through an external damped environment [57–60] (Fig. 1.14).
- Lag synchronization : Where two systems are separated by a constant phase, they are said to be in lag synchronization. Here $x_1(t) = x_2(t + \tau)$ where τ is the lag in time. Lag synchronization is mostly seen when two systems are coupled to each other with a time delay in the coupling term [54, 61–63] (Fig. 1.15).
- Generalized synchronization : Here the two systems are related with each other through a fixed functional form. i.e., $x_2 = f(x_1)$. Generalised synchronization occurs when one

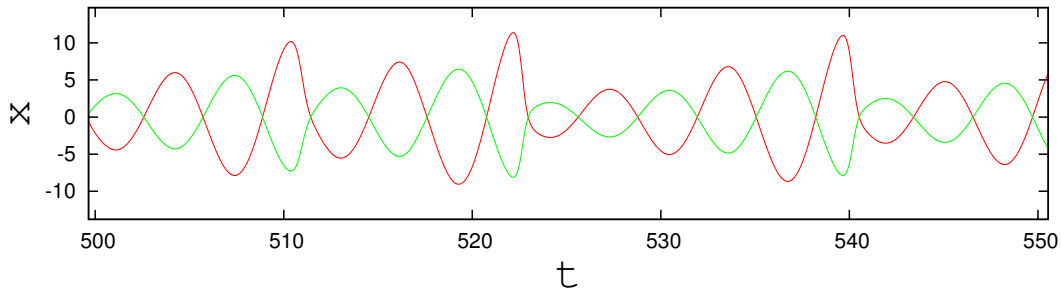

Figure 1.14: Time series showing anti-phase synchronization in two coupled systems

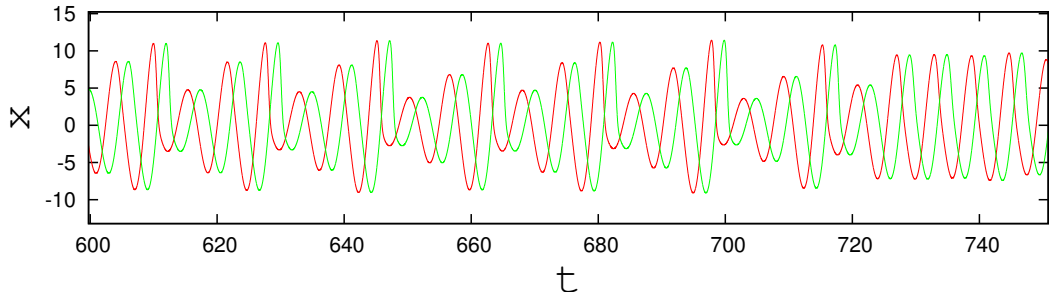

Figure 1.15: Time series showing lag synchronization in two coupled systems

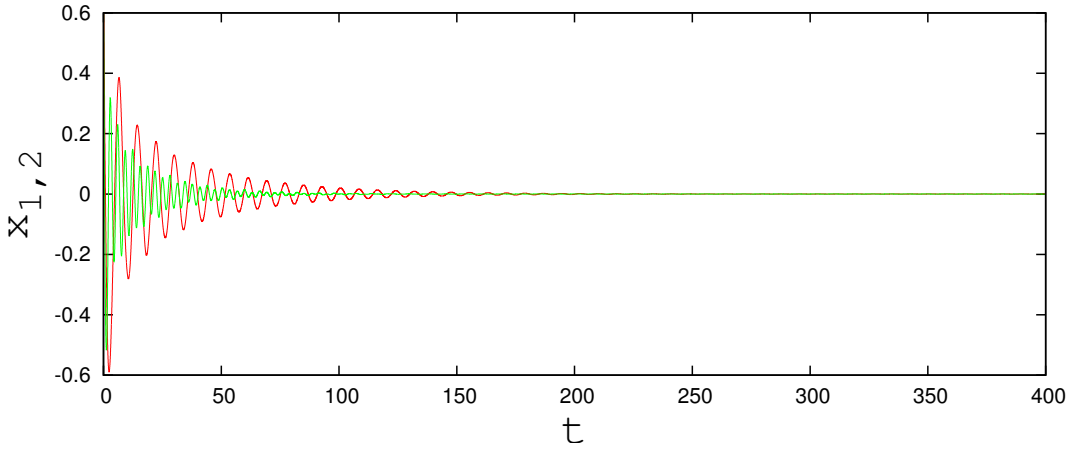

Figure 1.16: Time series showing amplitude death

system is unidirectionaly coupled to another system. To detect this state, another auxiliary system is attached to the master system. If the auxiliary system and the slave system are completely synchronized with each other, then the main master and slave system are in generalized synchronization [48, 64–69].

Amplitude death

Another important emergent phenomenon found in the context of coupled systems is amplitude death. In this case the systems go to a state of fixed point because of the coupling and the amplitudes become zero resulting in amplitude death. As we know the dynamical systems can have different fixed points which are stable or unstable. When the systems are coupled an existing unstable fixed point becomes stable, or because of the coupling new fixed point states can be generated [70, 71]. When the emergent phenomenon is such that all the systems go to the same fixed point, it will be a synchronized fixed point referred to as amplitude death. When the different systems go to different fixed points, it is a state of oscillation death [72, 73]. Studies have shown that non linear coupling [74], parameter mismatch, induced time delay conjugate coupling [75, 76], environmental coupling [77, 78] etc in coupled systems result in amplitude death state (Fig. 1.16). Oscillation death is found to occur with parameter mismatch, mean field diffusive coupling, with local repulsive link etc [79–83].

Cluster synchronization

One of the emergent phenomena observed in the context of complex networks is cluster synchronization. Each cluster will be synchronized but will be different in dynamics from another cluster. Studies have shown clusters in coupled Kuramoto phase oscillators [84, 85], where each cluster is defined by the group which has a small range of phase difference between each other, whereas the phase difference between two clusters are much larger but bounded [86–90].

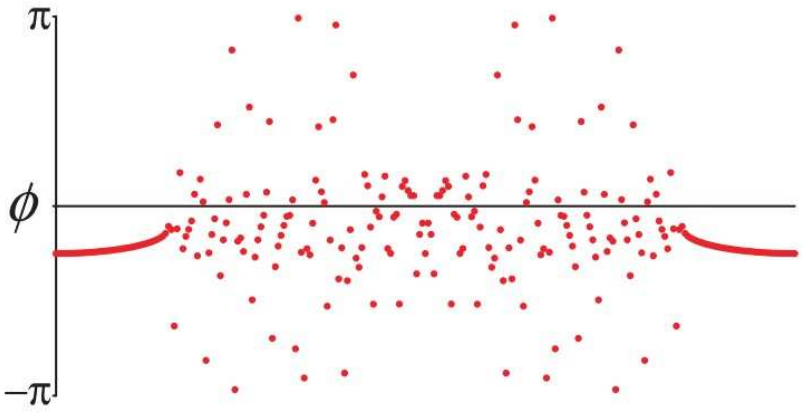

Figure 1.17: Chimera states in a ring of nonlocally coupled limit cycle oscillators, with the indices of the oscillators in x-axis and the phases ϕ in y-axis. (from [94])

Chimera states

Chimera state is an emergent state where coherent states and noncoherent states coexist in a network. This happens when a subset of many systems can be coherent to each other showing some sort of relation between them, like synchronization or amplitude death, whereas there exist other subsets of systems which do not show any coherence among themselves. [91–94] (Fig. 1.17)

1.4 Multi time scale phenomena

Other than dynamical complexity and complex patterns in interaction, complexity of many physical, biophysical, ecological, social systems can also arise from different time scales in the underlying processes [95–101]. When representing such systems using complex networks, we can model them by having subsystems evolving at different time scales. For example there are fast and slow processes that occur in modulated lasers and in chemical reactions [102, 103]. In biological processes it is known that dynamics with time scales of days coexist and interact with biochemical processes of sub-second time scales. Also many intercellular processes occur at different time scales which directly or indirectly affects the responses of neurons which act as subsystems in brain [104, 105]. On a global scale the weather and climate system of earth subsystems varying over wide time scales exist. In most of the cases these subsystems are also nonlinear and are strongly coupled with each other [106, 107].

In these contexts, some of the relevant questions that can be asked are how the slow dynamics affects the fast dynamics and whether new emergent phenomena are possible. If so what are the dynamical transitions among them? In engineering designs coupled slow and fast systems have relevance in the context of regulation and optimal control [108]. The major part of the study involves the method of adiabatic elimination of fast variables from the slow, which is effective only when the time scales are widely different [109, 110]. However when the time scales are not very different, such approximation schemes are not applicable, the analysis becomes much more interesting. A detailed study in this direction is the focus of research presented in the thesis.

In the remaining chapters we discuss the study to understand the emergent dynamics caused by complexity arising from heterogeneous dynamical time scales in interacting dynamical systems. We begin by considering two systems coupled diffusively but with different time scales and discuss the possible emergent dynamics that can occur due to various parameters involved. We also discuss coupled ocean-atmospheric model as an important application of two slow and fast coupled systems. This is discussed in the next chapter. In chapter 3 we extend our study to interacting slow and fast systems when they connected on a fully connected network. We also discuss possible dynamics on small motifs of networks. In chapter 4 we discuss the interaction of time scales between systems when connected on a random network and in chapter 5 we discuss the same in the context of a scale free network. In scale free network we study the spread of slowness as an effect of one node being slow at a stable dynamical situation such as synchronized state. The summary of the research work done and possible future directions are added in the final chapter.

Chapter 2

Coupled slow and fast systems

2.1 Introduction

We begin our study on slow and fast dynamics on complex systems by considering the most basic model of two coupled nonlinear systems that evolve with different time scales. This would mean that one of the systems has a slower time scale compared to the other. This can be introduced as a relative time scale or time scale mismatch parameter in the dynamical equations of one of the systems. We present the results of study in the specific cases of nonlinear periodic systems like coupled Landau-Stuart oscillators, periodic Rössler systems and extend to chaotic systems like Rössler and Lorenz systems in chaotic regime. We also establish the relevance of such studies by considering the case of coupled ocean-atmosphere model in climate studies where the convective dynamics of the ocean occurs at a much smaller time scale compared to that of the atmosphere. Our results in general indicate that with sufficient mismatch in the time scales of the system and strong coupling between them, both of them settle to a state of no oscillations called amplitude death state(AD) [70]. However if the mismatch in the time scale is small, with strong coupling the two systems go into a frequency synchronized state with a constant phase shift. In this case the resultant frequency is an intermediate frequency between the slow and fast intrinsic frequencies, which along with the amplitudes of the systems, decrease as they approach amplitude death state. We analyze the stability of amplitude death state and the transitions to this state as the parameters are tuned.

2.2 Coupled slow and fast systems

We construct a simple model of two coupled slow and fast dynamical systems by considering two identical dynamical systems that evolve with different time scales and interact through a coupling. The equations governing the model are given below as

$$\begin{aligned} \dot{\mathbf{X_1}} &= \tau_1 \mathbf{F}(\mathbf{X_1}) + \tau_1 \epsilon \mathbf{G}\mathbf{H}(\mathbf{X_1}, \mathbf{X_2}) \\ \dot{\mathbf{X_2}} &= \tau_2 \mathbf{F}(\mathbf{X_2}) + \tau_2 \epsilon \mathbf{G}\mathbf{H}(\mathbf{X_2}, \mathbf{X_1}) \end{aligned} \tag{2.1}$$

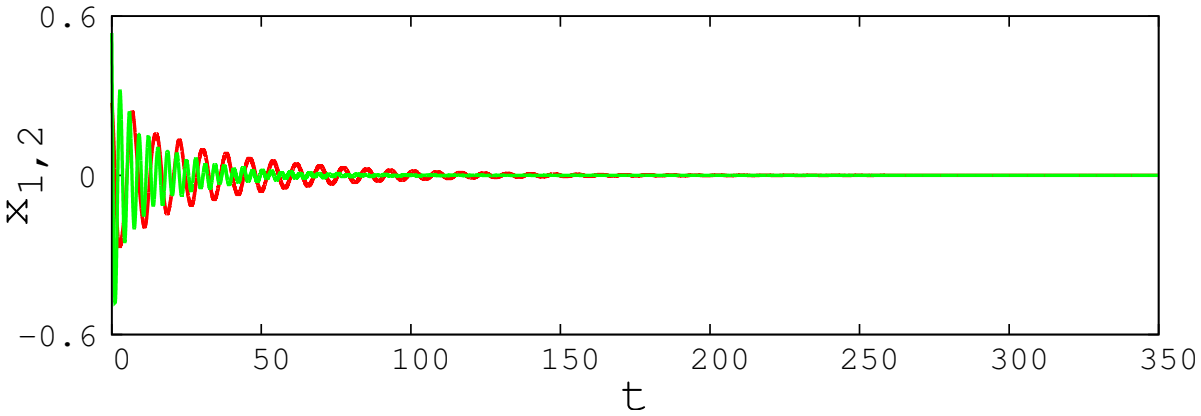

Figure 2.1: Time series of two coupled slow (red) and fast (green) Landau-Stuart oscillators in (2.2) showing amplitude death for $\tau = 0.4$ and $\epsilon = 0.3$.

Here $\mathbf{X_{1,2}} \in \mathbf{R^n}$, $\mathbf{F}$ is the intrinsic dynamics of the system, $\mathbf{H}$ denotes the coupling function and ϵ, the coupling strength. $\mathbf{G}$ is an n x n matrix which decides the variables to be coupled. The parameters τ_1 and τ_2 decide the difference in time scales. Without loss of generality, we can take $\tau_1 = \tau$ and $\tau_2 = 1$ with τ as the time scale parameter to be tuned, to vary the time scale mismatch between the two systems. In this case, in addition to the coupling strength ϵ, the time scale mismatch parameter τ also controls the asymptotic dynamics of the coupled systems.

2.2.1 Coupled slow and fast periodic oscillators

In this section we discuss the specific case of two coupled periodic systems with differing time scales. As an example of a periodic oscillator, we first consider two Landau-Stuart oscillators with slow and fast time scales, with diffusive coupling as described in Chapter 1. The coupled dynamics then evolves as

$$\begin{aligned} \dot{x}_1 &= \tau((a - {x_1}^2 - {y_1}^2)x_1 - \omega y_1) + \tau\epsilon(x_2 - x_1)) \\ \dot{y}_1 &= \tau((a - {x_1}^2 - {y_1}^2)y_1 + \omega x_1) \\ \dot{x}_2 &= (a - {x_2}^2 - {y_2}^2)x_2 - \omega y_2 + \epsilon(x_1 - x_2) \\ \dot{y}_2 &= (a - {x_2}^2 - {y_2}^2)y_2 + \omega x_2 \end{aligned} \tag{2.2}$$

The intrinsic Landau-Stuart oscillator has a limit cycle behaviour for $a > 0$ and a fixed point state for $a < 0$, as mentioned in the Chapter 1. Since we are interested in periodic orbits as intrinsic dynamics, in this case we take $a = 0.1$ and $\omega = 2$ and analyse the system numerically using Adams-Moulton-Bashforth algorithm [111] for equation (2.2). We observe that, for sufficiently large value of ϵ and small value of τ i.e strong coupling strength and large time scale mismatch, the two systems go into a state of amplitude death. This is shown in Fig. 2.1 where the time series of the x- variable of both systems are plotted for $\tau = 0.4$ and $\epsilon = 0.3$.

Amplitude death and stability analysis

The systems in equation (2.2) go into a state of amplitude death when the synchronized fixed point of the whole system has stabilized. One can obtain the parameters for which this happens by doing a linear stability analysis [35] of the system about the fixed point. For this we first calculate the synchronized fixed points of the systems in equation (2.2) by taking (x^*, y^*) equal to $(0, 0)$. As we know the eigenvalues of the Jacobian of the coupled slow and fast systems decide the stability of the AD state in this case. The Jacobian in this case is given by,

$$J = \begin{pmatrix} \tau(a-\epsilon) & -\tau\omega & \tau\epsilon & 0 \\ \tau\omega & \tau a & 0 & 0 \\ \epsilon & 0 & a-\epsilon & -\omega \\ 0 & 0 & \omega & a \end{pmatrix} \tag{2.3}$$

The characteristic equation of the Jacobian is a 4th order polynomial of the form

$$a_0\lambda^4 + a_1\lambda^3 + a_2\lambda^2 + a_3\lambda + a_4 = 0 \tag{2.4}$$

where

$$\begin{aligned} a_0 &= 1 \\ a_1 &= -2\tau a - 2a + \tau\epsilon + \epsilon \\ a_2 &= \tau^2a^2 + 4\tau a^2 - 4\tau a\epsilon - \tau^2\epsilon a + a^2 - \epsilon a + \omega^2 + \tau^2\omega^2 \\ a_3 &= -2\tau^2a^3 + 3\tau^2a^2\epsilon - 2\tau a^3 + 3\tau a^2\epsilon - 2\tau a\omega^2 + \tau\epsilon\omega^2 \\ &\quad -2a\tau^2\omega^2 + \tau^2\omega^2\epsilon \\ a_4 &= \tau^2a^4 - 2\tau^2a^3\epsilon + 2\tau^2a^2\omega^2 - 2\tau^2\omega^2a\epsilon + \tau^2\omega^4 \end{aligned} \tag{2.5}$$

- Routh-Hurwitz criterion

  From Routh-Hurwitz stability criterion [36], the solutions for the eigenvalue λ will have negative real parts if $a_i > 0$, $\forall\ i$ and,

$$Det\begin{pmatrix} a_1 & a_0 \\ a_3 & a_2 \end{pmatrix} > 0, Det\begin{pmatrix} a_1 & a_0 & 0 \\ a_3 & a_2 & a_1 \\ 0 & a_4 & a_3 \end{pmatrix} > 0$$
$$Det\begin{pmatrix} a_1 & a_0 & 0 & 0 \\ a_3 & a_2 & a_1 & a_0 \\ 0 & a_4 & a_3 & a_2 \\ 0 & 0 & 0 & a_4 \end{pmatrix} > 0 \tag{2.6}$$

  Hence

$$\begin{aligned} &a_1a_2 - a_0a_3 > 0 \\ &a_1a_2a_3 - {a_1}^2a_4 - a_0{a_3}^2 > 0 \\ &a_1a_2a_3a_4 - {a_1}^2{a_4}^2 - a_0{a_3}^2a_4 > 0 \end{aligned} \tag{2.7}$$

The above three conditions give three different transition curves as their solutions corresponding to the inequalities equal to zero. Thus, we identify the common region in the parameter plane (τ,ϵ) as the region enclosed by these curves where all of the above three conditions are satisfied. This is marked by the boundary line with red circles in Fig. 2.2. This thus indicates the region of amplitude death where the steady state of the coupled system is stable.

- Direct calculation of eigenvalues

  We also directly calculate the eigenvalues of J for different values of τ and ϵ using Mathematica software. By doing this we estimate the parameter values at which at least one of the eigenvalues changes from negative to positive. These are plotted to get the transition curves, shown in black in Fig 2.2. We observe that this boundary matches with the one estimated using Routh-Hurwitz criteria directly.

- Numerical calculations

  We also do a detailed direct numerical analysis of the coupled slow and fast systems in equation (2.2) for different values of these parameters scanning the parameter plane (τ, ϵ) using Adams-Moulton-Bashforth algorithm for integration of the equation of motion with 0.01 time step and 100000 iterations. To identify the region of amplitude death in this plane, we compute the index A_{diff} as the difference between global maximum and global minimum of the variable x for each system, calculated after neglecting the transients of 90000 iterations. Hence in this case $A_{diff} = 0$ for both systems would indicate the region of AD [77] .

  Using this method we isolate the region of amplitude death in the (τ, ϵ) plane where both the systems stabilize to the synchronized fixed point. This is shown in green in the Fig. 2.2. It is clear that this region of AD obtained by direct numerical simulation has good agreement with the analytical transition curves calculated by both Routh-Hurwitz criterion and the eigenvalue calculations from the Jacobian.

Frequency synchronization with phase shift under strong coupling

We now study the possible emergent dynamics of these systems outside the region of amplitude death. As we know from earlier studies, when the systems are coupled with their dynamics having equal time scales, i.e in this case $\tau = 1$, with strong enough coupling they completely synchronize with each other. In our studies additionally we introduce a time scale mismatch parameter τ and decrease it from 1, we find the systems cannot remain in identical or complete synchronization. They settle to a state of constant phase relation (Fig .2.3), which can be understood as a state of frequency synchronization with a phase shift between them.

To estimate the phase between the oscillators in this state, we calculate the difference between times of successive zero crossing $(t_k - t'_k)$ of the two oscillators over a sufficiently long interval of time after neglecting the transients. We average this time difference and call it ϕ. We observe that this phase shift changes with the time scale mismatch, and we study this variation of ϕ with τ for a fixed ϵ as shown in Fig .2.4. To calculate the frequency of each oscillator from the

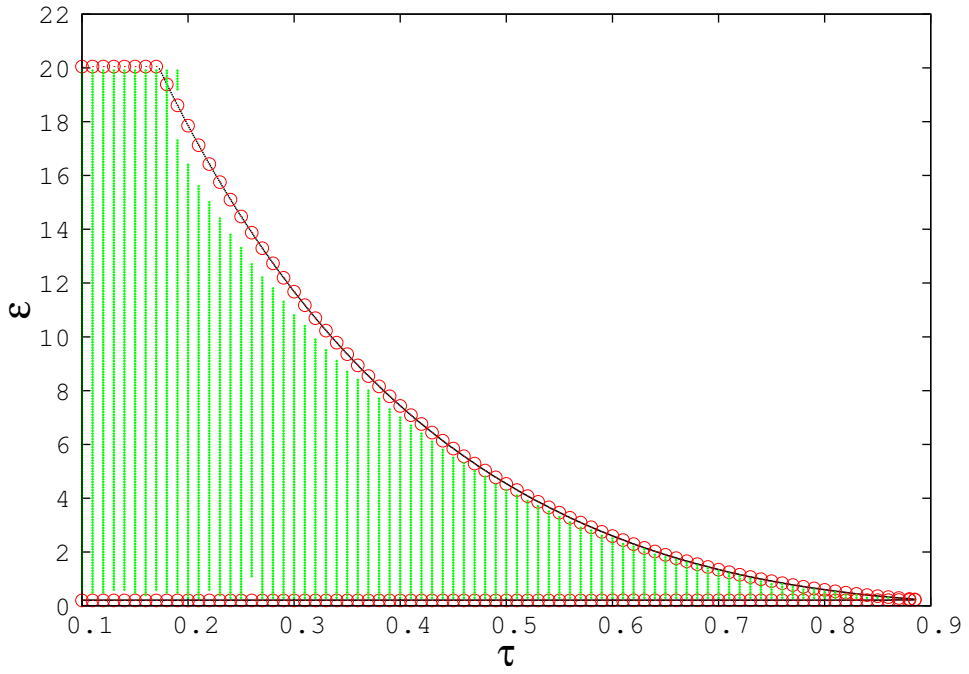

Figure 2.2: Amplitude death region (shown in green) for coupled slow and fast Landau-Stuart oscillators in the plane (τ, ϵ) obtained numerically. Black line corresponds to the transition curve to AD obtained from stability analysis while red circles show the transition obtained using Routh-Hurwitz criterion.

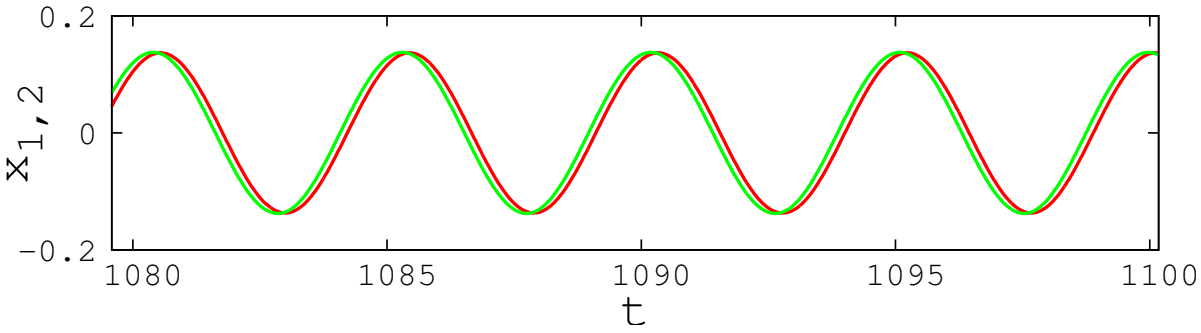

Figure 2.3: Frequency synchronized state with constant phase shift in coupled slow (red) and fast (green) Landau-Stuart oscillators. Time series shown is for $\tau = 0.4$ and $\epsilon = 10$.

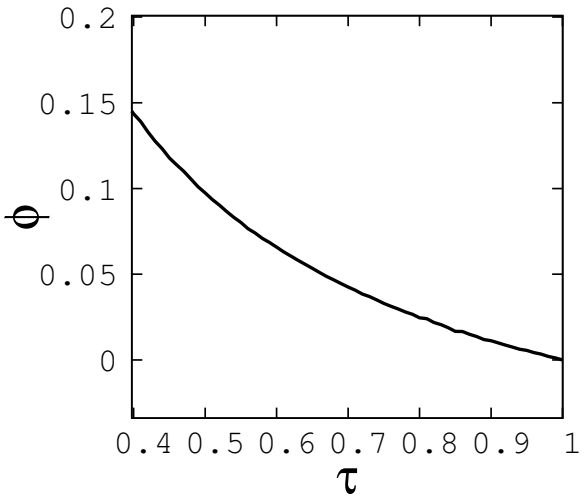

Figure 2.4: Phase shift ϕ between coupled slow and fast Landau-Stuart oscillators as τ is varied with $\epsilon = 10$.

time series we use the relation

$$\omega = \frac{1}{K}\sum_{k=1}^{K}\frac{2\pi}{(t_{k+1} - t_k)} \tag{2.8}$$

where t_k is the time of the k^{th} zero crossing point in the time series of the oscillator and K is the total number of intervals for which the zero crossings are counted. We find that for sufficiently large ϵ both oscillators settle into the same frequency, indicating the state of frequency synchronization with a phase shift. Moreover, this emergent frequency varies with the changes in values of τ and ϵ. This is shown in the contour plot of (τ, ϵ) plane with the emergent frequency of the oscillators(Fig .2.5a). We also study the variation of the intrinsic frequencies of both oscillators, their average frequency and the emergent frequency with τ. This is shown in Fig .2.5b. It is clear from the figure that because of the coupling the system with the greater frequency slows down, and the slower one speeds up to reach the common frequency. However this common frequency of the coupled system is always less than the mean of the frequencies of the uncoupled intrinsic oscillators. This indicates the phenomenon of **frequency suppression** [112, 113] (Fig .2.5). We also study how the amplitudes of coupled oscillators depend on the parameters τ and ϵ. For this we calculate the average amplitude for each oscillator over a period of time. This is calculated for different parameter values and Fig. 2.6 shows how average amplitude decreases to zero as amplitude death is reached along both directions of decreasing τ and ϵ.

Multi periodicity under weak coupling

We now discuss the dynamics with very low coupling strength corresponding to regions below the AD island. In this case we observe that when the coupling strength is very small ($\epsilon < 0.2$) and for a very small time scale mismatch such as $\tau = 0.9$ each system settles into a state of

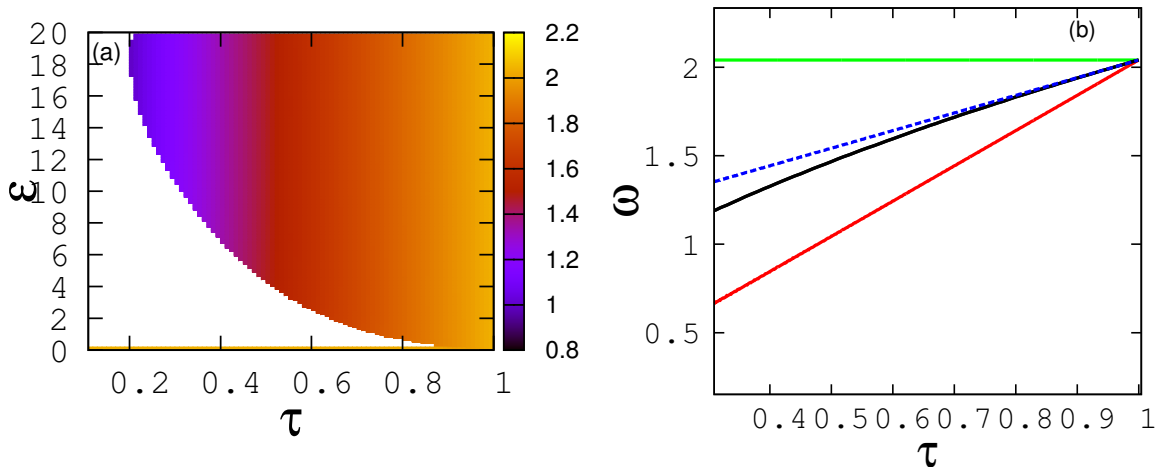

Figure 2.5: (a)Contour plot of emergent frequency of the two oscillators in equation (2.2) in (τ, ϵ) plane. (b) Frequencies of fast oscillator (green), slow oscillator (red), coupled oscillator (black) and mean frequency of both oscillators (blue dotted), as τ is varied, keeping $\epsilon = 10$. The emergent frequency is less than the mean frequency, indicating frequency suppression.

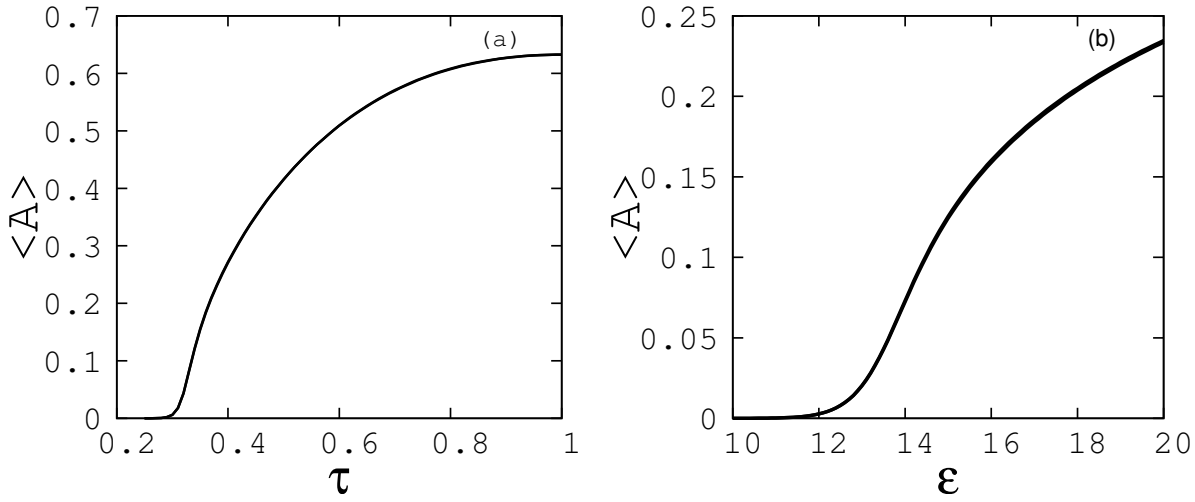

Figure 2.6: Average amplitude $\langle A \rangle$ of coupled slow and fast Landau-Stuart oscillators (a) varying τ at $\epsilon = 10$ and (b) varying ϵ at $\tau = 0.25$.

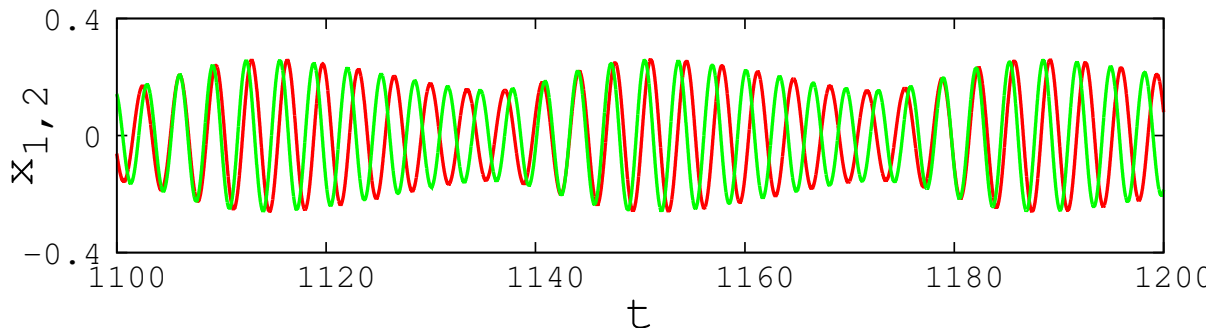

Figure 2.7: Two frequency state for coupled slow (red) and fast (green) Landau-Stuart oscillators. Time series shown is for $\tau = 0.9$ and $\epsilon = 0.11$.

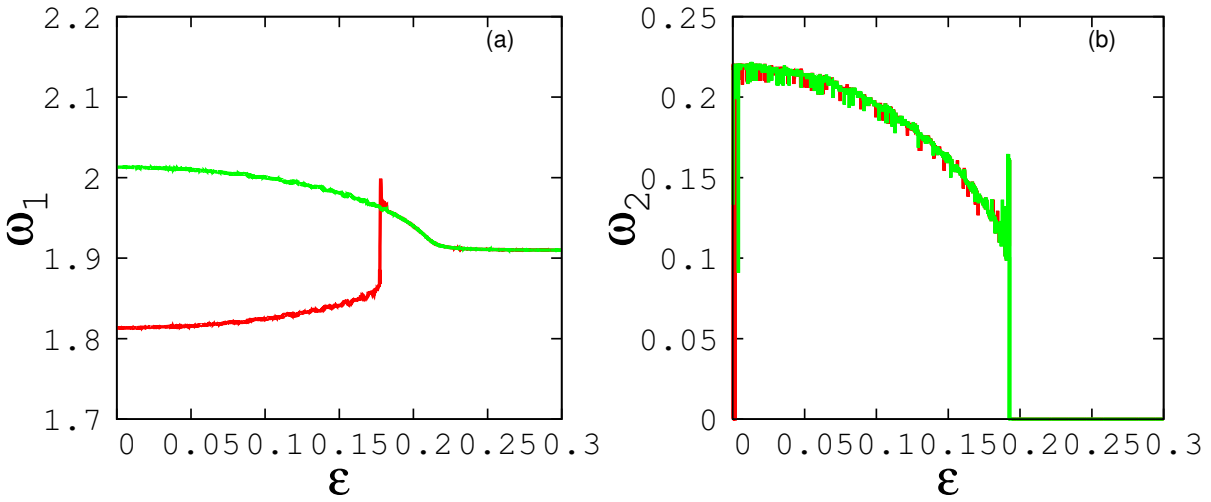

Figure 2.8: Variation of frequency with ϵ at $\tau = 0.9$.(a) Large frequency of fast (green) and slow (red) systems and (b) small frequency of both systems observed in coupled slow and fast Landau-Stuart oscillators.

two frequency oscillations as shown in Fig. 2.7. In this case, we calculate the larger or main frequency (ω_1) of each oscillator from the time series using eqn (2.8) as described earlier, while the small frequency (ω_2) is calculated by using the same equation but taking t_k as the time of k^{th} local maximum of all the maxima, i.e. where the maxima of the envelope of the time series is located in time. We find that the large frequencies (ω_1) are different in this state of weak coupling, but the small frequencies (ω_2) are the same for both oscillators. As the coupling strength increases the small frequency of envelope disappears and the large frequencies merge to get the two systems locked into the state of equal frequency, which is described in the previous section. The variation of ω_1 and ω_2 as ϵ increases is shown in Fig. 2.8a. We confirm this result by calculating the frequencies from Fourier transform of the time series of both oscillators.

We repeat the above analysis with periodic Rössler system as another example of coupled

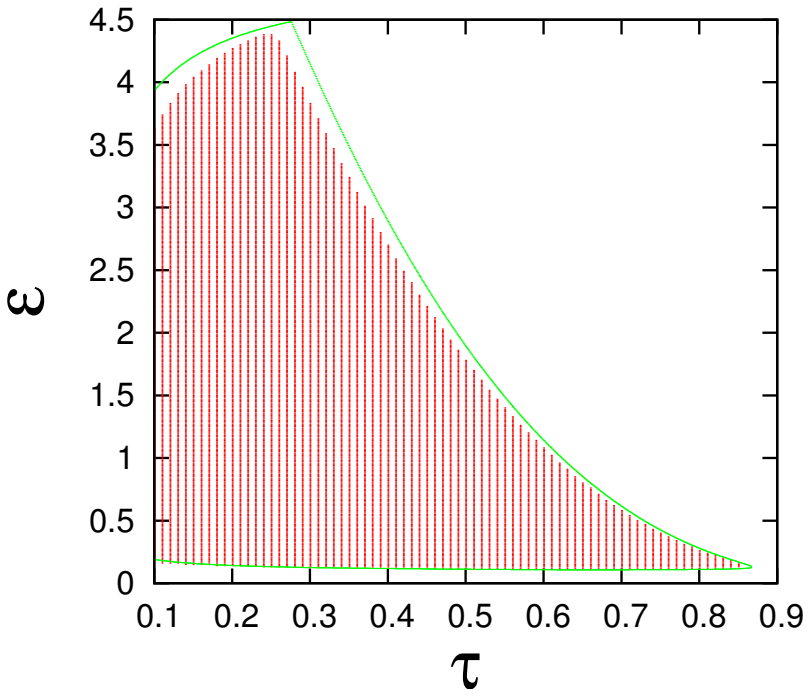

Figure 2.9: Parameter plane (τ, ϵ) showing region of amplitude death for coupled slow and fast periodic Rössler systems (shown in red). The green line shows boundary obtained using stability analysis.

periodic systems. The equations for two such coupled slow and fast systems are given by

$$\begin{aligned}
\dot{x}_1 &= \tau(-y_1 - z_1) + \tau\epsilon(x_2 - x_1) \\
\dot{y}_1 &= \tau(x_1 + ay_1) \\
\dot{z}_1 &= \tau(b + z_1(x_1 - c)) \\
\dot{x}_2 &= (-y_2 - z_2) + \epsilon(x_1 - x_2) \\
\dot{y}_2 &= (x_2 + ay_2) \\
\dot{z}_2 &= (b + z_2(x_2 - c))
\end{aligned} \tag{2.9}$$

In this case we take the intrinsic dynamics as periodic with parameters chosen as a=0.1, b=0.1 and c=4. Here also we observe qualitatively similar results with occurrence of amplitude death, phase locked frequency synchronization with phase shift for strong coupling (Fig. 2.10) and two frequency states for weak coupling (Fig. 2.12). We numerically isolate the amplitude death region in (τ, ϵ) plane and also obtain the transition curves from stability analysis around the fixed point. In Fig. 2.9 we show the island of AD in red and the boundary from the stability analysis in green. In this case the synchronized fixed point (x^*, y^*, z^*) is equal to $(\frac{c-\sqrt{c^2-4ab}}{2}, \frac{-c+\sqrt{c^2-4ab}}{2a}, \frac{c-\sqrt{c^2-4ab}}{2a})$.

We characterize the phase shift between oscillators in the frequency synchronized state with the variation of τ. We observe that the difference in amplitudes between slow and fast systems is

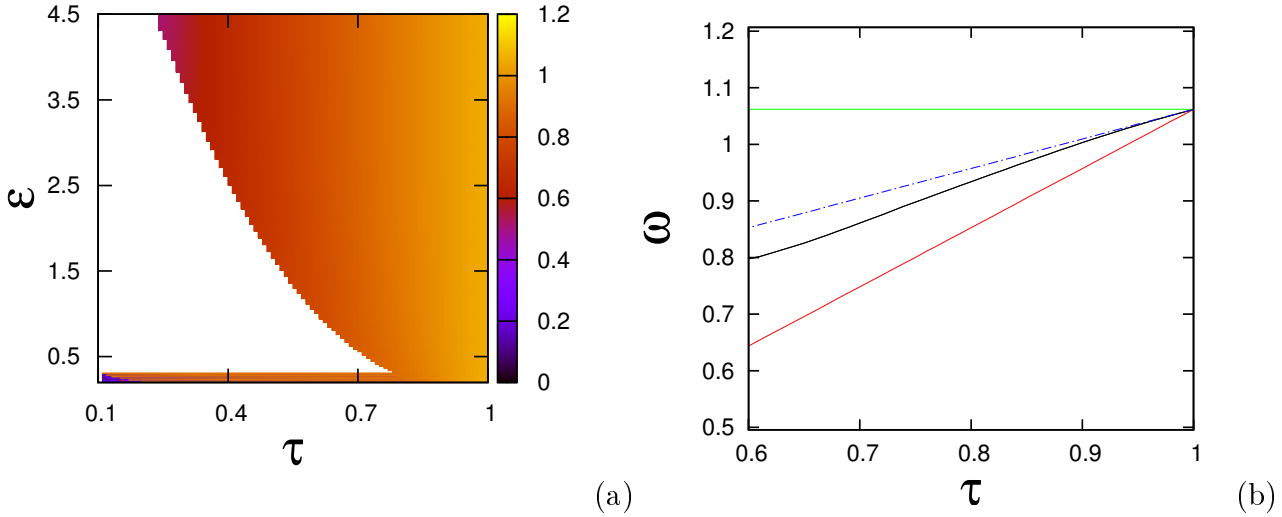

Figure 2.10: Frequency synchronized state in coupled slow and fast periodic Rössler systems showing a) contour plot of emergent frequency in (τ, ϵ) plane, b)Frequencies of fast oscillator (green), slow oscillator (red), coupled oscillator (black) and mean frequency of both oscillators (blue dotted), as τ is varied, keeping $\epsilon = 1$. The emergent frequency is less than the mean frequency, indicating frequency suppression.

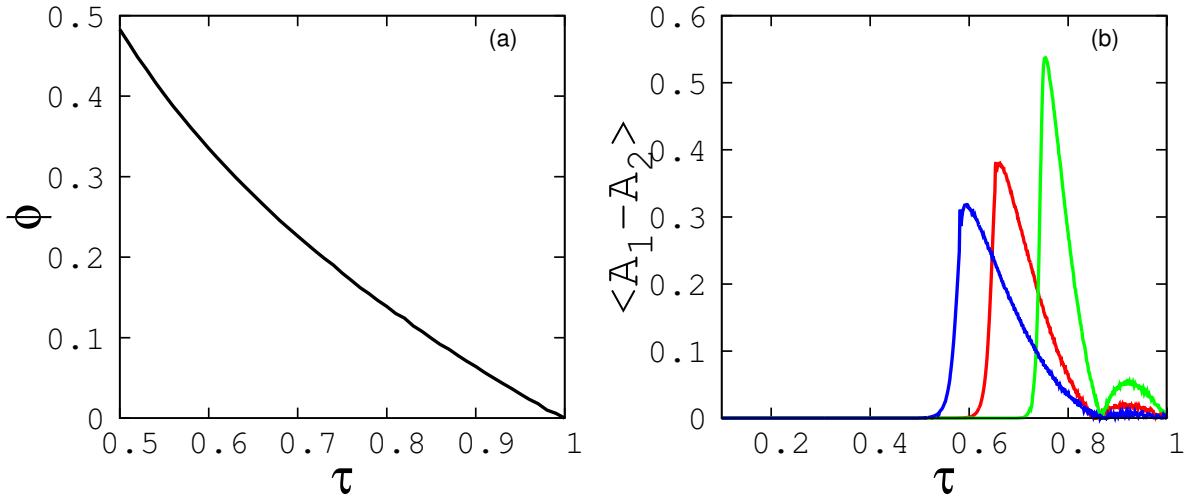

Figure 2.11: (a)Phase shift ϕ between slow and fast systems vs τ with ϵ =1 (b) Average amplitude difference $\langle A_1 - A_2 \rangle$ vs τ for ϵ=0.5(green), ϵ=1(red) and ϵ=1.5(blue) for coupled slow and fast periodic Rössler systems.

significant in this case and they depend upon the time scale parameter and the coupling strength in frequency synchronized state. The slow systems has less amplitude than the fast one and we calculate the amplitude difference between them with the variation of τ for different values of ϵ which is shown in the Fig. 2.11.

2.2.2 Coupled slow and fast chaotic Rössler systems

We extend the above study to two coupled chaotic Rössler systems with differing time scales, as in equation (2.9), but choosing the system parameters in chaotic regime as a=0.2, b=0.2, c=5.7.

For this case also we find that with sufficient time scale mismatch and strong coupling between the two systems both systems reach the state of synchronized fixed point described as AD in the previous sections. This region in (τ, ϵ) plane is isolated by numerical calculations as the region where the difference between global maxima to global minima for both systems reaches zero. This agrees with the boundary of AD calculated from stability analysis. The parameter plane for AD is shown in the Fig. 2.13.

We observe that for the case of coupled chaotic Rössler systems studied, the transition to AD is through a sequence of reverse period doubling bifurcations that results in periodic dynamics before reaching amplitude death. The bifurcations occur at the same parameter values for both the systems even when their amplitudes are different. The bifurcation diagram corresponding to these transitions as τ is varied for $\epsilon = 0.9$, is shown in Fig. 2.14. Once the systems reach the periodic state, we find qualitatively similar behaviour in the average phase shift and average amplitude as in the case of periodic oscillators described in the previous section. We take the time averaged Euclidian distance between the slow auxiliary systems X and X$'$ as D_x and fast auxiliary systems Y and Y$'$ as D_y. For the range of τ considered, as shown in the Fig. 2.16, we observe that D_x and D_y go to zero which is the indication of complete synchronization between

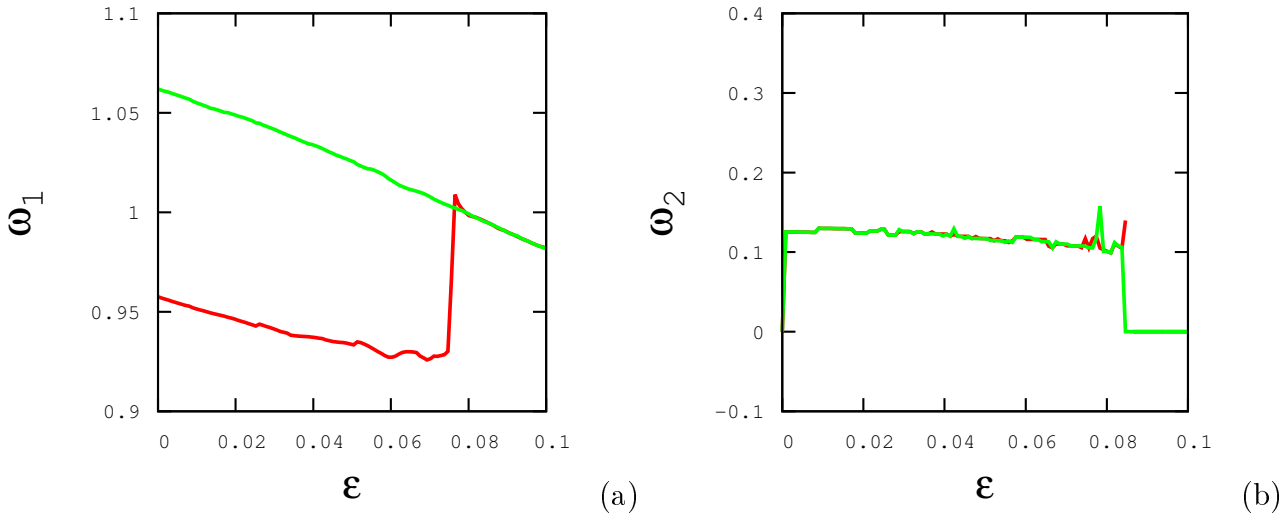

Figure 2.12: Two frequency states for weak coupling in periodic Rössler systems. a) large frequency of both systems which becomes equal with ϵ b) small frequency which becomes zero with increasing ϵ at $\tau = 0.9$

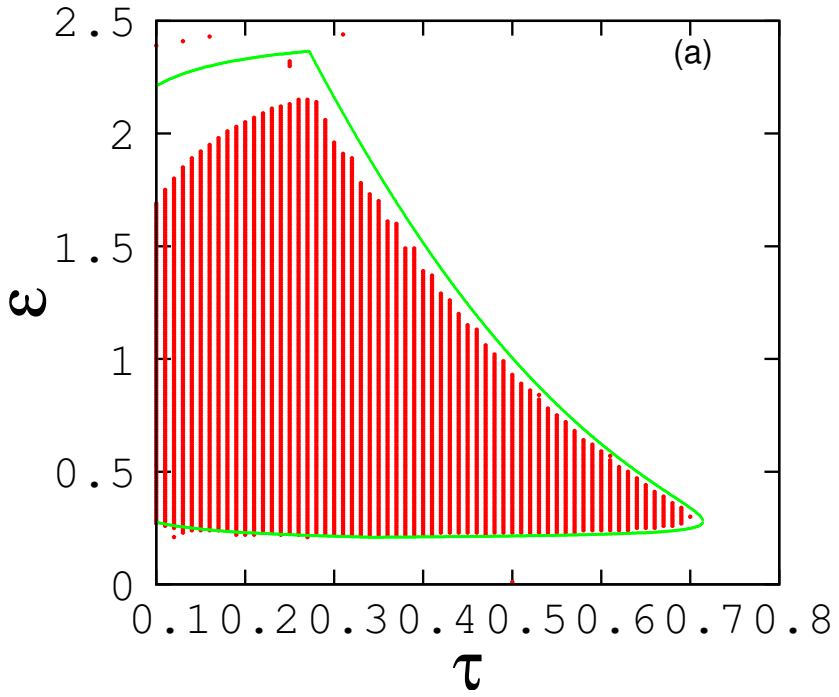

Figure 2.13: Parameter plane (τ, ϵ) showing region of amplitude death (shown in red) for coupled slow and fast chaotic Rössler systems. The green line shows boundary obtained using stability analysis.

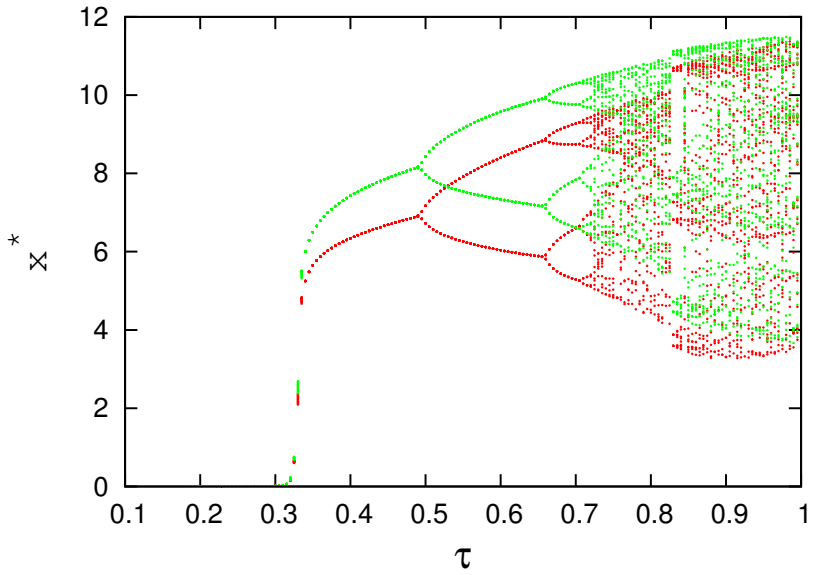

Figure 2.14: Bifurcation diagram obtained by plotting the maximum vales of the x variables of two coupled slow (red) and fast (green) chaotic Rössler systems for $\epsilon = 2$ as τ is varied.

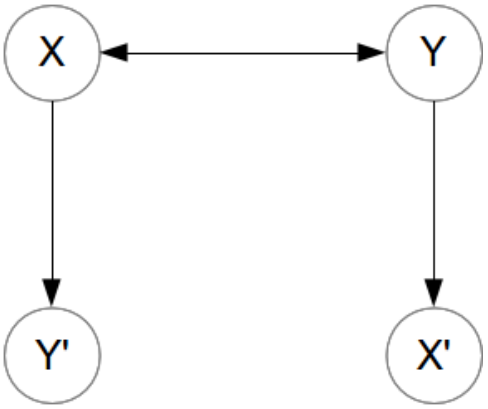

Figure 2.15: Auxiliary systems for coupled slow (X) and fast (Y) systems. X is connected to Y′ (fast) and Y is connected to X′ (slow) unidirectionally.

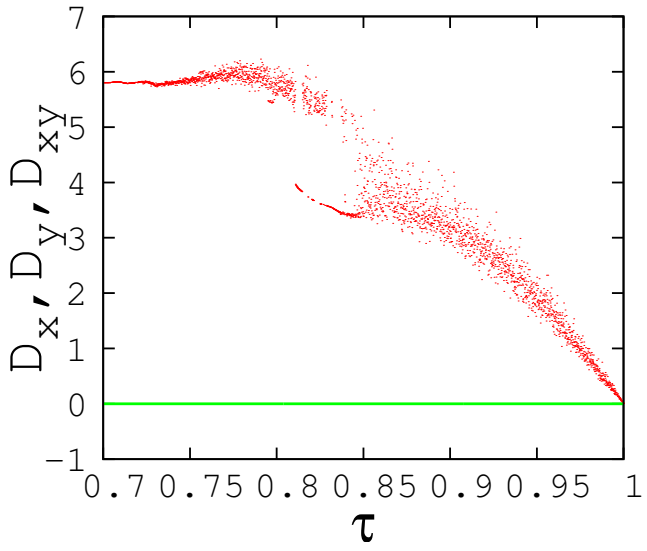

Figure 2.16: Euclidean distance between auxiliary systems for $\epsilon = 2$ as τ is varied. D_x, the distance between X and X$'$ which are auxiliary systems to the system Y and D_y, that between Y and Y$'$ which are auxiliary systems to the system X are shown in green. D_{xy}, the Euclidean distance between main slow and fast systems X and Y is also plotted (in red). D_x and D_y remain zero throughout the region, which indicates generalised synchronization between X and Y.

the auxiliary systems and therefore generalised synchronization in the slow and fast systems X and Y (Fig. 2.16).

2.2.3 Generalized synchronization

However when the dynamics of the oscillators are chaotic, for large τ, there is a region where we find the systems settle to a state of generalized synchronization with a functional relation between them. To study this, we attach one slow auxiliary system (X$'$) to the fast system (Y) and one fast auxiliary system (Y$'$) to the slow system (X) unidirectionally, as per the scheme described in [66, 69] for bidirectionally coupled systems (Fig. 2.15). So conceptually X and X$'$ become auxiliary systems to Y and Y and Y$'$ become auxiliary systems to X in this procedure.

2.2.4 Coupled Lorenz systems with differing time scales

We also consider two coupled slow and fast Lorenz systems as another example of coupled chaotic systems,

$$\begin{aligned} \dot{x}_1 &= \tau a(y_1 - x_1) + \tau\epsilon(x_2 - x_1) \\ \dot{y}_1 &= \tau(x_1(b - z_1) - y_1) \\ \dot{z}_1 &= \tau(x_1 y_1 - c z_1) \end{aligned}$$

$$\begin{aligned} \dot{x}_2 &= a(y_2 - x_2) + \epsilon(x_1 - x_2) \\ \dot{y}_2 &= x_2(b - z_2) - y_2 \\ \dot{z}_2 &= x_2 y_2 - c z_2 \end{aligned} \tag{2.10}$$

where a=10,b=28,c=8/3.

In this case also we find that amplitude death happens for sufficient strength of coupling and time scale mismatch. The region for which the coupled dynamics of both of the systems show AD in the plane (τ, ϵ) is obtained numerically and shows good agreement with the stability analysis from Jacobian of the coupled system. This is shown in Fig. 2.17.

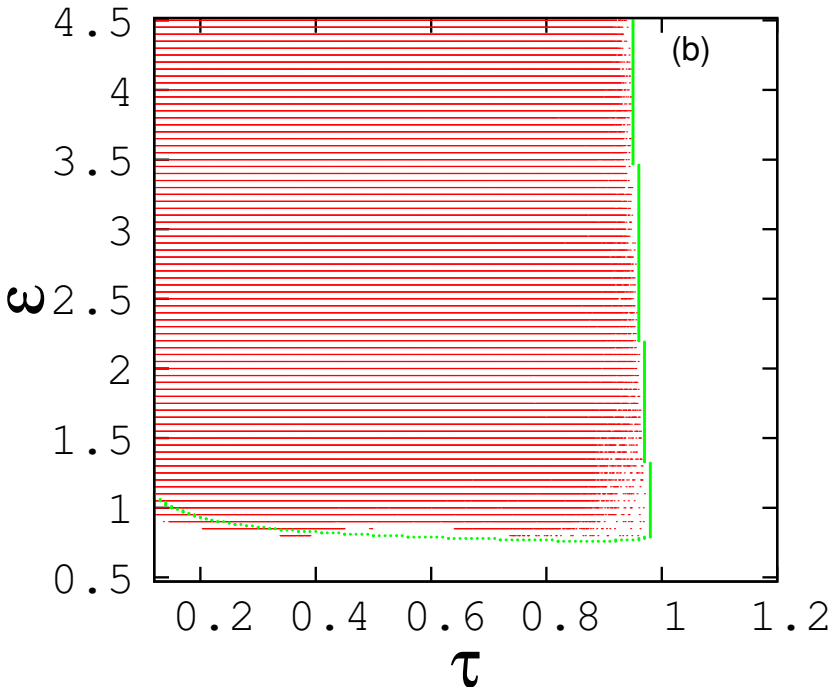

Figure 2.17: Parameter plane (τ, ϵ) showing region of amplitude death (shown in red) for coupled slow and fast chaotic Lorenz systems. The green line shows boundary obtained using stability analysis.

However for the coupled Lorenz systems the transition to AD is through an intermittency state. In this transition, the duration of the small amplitude oscillations present in Lorenz systems gets longer as τ is decreased. The time series of the coupled Lorenz systems are plotted for increasing values of τ with $\epsilon = 4.0$ in Fig. 2.18 which clearly indicate the intermittency route to AD for coupled chaotic Lorenz systems.

2.3 Coupled Ocean-Atmosphere model

As an important application of the phenomena introduced in the previous sections, we study the coupled ocean-atmosphere model used in climate studies [114, 115]. In this context, it is

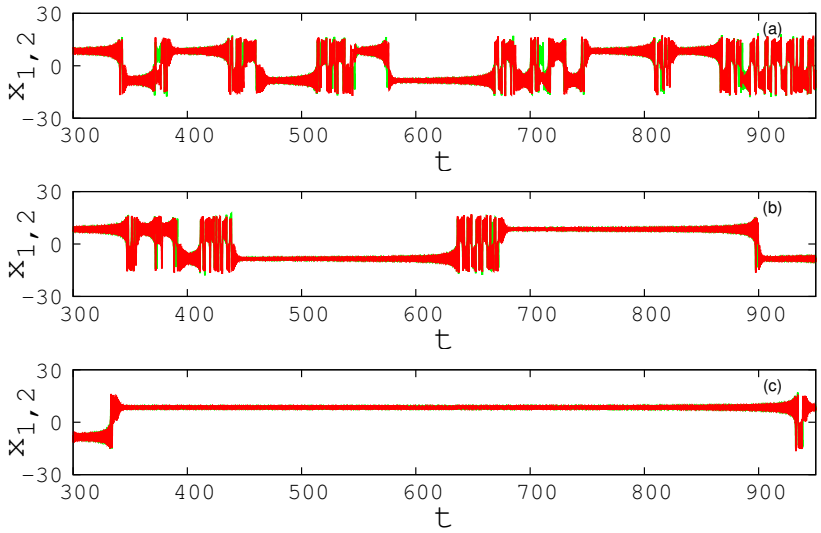

Figure 2.18: Transition to amplitude death in two coupled slow (red) and fast (green) chaotic Lorenz systems in (1.1). Time series plotted for $\epsilon = 4$ and (a)$\tau = 0.949$, (b) $\tau = 0.948$ and (c)$\tau = 0.947$ indicating intermittency in the transition.

usual to consider low dimensional Lorenz system as the model for basic dynamics and couple two versions of the same, one with fast and other with slow time scale. This then models the interactive dynamics of a fast oscillating atmosphere and slow-fluctuating ocean. The equations representing coupled convective dynamics studied earlier are given below [115].

$$\begin{aligned}
\dot{x}_1 &= \tau a(y_1 - x_1) - \epsilon x_2 \\
\dot{y}_1 &= \tau(x_1(b - z_1) - y_1) + \epsilon y_2 \\
\dot{z}_1 &= \tau(x_1 y_1 - c z_1) - \epsilon z_2 \\
\dot{x}_2 &= a(y_2 - x_2) - \epsilon x_1 \\
\dot{y}_2 &= x_2(b - z_2) - y_2 + \epsilon y_1 \\
\dot{z}_2 &= x_2 y_2 - c z_2 + \epsilon z_1
\end{aligned} \tag{2.11}$$

where a=10,b=28,c=8/3 and τ is the slow time-scale parameter.
We revisit this model to analyze it from the point of view of coupled systems and report the interesting dynamics that results in periodic and steady state convection due to the interaction with differing time scales. In this case unlike the previous cases, we observe two different fixed point attractors for the slow and the fast systems, indicating oscillation death. Moreover as an important result, we report multi stable periodic states for the coupled systems.

2.3.1 Oscillation death

We find that for a certain region in the parameter plane (τ, ϵ) i.e. for strong coupling strength and high time scale mismatch, the coupled dynamics of this model shows oscillation death (OD). In this state the two systems go to two different fixed points(Fig. 2.19). This region of OD is shown in the parameter plane (τ, ϵ) in red in Fig. 2.20. The region above the upper boundary

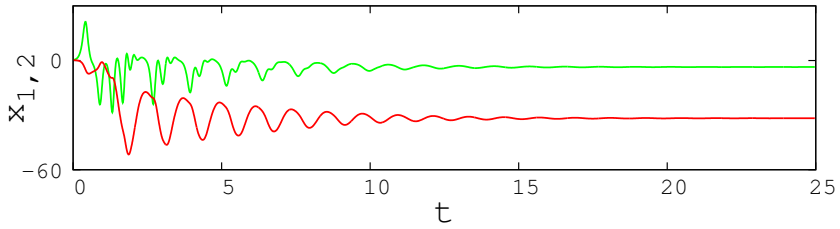

Figure 2.19: Time series of coupled ocean-atmosphere model at oscillation death for $\tau = 0.15$ and $\epsilon = 3$ where red corresponds to slow-fluctuating ocean and green corresponds to fast oscillating atmosphere.

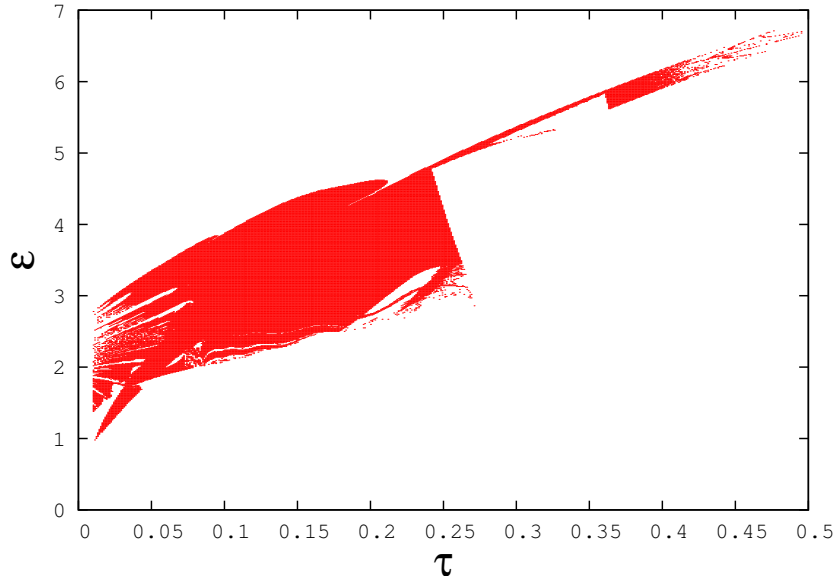

Figure 2.20: Region of oscillation death (shown in red) in coupled ocean-atmosphere system in (τ, ϵ) plane.

corresponds to unstable behaviour, while that below shows periodic dynamics and multi stable states.

2.3.2 Periodic oscillations and Multi stable states

We study the nature of dynamics in the region outside of OD state in the (τ, ϵ) parameter plane. We see that for large values of time scale mismatch as we increase the coupling between the oscillators, they show periodic behaviour in this model. This is shown in Fig. 2.21 where the phase plots of the oscillators in X-Y plane are shown, for different values of ϵ and τ below the OD region. The multi stable states occur due to the existence of different basins of attraction in the initial value space of the coupled system. We study this basin structure by scanning the (x_1, x_2) plane between $(-60, 60)$ keeping (y_1, z_1, y_2, z_2) fixed as shown in Fig. 2.22. Here we identify the regions in this plane, that lead to the different states possible from the four multi

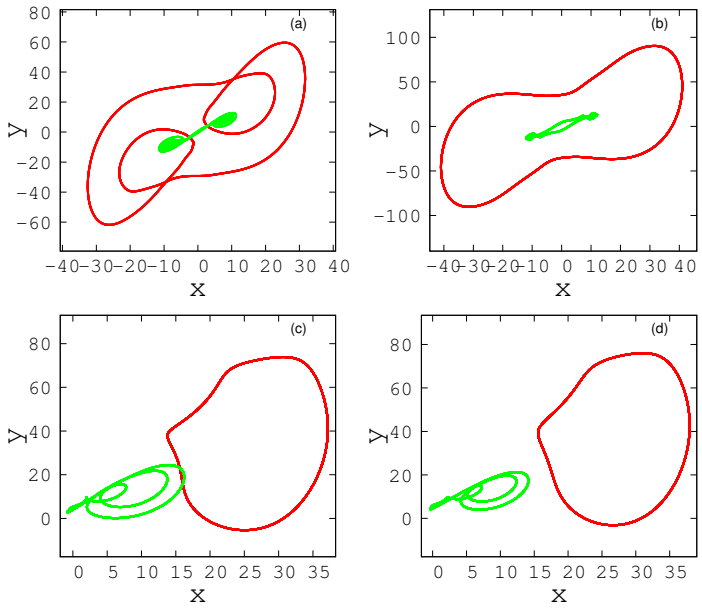

Figure 2.21: Attractors of coupled ocean-atmosphere model before reaching OD, (where red corresponds to slow oscillation of ocean and green corresponds to fast oscillation of atmosphere) for $\tau = 0.1$ (a)$\epsilon = 0.8$, (b)$\epsilon = 1.5$, (c)$\epsilon = 1.92$ and (d)$\epsilon = 2.02$ in X-Y plane.

stable states as shown in Fig. 2.22. This basin structure thus obtained is shown in Fig. 2.23. We also find multi stable states in this model, in the narrow region below the that of OD. Here for the same set of parameter values, different initial conditions show different behaviour such as oscillation death states and periodic states. We study these multi stable states, by keeping (y_1, z_1, y_2, z_2) constant as $(0.3, 0.4, 0.5, 0.6)$ and varying (x_1, x_2). Thus for (x_1, x_2)= $(0.8, 0.34), (0.1, 0.5), (0.4, 0.5), (40, -40)$ we get different possible states for the same values of $(\tau, \epsilon) = (0.312, 5.4)$. These states are shown in Fig. 2.22 a,b,c and d respectively. It is clear from the figures that the systems settle to two types of oscillatory states and two types of OD states indicating multi stability in both states.

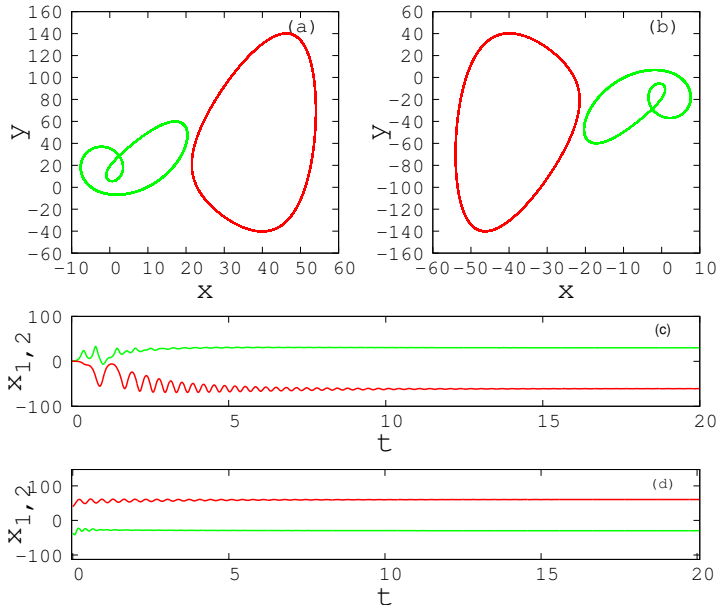

Figure 2.22: (a) and (b)Multistable periodic states and (c) and (d) oscillation death states of coupled ocean-atmosphere model (where red corresponds to slow oscillation of ocean and green corresponds to fast oscillation of atmosphere) at $\tau = 0.312$ and $\epsilon = 5.4$ for different initial conditions.

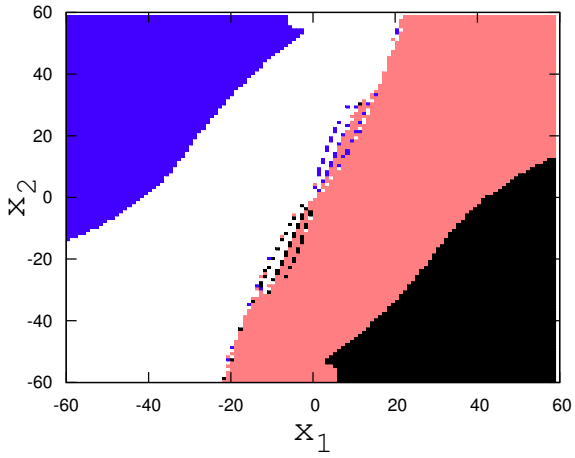

Figure 2.23: Basin structure for the multistable states in coupled ocean-atmosphere system for parameter values $\tau = 0.312$ and $\epsilon = 5.4$. The regions in blue and black form the basin for the oscillation death states shown in Fig 2.22(c) and (d)), while pink and white regions correspond to periodic oscillations shown in Fig 2.22 (a) and (b) respectively.

2.4 Summary

Our study shows that when two systems with different time scales are coupled together, the time scale mismatch causes their dynamics to go to a synchronized fixed point known as amplitude death. We characterize the parameter range in which such emergence can occur for different types of intrinsic dynamics like periodic Landau-Stuart, periodic and chaotic Rössler and Lorenz systems. We also observed that in periodic case, for strong coupling when the mismatch in time scale is not large, systems settle into an emergent state of synchronized frequency. The frequency observed in this case is in between the intrinsic fast and slow frequency leading to frequency suppression. For weak coupling the systems show a two frequency state. As an application we revisit and discuss the coupled ocean-atmospheric model as two coupled Lorenz systems of different time scales and report oscillation death, multistable states and corresponding basin structure. In this context the occurrence of periodic emergent states for coupled chaotic Lorenz systems is an interesting phenomena resulting periodically changing convection of different amplitudes for ocean and atmosphere. Similarly oscillation death results in steady state convection with varying rolls.

Chapter 3

Emergent dynamics of slow and fast dynamical systems on fully connected regular network

3.1 Introduction

In this chapter we present the study on the emergent collective behavior of interactive slow and fast systems that are connected to form a network. This can form the framework for understanding the dynamics of complex systems that have many interacting units or sub systems. In our study we consider the subsystems as nonlinear dynamical systems located at the nodes of the network, and we address the specific context of heterogeneity that arises from the difference in the dynamical time scales of nodal dynamics. To make this concept a specific feature and understand the effects arising only from time scale mismatch of interactive systems, we consider a regular or homogeneous topology for the network. One way to do this is to consider a fully connected network in which each node is connected to all the others. Thus in a network of N systems, each node is connected to (N-1) nodes making it a regular network of equal degree for all nodes. To introduce the effect of slow time scales or time scale mismatch, we take m of the N systems to be evolving at a slower time scale compared to others and study how this affects the dynamics of the whole network. In this system, we observe emergent dynamical states like synchronized clusters, multi frequency states, phase synchronized states and phenomenon like amplitude death. More importantly, we find an interesting novel cross over behavior in the collective dynamics as the number of slow systems is varied for chosen values of mismatch in time scales and coupling strength. We also present a detailed study on small motifs of minimal systems that can build up the full network and hence contribute to understanding the dynamics of the full complex network.

3.2 Network of slow and fast systems

We construct a network of N identical n dimensional systems. Among these N systems, m evolve on a slower time scale. This subset of slow oscillators is named as S. The equation governing

the dynamics of the i^{th} node of the network is given by

$$\dot{X}_i = \tau_i F(X_i) + G\epsilon\tau_i \sum_{j=1}^{N} A_{ij}(X_j - X_i) \tag{3.1}$$

where $\tau_i = \tau$ if $i \in$ S, $\tau_i = 1$ otherwise. G is an n x n matrix which decides which variables are to be coupled. Here we take G = diag(1, 0, 0 ..) which means x variable of the i^{th} oscillator is coupled diffusively with the x variable of j^{th} oscillator. A_{ij} is the adjacency matrix of the network defining its topology or connectivity. Since we consider a fully connected network, $A_{ij} = 1$ for all i and j except i=j.

3.2.1 Dynamics of slow and fast periodic systems on fully connected network

In this section we study the dynamics of slow and fast periodic oscillators on a fully connected network. We take first the dynamics at each node as a periodic Rössler system and study the case of a network of N systems with N=100 and analyze how the slowness of m of the systems can affect the dynamics of the whole network.

$$\begin{aligned} \dot{x}_i &= \tau_i(-y_i - z_i) + \tau_i\epsilon \sum_{j=1}^{N} A_{ij}(x_j - x_i) \\ \dot{y}_i &= \tau_i(x_i + ay_i) \\ \dot{z}_i &= \tau_i(b + z_i(x_i - c)) \end{aligned} \tag{3.2}$$

The parameters are chosen as a=0.1, b=0.1 and c=4 so that dynamics corresponds to the periodic regime. With slow time scale introduced in the dynamical equations, the frequency of the intrinsic oscillation depends linearly upon the value of the time scale parameter τ. However when m such slow systems are coupled with (N-m) fast ones to form the network, the emergent frequency of the whole network might depend additionally on other parameters like number of slow systems and the coupling parameter.

Our study shows the suppression of dynamics of the whole network is the main result with amplitude death in all systems. This happens for sufficient time scale mismatch, coupling strength and for a range of values of m. To calculate this range m, for a chosen value of τ and ϵ, we calculate the difference between global maximum and global minimum of the x-variable of each system after neglecting the transients and average this quantity over all the oscillators to get A_{diff}. We plot this quantity with varying number of slow systems m to detect the region for which $A_{diff} = 0$ corresponding to the amplitude death region. This region is shown in Fig. 3.1 for N=100, marked as region 2, which is for a moderate range of m. As shown in the same Fig. 3.1, there are regions 1 and 3 for lower and higher range of m respectively in which AD is not seen, where we observe other dynamical states like synchronized clusters. We discuss the dynamical states for these regions in detail in the subsequent sections.

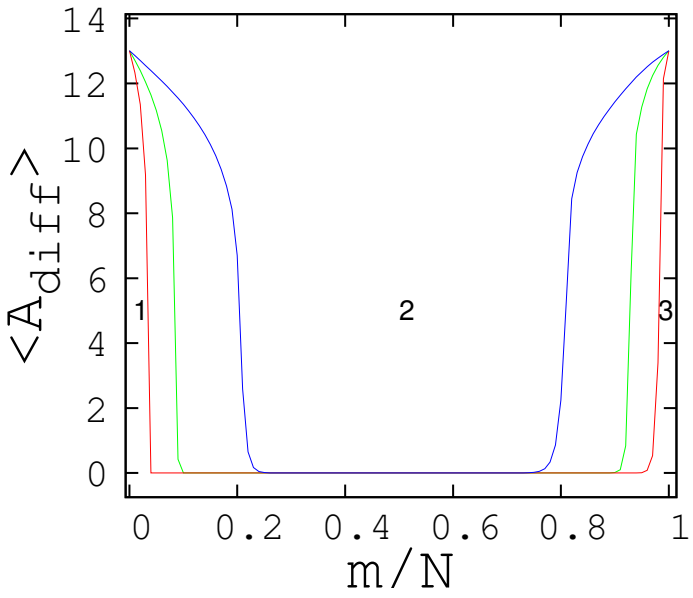

Figure 3.1: Average difference in amplitudes, $< A_{diff} >$, of N coupled Rössler systems plotted with the fraction, m/N of slow systems. Here $N = 100$, $\epsilon = 0.03$ and $\tau = 0.1$(red), 0.35(green), 0.5(blue). Region 2, where $< A_{diff} >= 0$ corresponds to AD.

3.2.2 Synchronized clusters, multi-frequency states and frequency synchronization for small m

In the region 1 of Fig. 3.1, where the number of slow systems m is small ($m \approx 10$) all the systems are found to show oscillatory behavior and have a nonzero value for amplitude as shown in the Fig. 3.1. In this range under the influence of strong coupling, the whole network splits into two separate clusters, one of slow and the other of fast systems. The dynamics of the oscillators within each cluster is synchronized among themselves, however, that of the two clusters is only frequency synchronized with each other with a phase shift between them. We show the time series of x-variable of the systems to demonstrate this cluster formation in Fig. 3.2 for $\tau = 0.5$, $\epsilon = 0.03$. We note that in this region 1 with low m, the amplitude of the cluster of fast systems is larger than that of the slow one throughout the parameter plane (τ, ϵ). As time scale mismatch increases, the difference in amplitudes between clusters also increases.

To check the synchronization within each cluster we calculate the variance of all oscillators within that cluster, var_s and var_f being this value for slow and fast clusters respectively. They are shown in Fig. 3.3. As time evolves, we see that the variance goes to zero for each cluster indicating identical synchronization for all systems within each cluster. For very weak coupling ($\epsilon \approx 0.001$) and large $\tau \approx 0.8$, the dynamics within each cluster is completely synchronized. However, the dynamics within the cluster of slow systems show two frequency state with smaller amplitude and that in the fast cluster is single frequency oscillations with larger amplitudes. Fig. 3.4 demonstrates this interesting phenomenon.

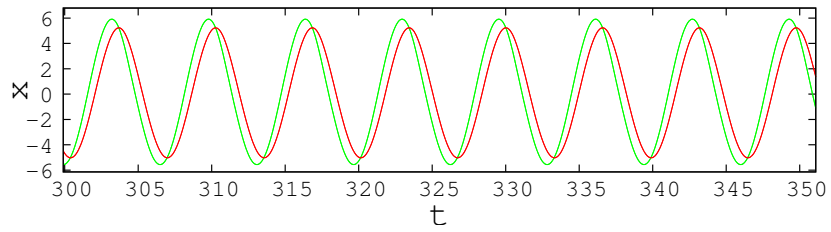

Figure 3.2: Synchronized clusters of slow and fast dynamics in the network for $\tau = 0.5$, $\epsilon = 0.03$, $m = 10$ and $N = 100$. Here the time series of the x variables are plotted for 3 typical slow(red) and 3 fast(green) systems.

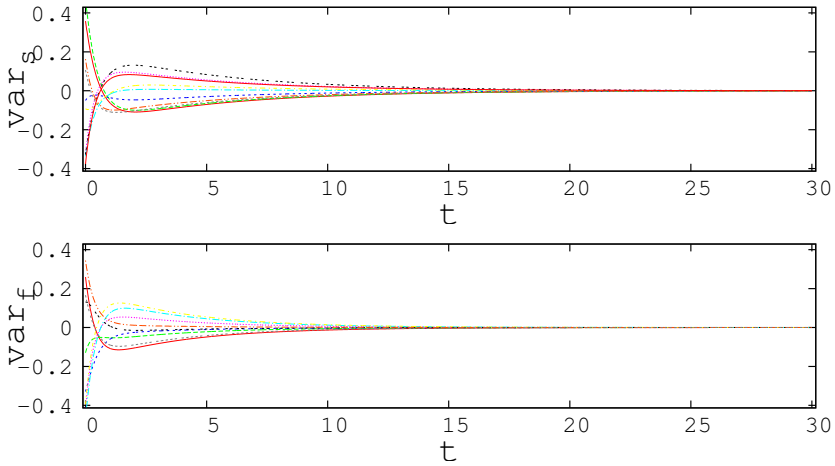

Figure 3.3: Variance of slow oscillators var_s and that of fast oscillators var_f are plotted with time for $\tau = 0.5$, $\epsilon = 0.03$. After transients, $var_s = 0$ and $var_f = 0$, indicating that the dynamics within each cluster sets them completely synchronized.

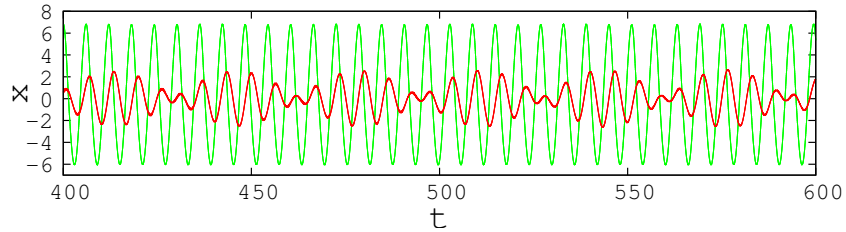

Figure 3.4: Time series of x variables are plotted for 3 slow and 3 fast systems. This plot shows two frequency state for slow(red) systems while fast(green) systems show large amplitude oscillations of single frequency. Here $\tau = 0.8$, $\epsilon = 0.001, m = 10$ and $N = 100$.

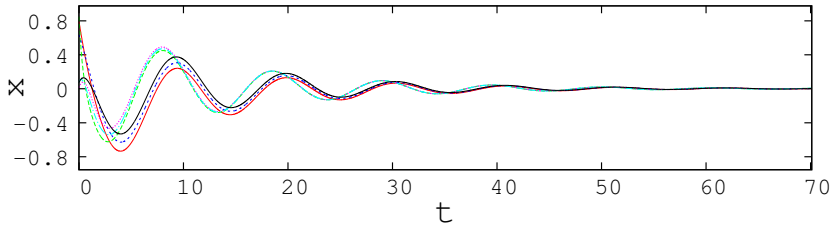

Figure 3.5: Amplitude death state for fully connected network of slow and fast systems for $\tau = 0.35$, $\epsilon = 0.03, m = 50, N = 100$. Here the time series of x variables of 3 fast and 3 slow systems are plotted.

3.2.3 Suppression of dynamics and frequency synchronization for moderate m

As the number of slow systems m is increased to moderate values corresponding to region 2 in the Fig. 3.1, we observe that the interaction between slow and fast systems causes suppression of dynamics in the whole network resulting in AD. This is observed for a specific range of (τ, ϵ) where time scale mismatch and coupling strength between slow and fast systems are high. This state of AD is shown in Fig. 3.5. We can identify the region of AD in (τ, ϵ) parameter plane for any value of m chosen from the region 2 of Fig. 3.1. For this we numerically calculate the difference between global maximum and global minimum (A_{diff}) of each system in the network and mark the region where A_{diff} is zero for all the systems. This region of AD thus isolated is shown in red in Fig. 3.6.

Now we study the nature of dynamics outside the region of amplitude death. In this case for weak coupling and large τ, the systems go into two frequency states as shown in Fig. 3.7. While there exists slow and fast clusters, the oscillators within each cluster are synchronized with each other. The small frequencies, which define the frequency of envelope is same for both the clusters. For all the cases of synchronized clusters mentioned above, synchronization is verified by calculating the variances that behave qualitatively similar to Fig. 3.3.

As the coupling strength increases in this range of m, we observe for a large range in parameter plane, outside region of AD, the whole network settles to a state of frequency synchronization. However the network still has two clusters of slow and fast systems, such that the states of the two clusters are separated by a phase shift. This is qualitatively similar to the dynamics shown in Fig. 3.2. We calculate the frequency of this emergent state from the time series, as reported in the earlier work [116]. The dependence of this frequency on the parameters ϵ and τ is shown in the colour coded plot in Fig. 3.8a. In Fig. 3.8b the emergent frequencies of the oscillators are plotted along with the intrinsic fast and slow frequencies as τ is varied. For this range of τ and ϵ, the emergent frequencies are less than the average of intrinsic fast and slow frequencies indicating frequency suppression.

3.2.4 Crossover behavior in dynamics for large m

In the range of large m which is marked as region 3 in the Fig. 3.1, we observe that the network regains the dynamics from the amplitude death state but in general follows a slower time scale.

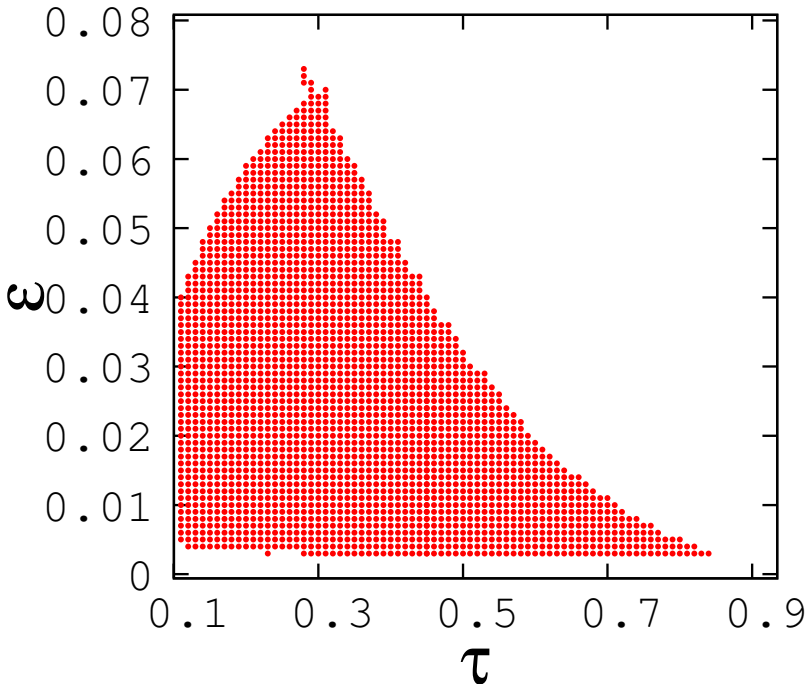

Figure 3.6: Region of amplitude death in (τ, ϵ) plane for $m = 50$ and N=100.

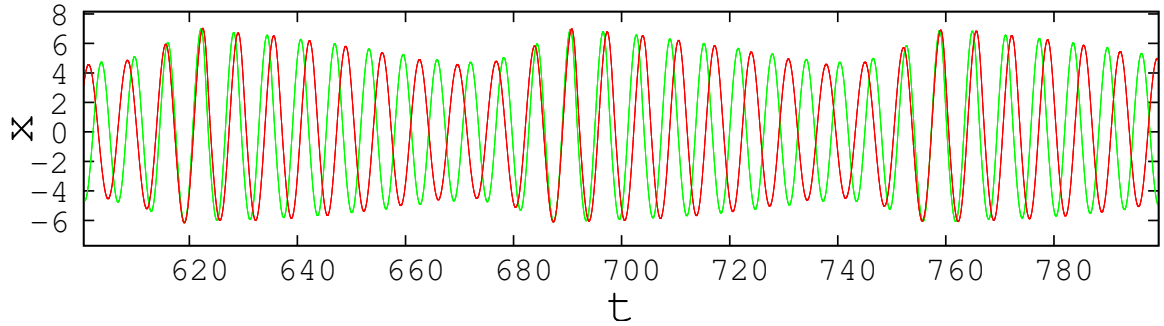

Figure 3.7: Time series of x variables are plotted for 3 slow and 3 fast systems out of 100 systems in the network. This shows two frequency states of slow(red) and fast(green) systems synchronized within the clusters for $m = 50$, $\tau = 0.9$ and $\epsilon = 0.001$.

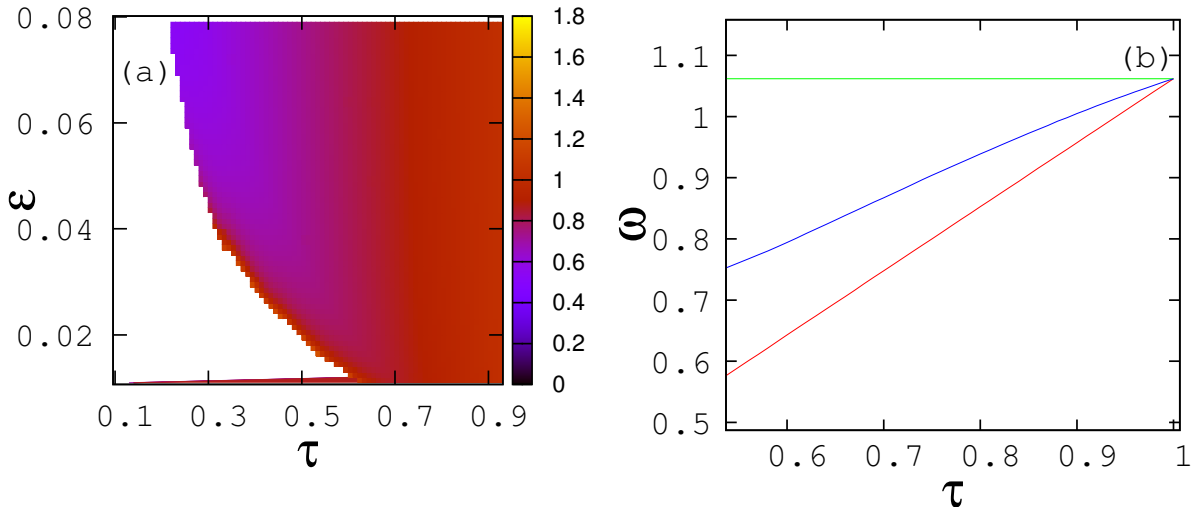

Figure 3.8: a) Variation of the emergent frequency in (τ, ϵ) plane for $m = 50$ in the frequency synchronized state. The color code is as per the value of the frequency of the emergent state. b) Variation of intrinsic frequency of fast systems (green) and that of slow systems(red) compared with the emergent frequency (blue) as τ is varied for $\epsilon = 0.03$ and $m = 50$.

When the time scale mismatch is not large or for large τ, the systems show synchronized clusters being frequency synchronized as described before. But in this case the cluster of slow systems has larger amplitude than that of fast systems. This is thus a clear indication of a crossover behavior in the collective dynamics of the network as m varies. This phenomenon is studied in two ways, by considering the emergent frequency of the frequency synchronized states and the average amplitude of the synchronized clusters.

We observe that the emergent frequency in the frequency synchronized state decreases with the increase of m, which makes all the systems evolve in a slower time scale. This is shown in Fig. 3.9a for a particular value of τ and ϵ. Moreover the frequency becomes less than the average of intrinsic fast and slow frequencies at a particular value of m, say m_1. This value of m_1, which gives the critical value where frequency suppression sets in, depends on the parameters τ and ϵ.

We also observe another crossover behavior in the amplitudes of oscillations of slow and fast systems when m is increased. To study this we plot the average amplitudes of the fast cluster and slow cluster separately in Fig 3.9 for each m for a particular value of τ and ϵ. The crossover from a state where the amplitudes of systems in the fast cluster are larger, to one where that of slow cluster are larger, happens at a value of m say m_2, which again is a crossover in dynamics. We find both these crossover points vary with the parameters τ and ϵ, as is clear from the plot of m_1 and m_2 values for $\epsilon = 0.03$, with different τ values (Fig. 3.10).

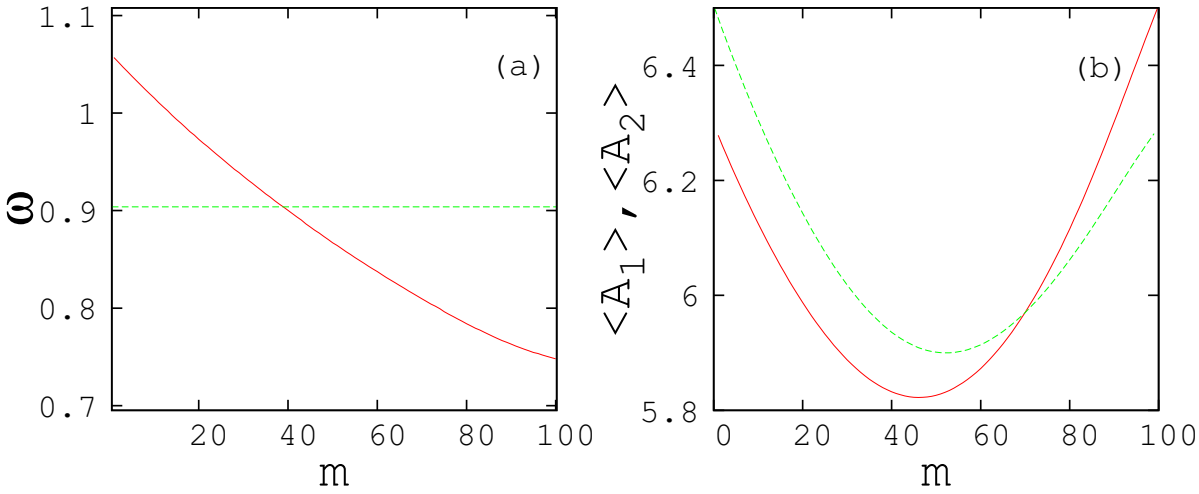

Figure 3.9: a)Variation of emergent frequency with m for $\epsilon = 0.03$ and $\tau = 0.7$ (shown in red). Green line shows the average of intrinsic fast and slow frequencies. Here frequency suppression happens for m greater than $m_1 = 38$ at which red and green lines intersect. b) Average amplitude of slow (red) and fast (green) oscillators with m, showing crossover behavior at $m_2 = 70$ for $\epsilon = 0.03$ and $\tau = 0.7$.

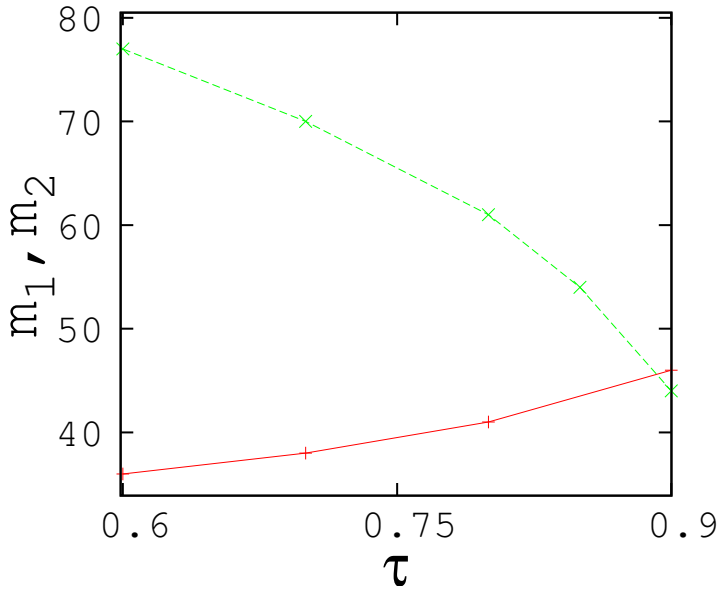

Figure 3.10: Variation of crossover thresholds with τ for $\epsilon = 0.03$. Red line denotes the critical number of slow systems (m_1) at which frequency suppression starts and green line denotes the same (m_2) for crossover in amplitudes.

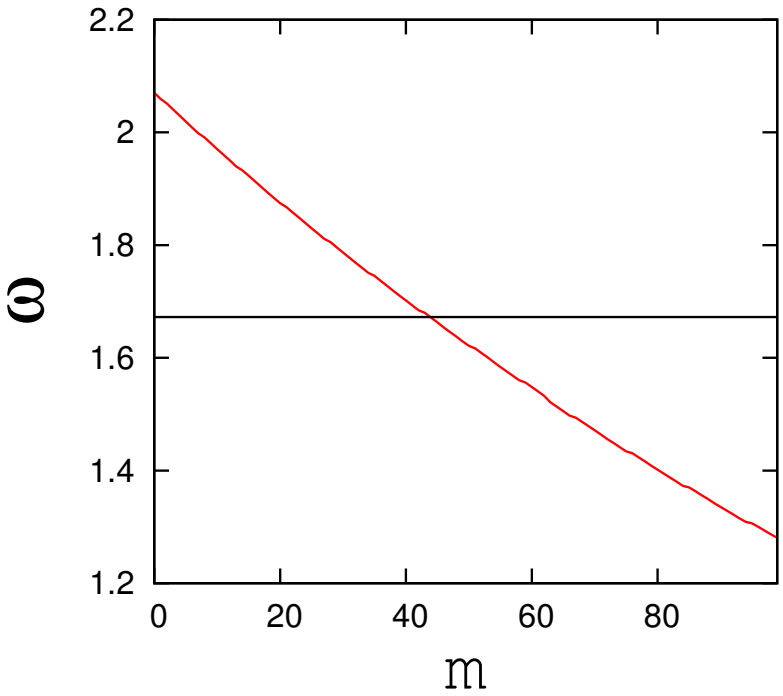

Figure 3.11: Frequency vs m (in red) is plotted with mean frequency (in black) to show crossover for Landau-Stuart oscillators with m for $\tau = 0.6$, $\epsilon = 0.15$ and N=100. Crossover happens at $m_1 = 43$ where the red line crosses the black line

3.2.5 Network of Landau-Stuart oscillators

We continue the study on the interaction of slow and fast systems on the fully connected network for another periodic limit cycle oscillator, viz. Landau-Stuart oscillator. We consider the intrinsic dynamics of each node of the network with N systems as given in the eqn(3.3) where m of them are slow.

$$\begin{aligned} \dot{x}_i &= \tau_i((a - {x_i}^2 - {y_i}^2)x - \omega y_i) + \tau_i \epsilon \sum_{j=1}^{N} A_{ij}(x_j - x_i) \\ \dot{y}_i &= \tau_i((a - {x_i}^2 - {y_i}^2)y + \omega x_i) \end{aligned} \tag{3.3}$$

We observe qualitatively similar results as in the case of periodic Rössler systems. Thus there exists a range of intermediate values of m which leads to suppression of dynamics of the whole network. For lower and higher ranges of m, we find clusters of slow and fast systems showing frequency synchronization between them. We also observe crossover for large m in terms of amplitudes and frequencies similar to Rössler systems. Here in Fig.3.11 crossover for frequency suppression is shown with m, for $\tau = 0.6$ and $\epsilon = 0.15$. The crossover happens at $m_1 = 43$. For the moderate range of m, we isolate the region of AD in (τ, ϵ) plane which is shown in Fig. 3.12 for $m = 50$ and N=100. Outside this region of amplitude death, we find clusters of slow and fast oscillators as discussed before.

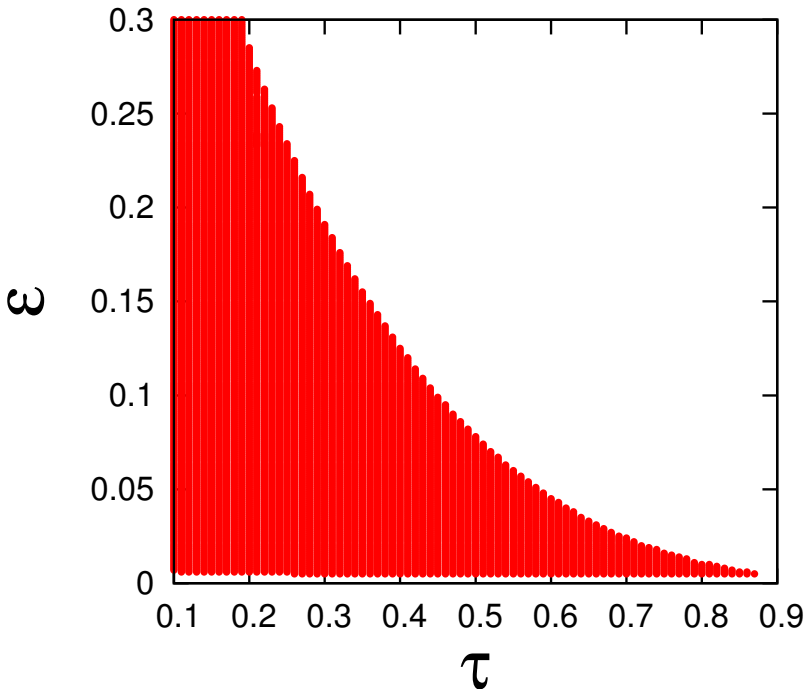

Figure 3.12: Region of amplitude death for Landau-Stuart oscillators in (τ, ϵ) plane for $m = 50$ and N=100.

3.3 Fully connected network of chaotic systems with differing time scales

In this section we report the results of our study on emergent dynamics of chaotic systems on fully connected network with each node having chaotic nonlinear dynamical system with differing time scales. We present the results for standard chaotic Rössler systems and Lorenz systems.

3.3.1 Network of chaotic Rössler systems

Each node of the network follows the dynamics of Rössler system using eqn(3.2) with parameters a=0.2, b=0.2 and c=5.7 which gives the intrinsic dynamics as chaotic. Here out of N nodes, m are slow and evolve with a time scale mismatch of τ. In our calculations we take N as 100 and find AD region for moderate m in (τ, ϵ) plane. This island of AD is shown in Fig. 3.13 for 50 slow systems out of 100 nodes. The transitions to amplitude death is through reverse period doubling bifurcations as τ is decreased from 1 for a fixed ϵ. (Fig. 3.14)

Throughout the bifurcation region, the systems show clusters of slow and fast systems for periodic as well as chaotic oscillations. For low and high ranges of m, the systems settle into frequency synchronized periodic clusters of slow and fast systems for large time scale mismatch and strong coupling. (Fig. 3.15)

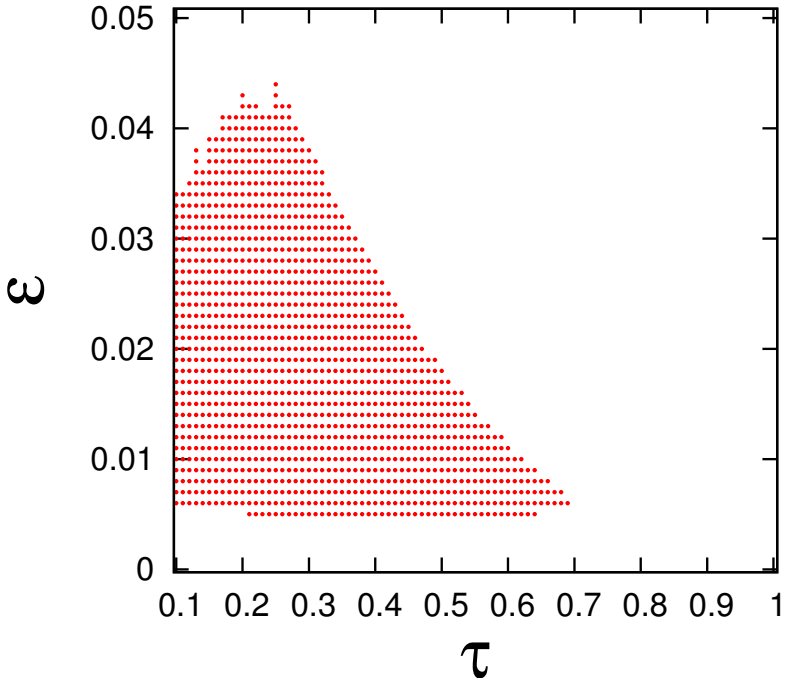

Figure 3.13: Region of amplitude death for chaotic Rössler system in (τ, ϵ) plane for $m = 50$ and N=100.

3.3.2 Network of chaotic Lorenz systems

We analyze the behavior of slow and fast Lorenz systems when they are interacting with each other on a fully connected network. For this the AD region in (τ, ϵ) plane for m value in the range $\approx (10 - 90)$ is shown in the Fig. 3.16. The transition to AD is very sharp where the systems go to AD with a very small change in τ.

The dynamics outside the region of AD indicates separate clusters of slow and fast systems with chaotic oscillations.

For low and high ranges of m, we see that even with increasing mismatch in time scale, systems do not go to AD state. They remain clustered in the chaotic state, with increasing phase shift and amplitude difference between them as τ is decreased. (Fig. 3.17, 3.18)

3.4 Suppression of dynamics in minimal networks with differing time scales

In this section, we discuss in detail the onset of amplitude death and transitions due to difference in time scales on minimal configurations of network. For this we consider 3 and 4 systems connected to make all the possible configurations. These configurations are important as they represent the basic interaction patterns that can recur and thus make up the full networks of larger sizes [117–119]. Hence, they serve as possible motifs in such large networks and are

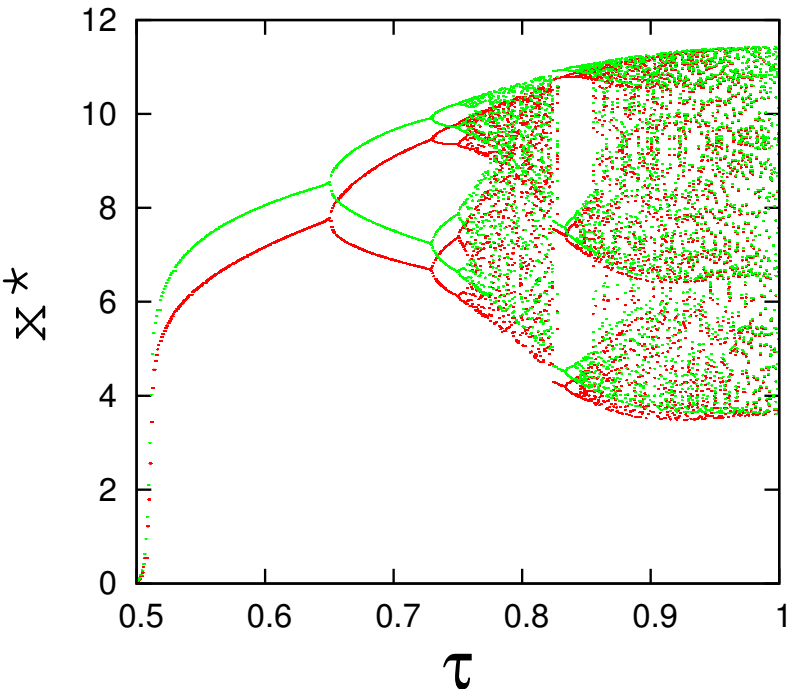

Figure 3.14: Reverse period doubling bifurcation for chaotic Rössler system with τ for $\epsilon = 0.02$, $m = 50$ and N=100. Red(slow cluster), green(fast cluster)

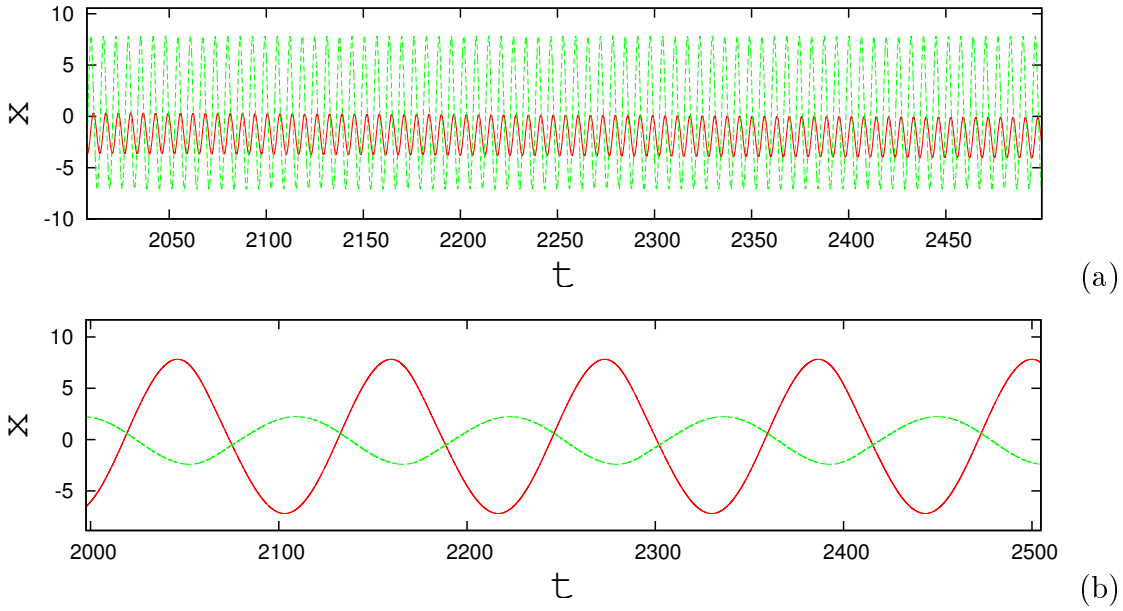

Figure 3.15: Time series showing periodic frequency synchronized states for high time scale mismatch and strong coupling for both low and high m for fully connected network of chaotic Rössler system a)$m = 5$, $\tau = 0.055$, $\epsilon = 0.03$ b)$m = 95$, $\tau = 0.055$, $\epsilon = 0.012$. N=100. red (slow cluster), green (fast cluster)

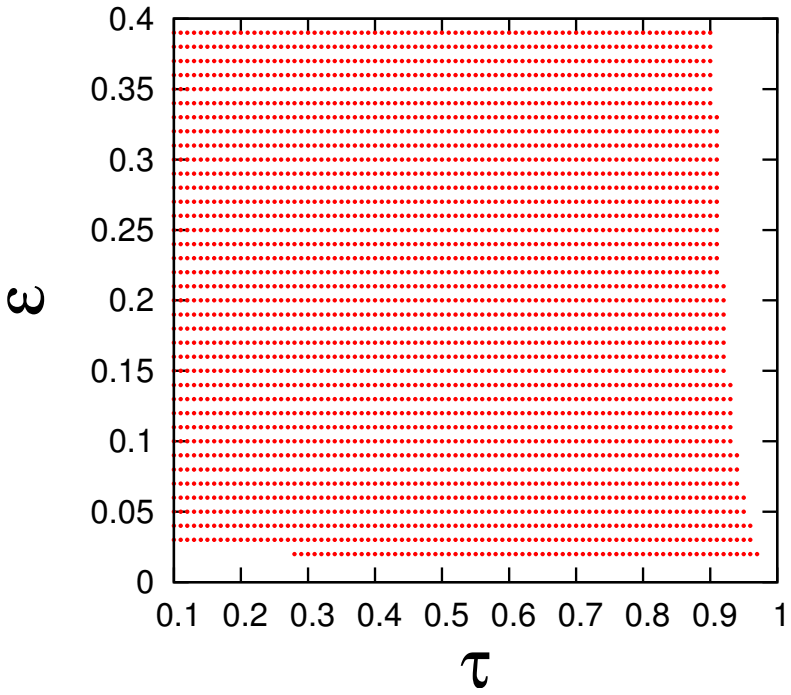

Figure 3.16: Region of amplitude death for chaotic Lorenz system in (τ, ϵ) plane for $m = 50$ and N=100.

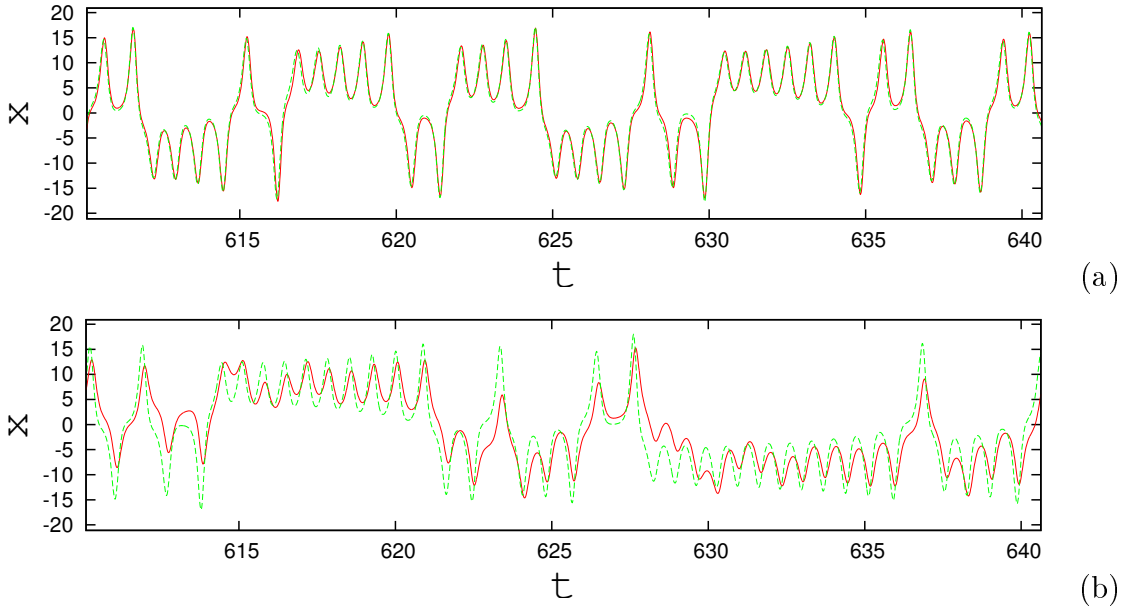

Figure 3.17: Time series showing slow(red) and fast(green) clusters of Lorenz systems for low $m = 5$, for a)$\tau = 0.9$ b)$\tau = 0.3$ for $\epsilon = 0.3$. Here x-variable of three typical systems are plotted for each cluster.

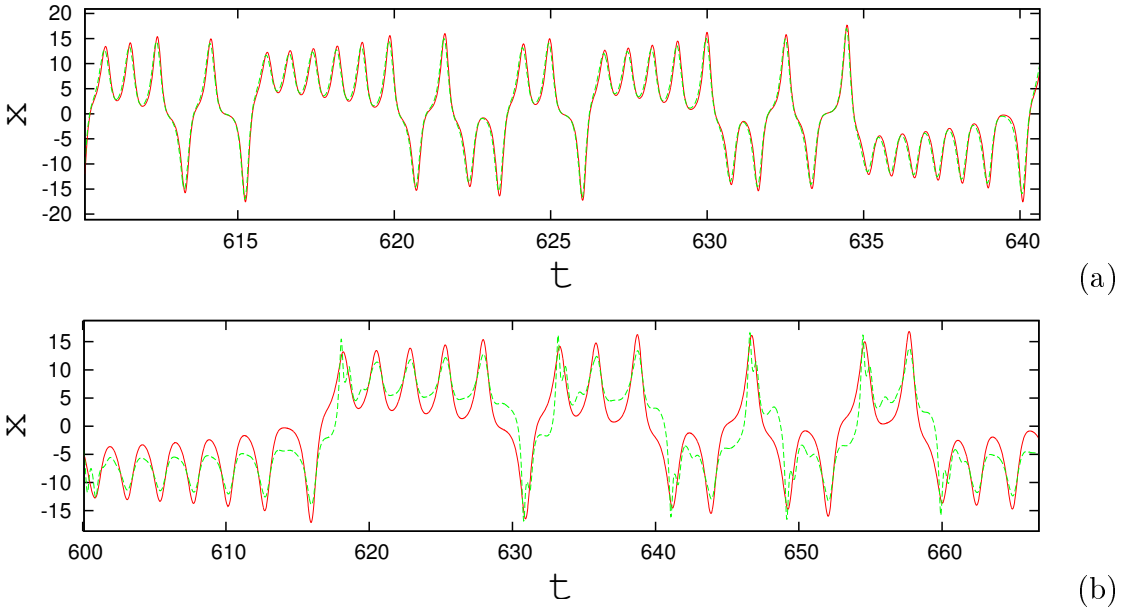

Figure 3.18: Time series showing slow(red) and fast(green) clusters of Lorenz systems for high $m = 95$, for a)$\tau = 0.9$ b)$\tau = 0.3$ for $\epsilon = 0.3$. Here x-variable of three typical systems are plotted for each cluster.

important as repeating sub-graphs of any network. Moreover, in the present study, they are relevant as it is feasible to understand their dynamical states and transitions in them using analytical study. We consider in Fig. 3.19, all possible configurations of the minimal networks for N=3 and N=4 two different time scales, marked as S (slow) and F (fast). In addition to fully connected motifs, we also include in our study all other configurations like open, bipartite etc. which will be instructive when we consider complex networks later. Thus for $N = 3$, we get a total of six unique possible configurations with m as 1 and 2. In the case of 4 systems, we consider 9 configurations in total, by choosing specific topologies of ring, bipartite and fully connected structures and with m as 1, 2 and 3 for each of them.

3.4.1 Analytical calculations

The state of AD corresponds to the occurrence of a stable common fixed point for the whole system. Thus this state can be analytically studied and the corresponding parameters derived from the stability analysis of the fixed point of the system (x^*, y^*, z^*). For this we calculate the eigenvalues of the Jacobian of each configuration shown in Fig. 3.19, around the fixed point (x^*, y^*, z^*). The values of τ and ϵ for which all eigenvalues have negative real parts correspond to the stable fixed point or region of AD.

The generic form of Jacobian of any of the motifs of slow and fast systems can be written as

$$\mathbf{J} = (\tau.\mathbf{I})\mathbf{xF} + (\tau.\mathbf{A})\mathbf{xH} \tag{3.4}$$

where τ is an NxN matrix in which τ_{ij} corresponds to τ_i of eqn(3.1) for all j. $\mathbf{I}$ is NxN identity matrix. Dot product (.) is defined here by the element wise product of two matrices, and cross

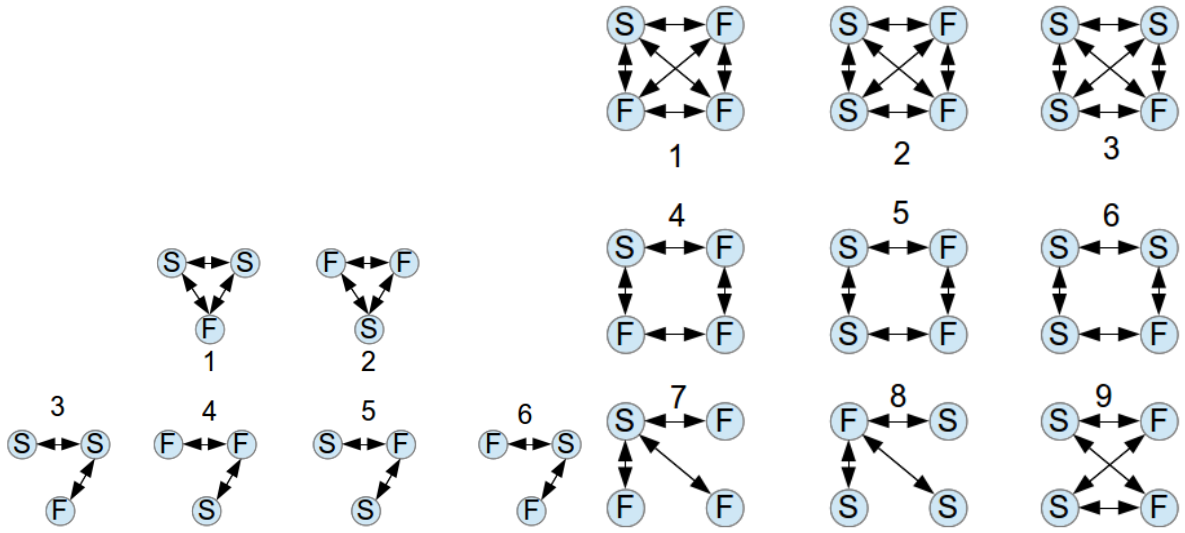

Figure 3.19: Configurations of minimal networks with 3 systems and 4 systems having different possible m.

product (**x**) is defined as each element of the former matrix being multiplied by the later matrix as a block. **A** is the adjacency matrix. **F** is system specific and is an nxn matrix, where n is the dimension of a single system on each node. In the case of Rössler systems with coupling function as given in eqn(3.2), we have

$$\mathbf{F} = \begin{pmatrix} -k\epsilon & -1 & -1 \\ 1 & a & 0 \\ z* & 0 & (x*-c) \end{pmatrix}, \mathbf{H} = \begin{pmatrix} \epsilon & 0 & 0 \\ 0 & 0 & 0 \\ 0 & 0 & 0 \end{pmatrix}, \tag{3.5}$$

$$\mathbf{0} = \begin{pmatrix} 0 & 0 & 0 \\ 0 & 0 & 0 \\ 0 & 0 & 0 \end{pmatrix} \tag{3.6}$$

Here, $(x^*, y^*, z^*) = (\frac{c-\sqrt{c^2-4ab}}{2}, \frac{-c+\sqrt{c^2-4ab}}{2a}, \frac{c-\sqrt{c^2-4ab}}{2a})$.

k is the number of non zero elements in the i^{th} row of **A**. For example in the case of N=4, the Jacobian of the configuration 9 in Fig. 3.19 can be written as

$$J = \begin{pmatrix} \tau\mathbf{F} & \mathbf{0} & \tau\mathbf{H} & \tau\mathbf{H} \\ \mathbf{0} & \tau\mathbf{F} & \tau\mathbf{H} & \tau\mathbf{H} \\ \mathbf{H} & \mathbf{H} & \mathbf{F} & \mathbf{0} \\ \mathbf{H} & \mathbf{H} & \mathbf{0} & \mathbf{F} \end{pmatrix} \tag{3.7}$$

Here $k = 2$ in the matrix **F** as **A** has 2 entries of 1 in each row.

We now calculate the eigenvalues of the Jacobian for each configuration for a range of values of τ and ϵ in the parameter plane and identify the transition to AD as the point where the real part of at least one eigenvalue of J goes from negative to positive. This analysis is repeated for all the configurations of $N = 3$ and $N = 4$ as shown in Fig. 3.19. The transition curves thus

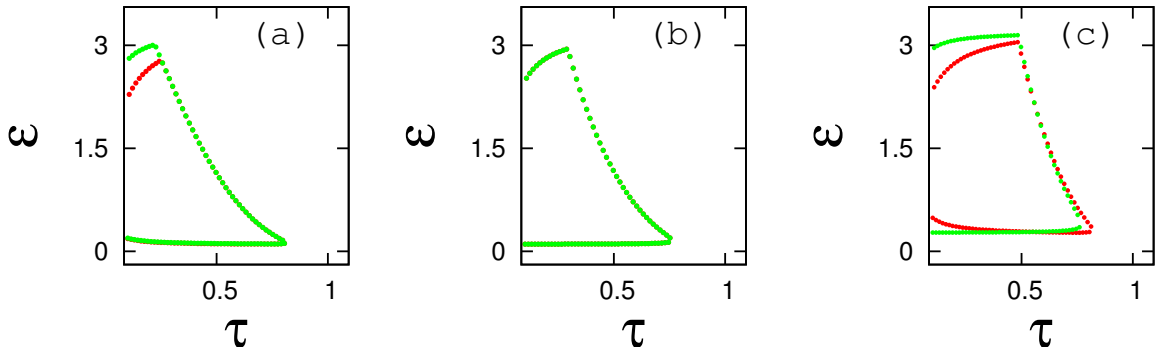

Figure 3.20: Transition curves for AD with 3 systems for configurations a) 1(red) and 5(green) b) 2(red) and 6(green) showing fully connected and bipartite cases with identical transitions, c) 3(red) and 4(green) with different transition curves.

obtained in the (τ, ϵ) plane are shown in the Fig. 3.20 and Fig. 3.21 for periodic Rössler systems. In all these figures top left part of the transition curve gives the transition to instability, while the other two curves represent the transitions from amplitude death to oscillations.

When we compare these transition curves among different configurations for a fixed N, we observe that in general the curves depend mainly on the number of slow systems m. Thus for the same m, the configurations of all-to-all and bipartite structures have identical transition curves.

For N=3 and $m = 1$, configurations 1 and 5 have identical transitions (Fig. 3.20a). In this case, out of the nine eigenvalues of the Jacobian, six are common. Among these six common eigenvalues the real part of one of the common complex conjugate pair crosses zero at the transition, for the same set of parameter values indicating a Hopf bifurcation. Similar results are obtained for configurations 2 and 6 with $m = 2$(Fig. 3.20b). However for the configurations 3 and 4, with different m which are neither all-to-all nor bipartite, transition curves are different (Fig. 3.20c). Similarly for the case of motifs with four systems we get such pairs of all-to-all and bipartite structures with each value of m chosen. Thus, configurations 1 and 7 ($m = 1$), 2 and 9 ($m = 2$) and 3 and 8 ($m = 3$) have the same transition curves as shown in Fig. 3.21a, b and c respectively. In this context, each pair has a common pair of eigenvalues that cross zero at the transition just like the case of 3 systems. However, we find configurations 4, 5 and 6, which are ring topologies with different m, show different transition curves (Fig. 3.21d).

In the region outside of amplitude death, we see clusters of slow and fast systems for fully connected and bipartite configurations in both cases of N=3 and 4. The clusters are always frequency synchronized with each other but evolve with a phase shift in each configuration. As we see that the transition curves and dynamics outside AD is similar for the pairs discussed. However we note that the dynamics of the all-to-all configuration is phase shifted from that of the bipartite one, even when they start from the same initial conditions. In the network of three systems the configurations 3 and 4 exhibit frequency synchronized states with no clusters. In the network of four systems with ring topology, in configuration 4, the two fast systems directly connected to the slow one, form a cluster while the other fast system evolves separately with a phase shift being frequency synchronized. We see similar behavior for configuration 6 where the two slow systems directly connected to the fast form a cluster. Also in configuration 5, we see

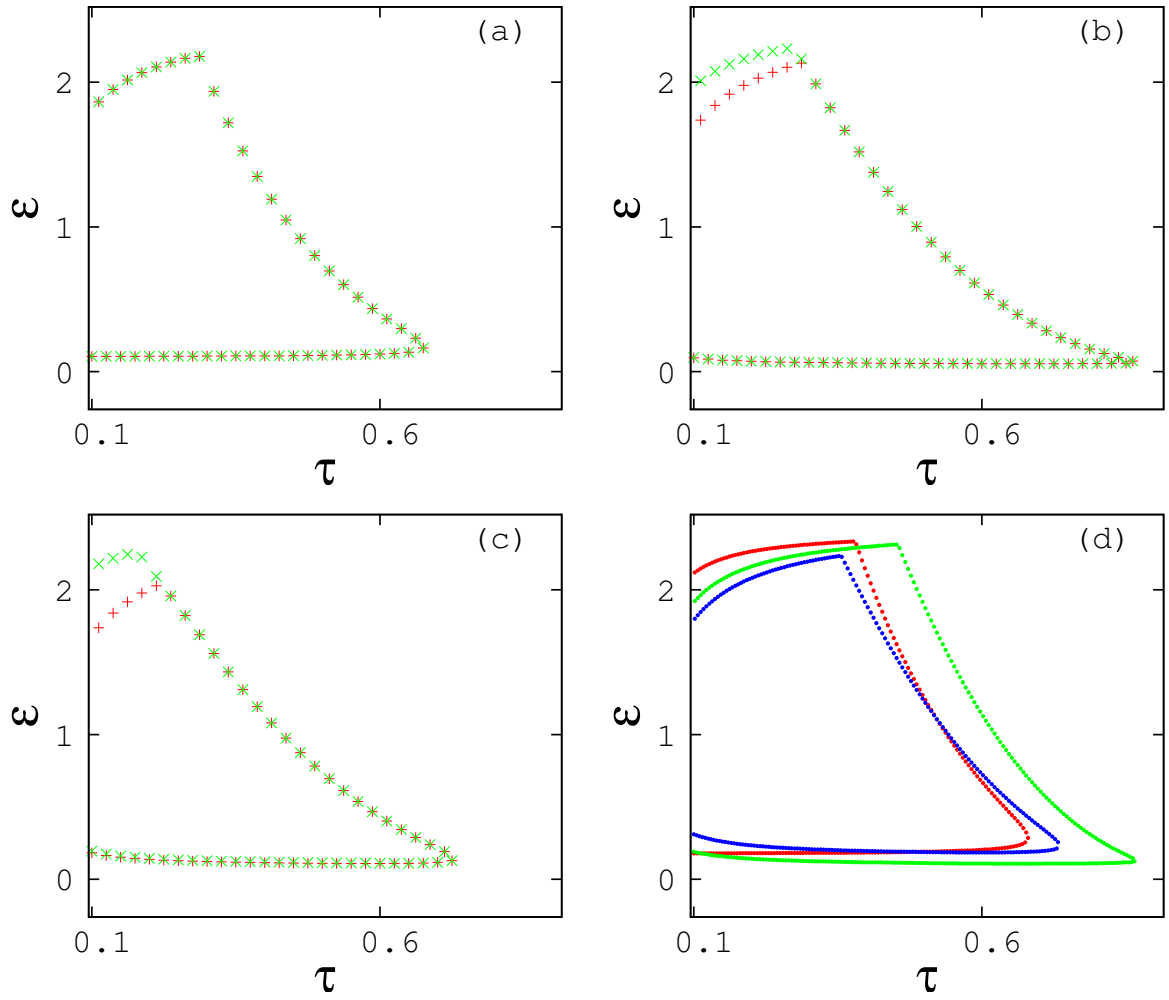

Figure 3.21: Transition curves for AD with 4 systems for configurations a) 1(red) and 7(green) b) 2(red) and 9(green) c) 3(red) and 8(green) showing fully connected and bipartite cases with identical transitions, d) 4(red), 5(green) and 6(blue) with different transition curves.

clustering states of slow and fast systems.

3.5 Summary

In this chapter we present the results of our study on possible emergent dynamics when nonlinear dynamical systems with different time scales are interacting with each other through a fully connected network. Our study covers the periodic and chaotic intrinsic dynamics taking three standard dynamical systems. In all cases, we observe amplitude death as the most common emergent phenomena. We characterize the parameter regime for such emergence in the whole network in terms of number of slow systems, time scale mismatch and coupling strength between systems. As another important emergent dynamics we observe is formation of synchronized clusters of slow and fast systems in such networks. Our results also show interesting crossover behavior in dynamics observed in the context of amplitude and frequency, as the number of slow systems m is increased. The critical values of m at crossover and their dependence on other parameters are studied. Towards the end we present analytical study on the behaviors of connected slow and fast systems on minimal networks of three and four systems, which form motifs or sub groups of the large networks. In these systems, the transition curves of AD computed from the eigenvalues of the Jacobian indicate the role of symmetry in connections in deciding the transitions. In the next chapter, we will consider dynamics of complex networks with differing time scales so that the interplay of time scales and topology on the emergent dynamics can be understood.

Chapter 4

Dynamics of slow and fast systems on complex networks

In this chapter we present the study on how complexity in connections or interactions among systems with multiple time scales affect their collective behavior. We include in our study two standard network topologies, which are very prevalent in real world systems, viz random and scale free. We report the variations in collective behaviour and dynamical transitions as parameters of network topology are changed. The study of dynamics on random network with systems of differing time scales are reported in this chapter and that on scale free networks in the next chapter.

4.1 Random network of slow and fast periodic systems

We construct a random network of N nodes where each node represents a dynamical system. In that network out of N identical systems m evolve on a slower time scale. The topological connectivity of the network is defined by a parameter p, where p is the probability with which any two nodes of the network are connected such that $A_{ij} = 1$. First we discuss the case where each node of the network has a dynamics of periodic system on a random network of N=100 and analyse how the slowness of m of the systems can affect the dynamics of the whole network. We consider two standard nonlinear systems, periodic Rössler and Landau Stuart oscillator. For periodic Rössler, the dynamical equations of the systems at each node are given by eqn.(4.1) with the parameters chosen as a=0.1, b=0.1 and c=4. The subset of oscillators of smaller timescale is defined as S. The equations that govern the dynamics are then

$$\begin{aligned} \dot{x}_i &= \tau_i(-y_i - z_i) + \tau_i\epsilon\sum_{j=1}^{N} A_{ij}(x_j - x_i) \\ \dot{y}_i &= \tau_i(x_i + ay_i) \\ \dot{z}_i &= \tau_i(b + z_i(x_i - c)) \end{aligned} \tag{4.1}$$

Where i=1, 2, ... N.

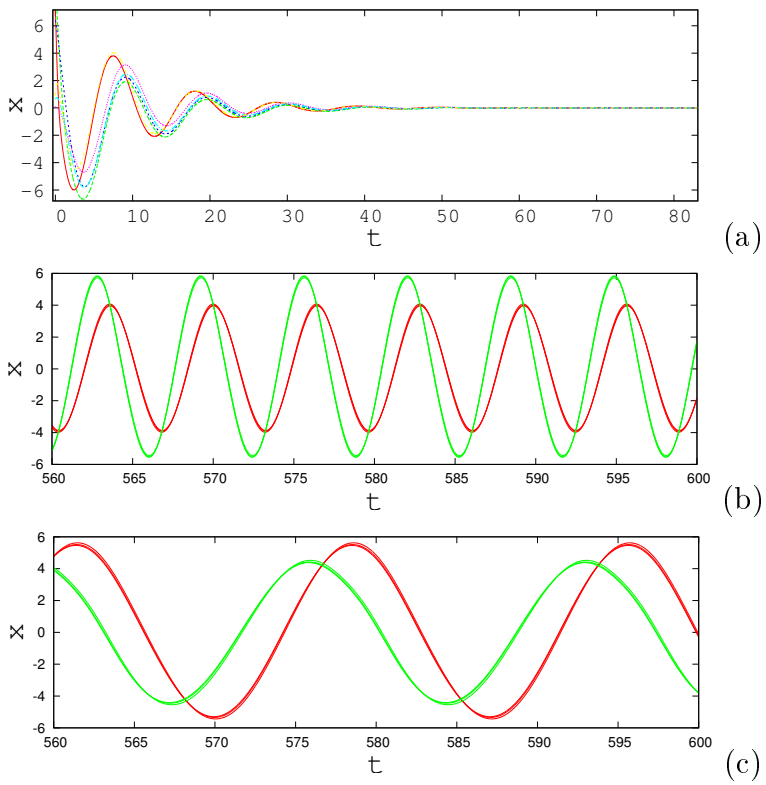

Figure 4.1: Time series of x variables in a random network of slow and fast systems showing a)amplitude death state for $m = 50$, b) oscillatory frequency synchronized state for $m = 5$ and c) oscillatory frequency synchronized state for $m = 95$ for τ=0.35, $\epsilon = 0.05$. For (b) and (c) red curves represent slow and green curves represent fast systems.

4.1.1 Region of amplitude death, onset and recovery

In this section we study in detail the onset of amplitude death in the random network of slow and fast systems. This onset of AD will also depend on the probability of connection of the network (p), in addition to the time scale mismatch (τ), number of slow systems (m), and coupling strength of connection (ϵ). The different dynamical states possible for a range of sufficient time scale mismatch, strong coupling and moderate probability of connection, but for three different values of m (50,5 and 95 respectively) are clear from Fig. 4.1. Thus while amplitude death occurs for a moderate number of slow systems, oscillatory states of collective behaviour are possible for very small and very large number of slow systems. As we can see in the oscillatory states the time period of oscillations vary according to the number of slow systems.

To identify the region for occurrence of amplitude death in terms of number of slow systems present in the network, we fix appropriate values for the probability of connection, time scale mismatch and coupling strength and calculate the average difference between global maxima to global minima (A_{diff}) over time for each oscillator. This is averaged over all the systems and plotted for different values of m, the number of slow systems. This brings out the intermediate region where time scale mismatch can induce AD in the whole network. We plot this region for

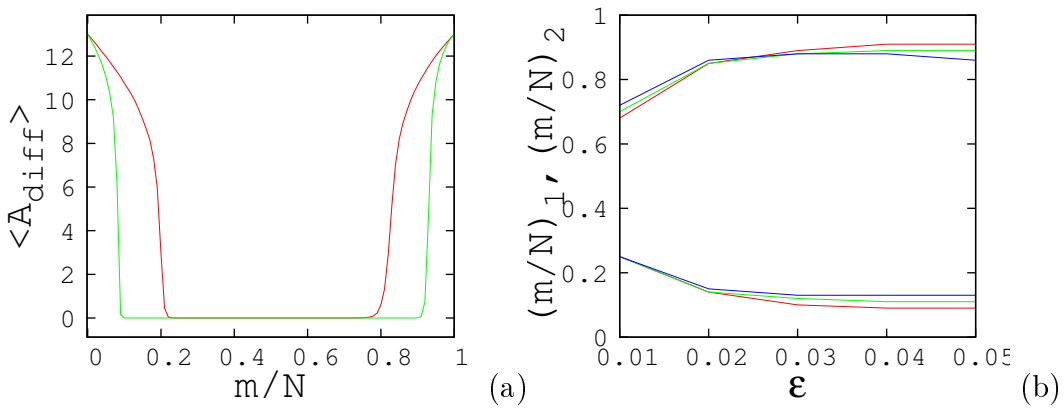

Figure 4.2: Variation of average A_{diff} with m/N ratio. Here τ=0.35 and ϵ=0.01 for red curve and τ=0.35 and ϵ=0.05 for green curve. N=100, p=0.5. b)critical values for onset of AD at $(m/N)_1$ and recovering from AD at $(m/N)_2$ with ϵ for τ=0.3 (red), 0.35 (green) and 0.4 (blue). Here p=0.5.

two sets of τ and ϵ. (Fig. 4.2a) Thus there exists a minimum number of slow systems required for onset of AD, as $(m/N)_1$, and maximum number required for recovery from AD as $(m/N)_2$, both depend on τ, p and ϵ. The dependence of these two critical m values on ϵ, for different τ values is shown in Fig. 4.2b

For the region of m/N in Fig. 4.2 where AD occurs, we isolate the region of amplitude death in τ, ϵ plane by calculating the difference between global maxima to the global minima of x variable of the time series. This is done for a chosen probability of connections p. (Fig. 4.3a)

In this parameter plane for moderate m, we study the possible dynamical behaviour outside the region of AD. We observe a region of strong coupling strength and low time scale mismatch where all the systems show a frequency synchronized state, with the synchronized or common frequency in between the slow and fast intrinsic frequency. The common frequency changes with the time scale, indicating frequency suppression. The random network does not show clearly separated synchronized clusters as in the case of fully connected network. In this case the oscillations of slow systems are relatively close in phase and so do fast oscillators but the phase difference between slow and fast sets are relatively large. For weak coupling strength and small time scale mismatch the oscillators show two frequency states and as time scale mismatch increases they become periodic with separate time scales. For very high coupling strength all the systems go to a state of instability (Fig. 4.3b).

4.1.2 Crossover in emergent dynamics at large m

For both the regions of low m/N ratio and high m/N ratio there is no amplitude death region in the parameter plane. However in this region we observe frequency synchronized oscillations for all the oscillators for strong coupling strength. These oscillations are separated by clusters of slow and fast systems. However within one cluster complete synchronization is not observed, instead the members of one cluster are separated by very small phase shifts between them. These oscillations are shown in Fig. 4.1 for very small number of slow systems and very large

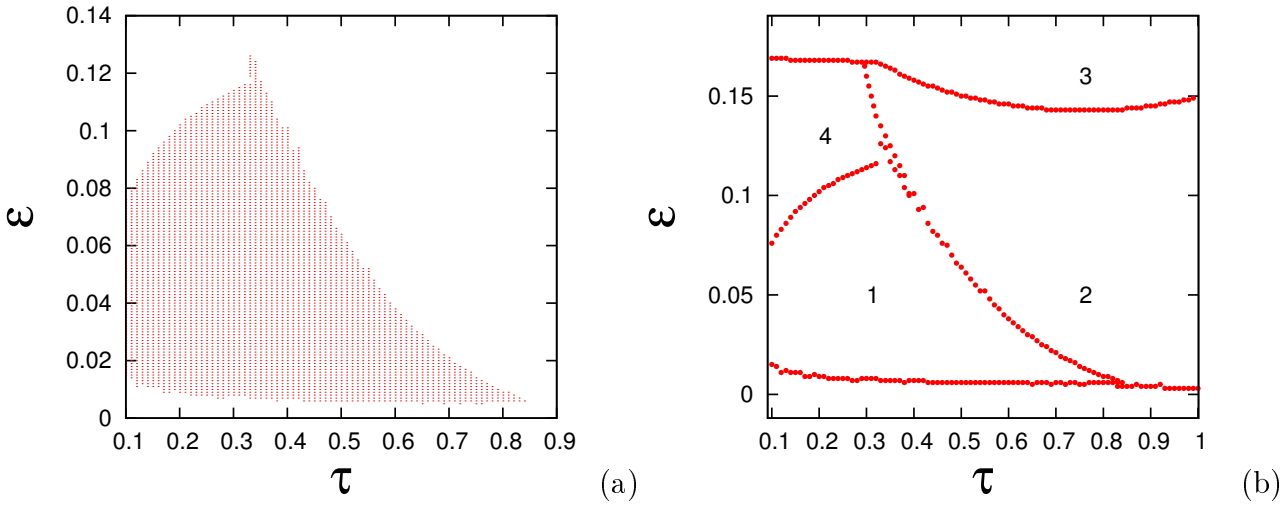

Figure 4.3: a)Region of AD in (τ, ϵ) plane b) Boundaries of different dynamical states in this parameter plane. 1 corresponds to AD, 2 corresponds to frequency synchronization, 3 is unstable state and 4 is a state where systems start diverging from fixed point state before reaching unstable state. Here $m = 50$,p=0.5,N=100

number of slow systems. It is also observed that the synchronized frequency is high for low m and very low for high m. This phenomena can be observed as **frequency crossover**. We take a suitable point from the (τ, ϵ) plane where irrespective of m frequency synchronization happens. We calculate the synchronized frequency for all the oscillators and plot it with m. For each particular τ there exist a mean of intrinsic slow and fast frequencies (shown by black lines in Fig. 4.4). When the synchronized frequency for that τ crosses the mean and decreases with the increase of m, frequency suppression happens. The value of m for which this happens is noted as crossover point for frequency.

While we have frequency synchronization in the oscillatory state, the amplitudes of slow and fast systems vary from each other. We observe that for the lower m amplitudes of slow systems are lower than those of fast systems, while for higher m this behavior gets reversed indicating crossover behavior in amplitude. We calculate the average amplitude of all the slow systems and that of all the fast systems for different number of slow systems. We do this for a suitable value of τ and ϵ where frequency synchronization happens. We note that at a critical value of m the amplitude of slow and fast systems get reversed as m increases. This point is called the crossover point in terms of amplitude. This crossover behavior is shown in Fig. 4.5.

4.1.3 Transition to amplitude death and connectivity of network

In order to understand the transition to amplitude death based on connectivity of the network, we study the collective behavior of all the systems by varying p, for a chosen number of slow systems that lie in the AD region of Fig. 4.2 and values of τ and ϵ that lie in the AD region in the parameter plane (Fig.4.3). As p goes from 0 to 1, the network topology goes from sparsly randomly connected to fully connected. In this scenario for each p we take 100 realizations of the

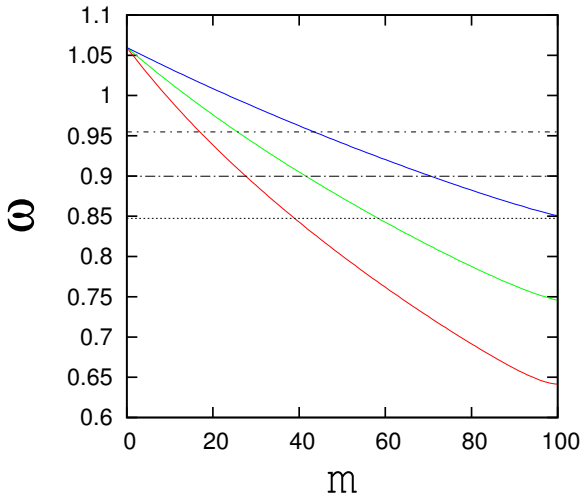

Figure 4.4: Frequency vs m ϵ=0.05 for τ=0.6(red),0.7(green) and 0.8(blue) showing crossover in frequency as the value crosses the mean value of fast and slow frequencies shown by corresponding black lines(increasing order of τ from below to above) . p=0.5.

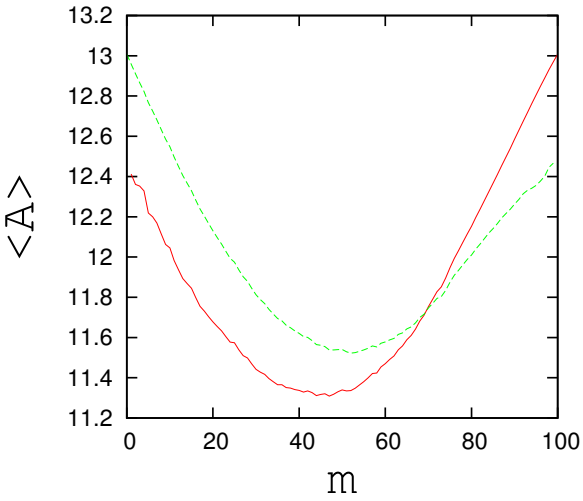

Figure 4.5: Crossover behavior in amplitude showing for large m in random network for slow (red) and fast (green) systems. Here p=0.5, $\tau = 0.7$, $\epsilon = 0.05$

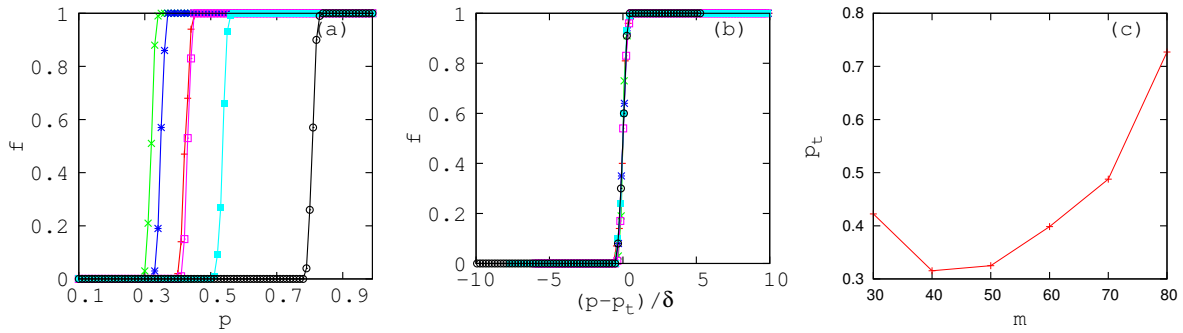

Figure 4.6: a)Fraction of realizations for transition to AD, f, with the probability p of network, b) normalized transition curve for m=30(red), 40(green), 50(blue), 60(magenta), 70(cyan), 80(black) and c) Variation of critical p with m. Here $\tau = 0.35$, $\epsilon = 0.01$

network and check what fraction of them go to an amplitude death state for the whole network. The corresponding transition curves of fraction of realizations are plotted against p, different values of number of slow systems. We observe that as m increases, the transition to AD occurs at a lower value of p, till an optimum value of m where this is lowest. As m is increased further this transition moves to the higher side of p. The threshold value for the transition, where half of the realizations follow global amplitude death, is taken as at $p = p_t$, For random network of periodic Rössler systems this p_t is observed to be minimum when the number of slow systems is 40 . The width of the transition is calculated as δ. We normalize the transition curves by replacing p with $(p - p_t)/\delta$ so that all the curves fall on top of each other revealing a universal behavior. This is shown in the Fig. 4.6.

Random networks of differing system sizes

We also calculate the transition curves for different network sizes, with N=100, 150, 200, 300, 500, 600, keeping m/N ratio fixed at 0.5. We notice the larger the network size the earlier transition takes place in terms of probability of connections. This helps us to calculate the scaling properties of the transitions by fitting the transition curve with the function form $f = (p - p_c)^{\alpha}$. The value of p_c is chosen as the one where the function gives best fit. This then gives the value of the scaling index α for each transition curve. We observe that the index α varies with the network size N and as 1/N approaches 0 or N approaches infinity, the scaling factor reaches a value of 0.68 or within numerical errors, 2/3. (Fig. 4.7)

Here also we calculate the threshold p for which the transition occurs. We plot the variation of p_t with the system size N which suggests that it decreases with increase of N. We also notice that the width of the transition decreases with the increase of system size which suggests sharper transitions for higher N. These variations are shown in Fig. 4.8.

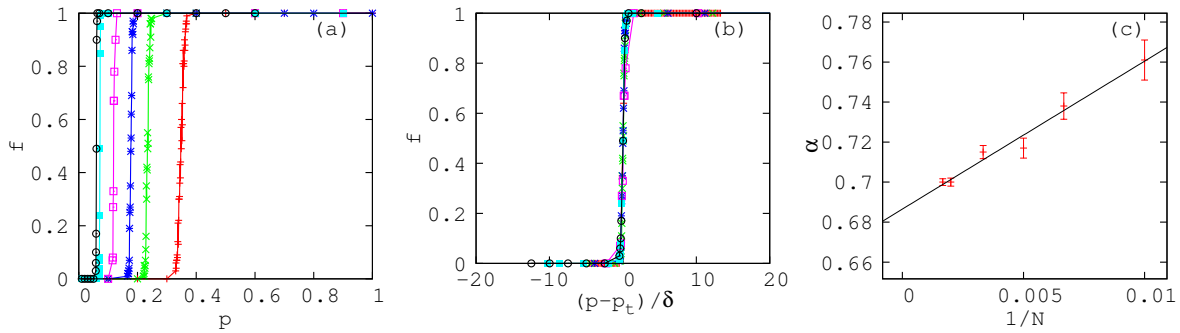

Figure 4.7: Fraction of realizations f for the transition to AD with the probability p for N=100(red), 150(green), 200(blue), 300(pink), 500(sky blue), 600(black), $\tau = 0.35$, $\epsilon = 0.01$, keeping $m/N = 0.5$. b) Normalized transitions with $p - p_t/\delta$ for different N. c) Variation of scaling coefficient with 1/N with errorbar shown in red.

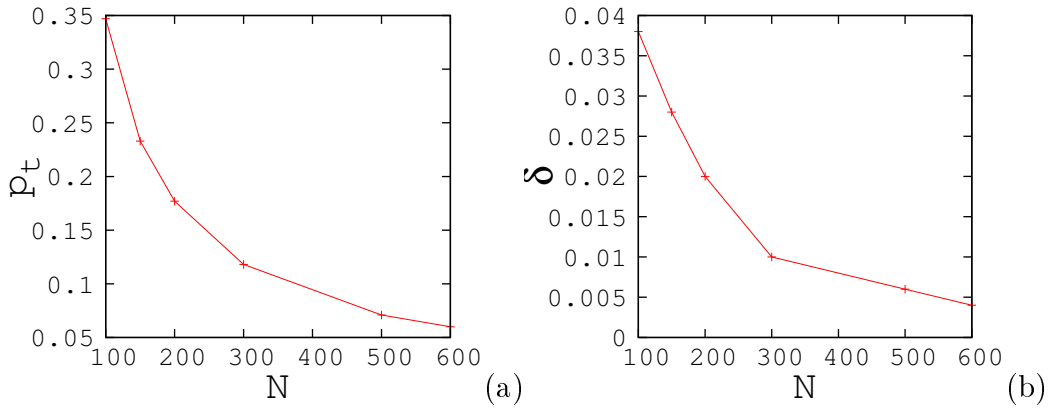

Figure 4.8: a) Threshold value of p (p_t)where f becomes 0.5, plotted with N, $\tau = 0.35$, $\epsilon = 0.01$ b)width of transition δ with N. $\tau = 0.35$, $\epsilon = 0.01$

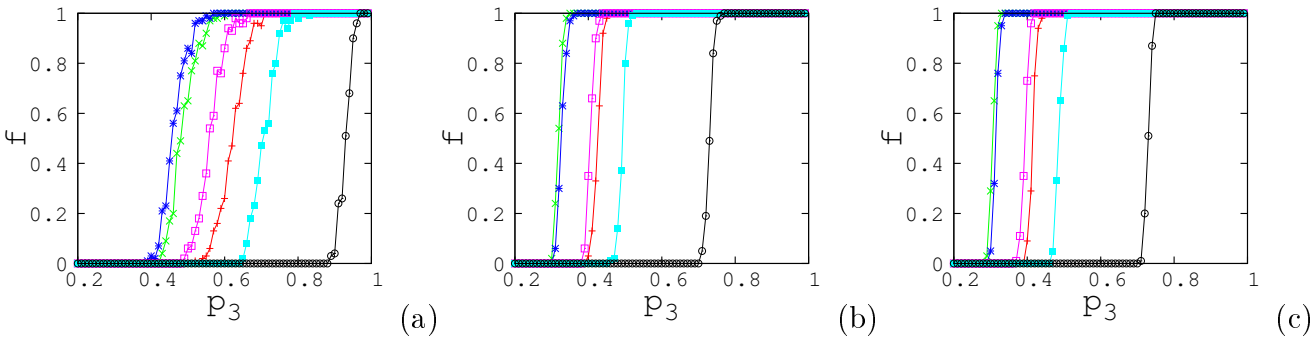

Figure 4.9: Fraction of realizations for transition to AD for random network of heterogeneous probabilities for a)p1=0,p2=0, b)p1=0.3,p2=0.3 c)p1=0.8,p2=0.8, varying p3. $\tau = 0.35$, $\epsilon = 0.01$. m=30(red), 40(green), 50(blue), 60(magenta), 70(cyan), 80(black)

4.1.4 Random network with non uniform probabilities of connections

In the discussion above, the probability of connections for generating the random network is taken as p for slow and fast nodes. We now consider a much more heterogeneous random network generated with three types of probabilities and study the effect of slow and fast dynamics on it. The probability at which a slow system connects to another slow system is taken as p_1, a fast system connects with another fast system is p_2 and a slow systems connects with a fast systems is p_3. We compute the fraction of realizations for obtaining amplitude death in this random network of slow and fast systems by varying p_3 for different sets of values of p_1 and p_2. We observe that the connection between slow systems and fast systems as a bipartite structure, i.e. keeping $p_1 = 0$ and $p_2 = 0$ but non zero p_3 alone can result in an amplitude death state. However, having a non zero value of p_1 and p_2 helps the network to reach amplitude death state at lower values of probability p_3 and the minimum p_3 for this transition becomes smaller with increasing p_1 and p_2 (Fig. 4.9). We also calculate the fraction of realizations for AD when there is no connection between slow systems and the probability of slow to fast connection is varied keeping fast to fast probability fixed. We repeat the same with no connection between fast to fast systems and slow to fast probability is varied keeping slow to slow connection as fixed. This is done for $p_1 = 0.8$ and $p_2 = 0.8$ in the respective cases, where p_3 is varied (Fig. 4.10).

4.1.5 Random network of Landau Stuart systems

We do a similar study for slow and fast Landau Stuart oscillators on random networks. The results are qualitatively similar for amplitude death and oscillatory behaviors. The region of AD is numerically calculated and shown for p=0.5, $m = 50$, N=100 in τ, ϵ. Choosing the τ and ϵ from the region of AD one can show the variation for fraction of realizations of AD while p varies. In this case also the optimum number of slow systems is seen for which the transition curve occurs at minimum probability value.

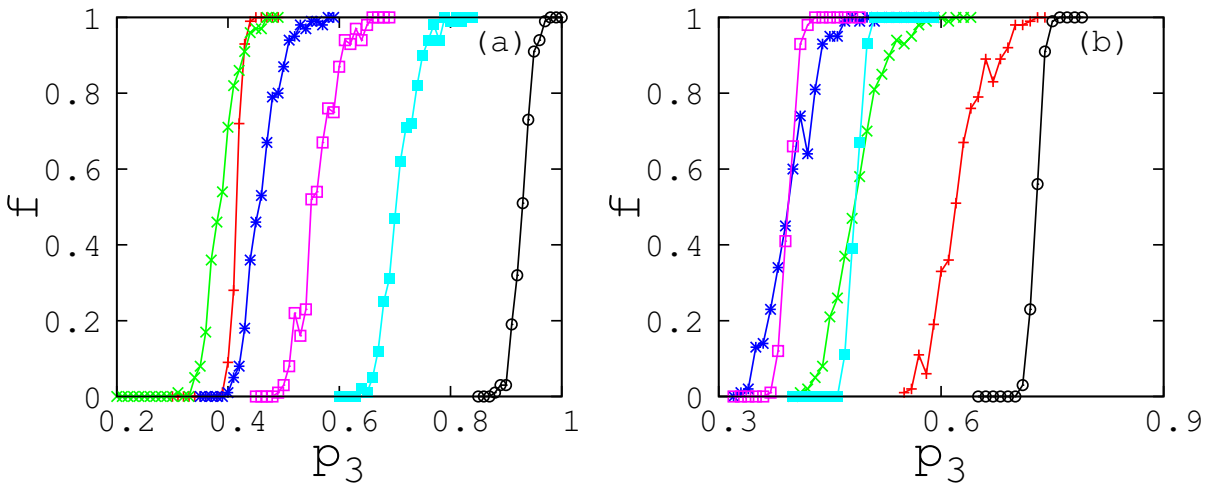

Figure 4.10: Fraction of realizations for transition to AD for random network of heterogeneous probabilities for a)p1=0,p2=0.8, b)p1=0.8,p2=0, varying p_3, $\tau = 0.35$, $\epsilon = 0.01$. m=30(red), 40(green), 50(blue), 60(magenta), 70(cyan), 80(black)

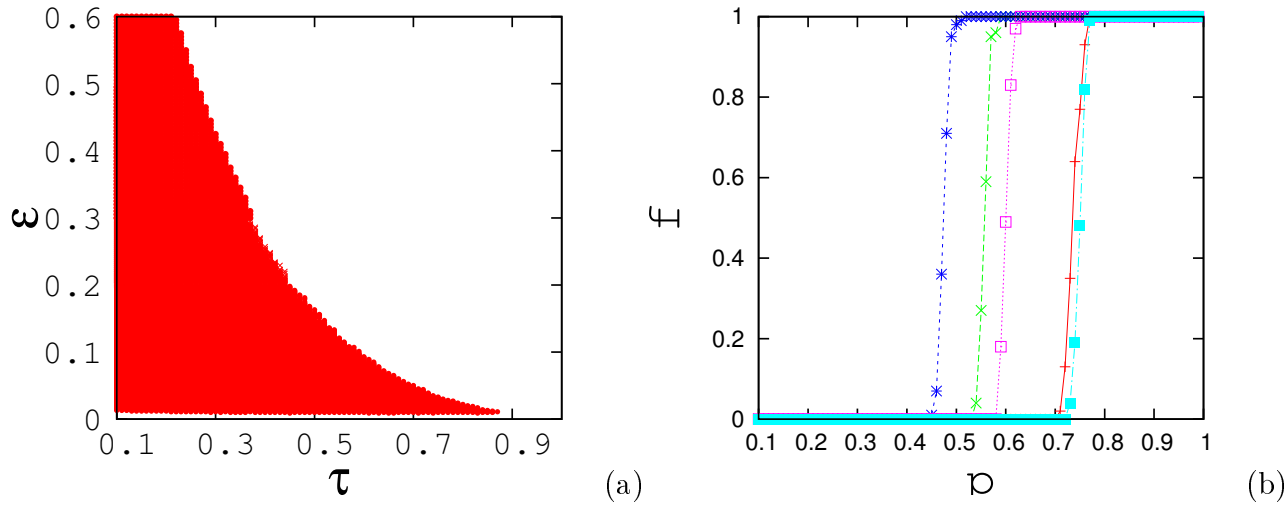

Figure 4.11: (colour online)a)Region showing AD in τ, ϵ plane for Landau-Stuart systems on a random network, $p = 0.5$, $m = 50$, $N = 100$, b) variation of fraction of realizations with p for $\tau = 0.35$, $\epsilon = 0.01$. m=30(red), 40(green), 50(blue), 60(magenta), 70(cyan)

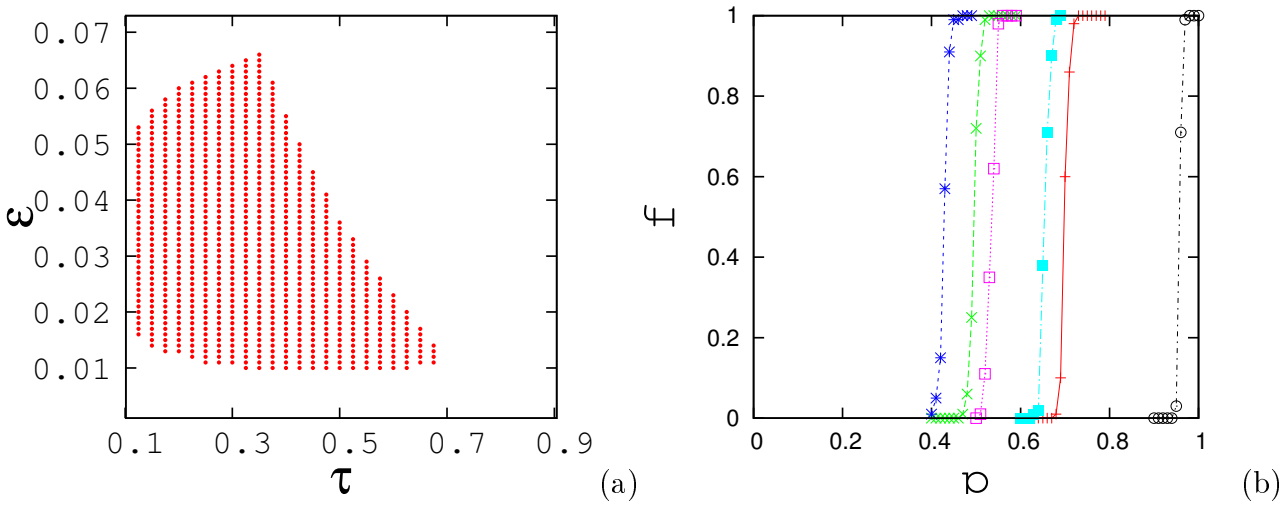

Figure 4.12: a)Region showing AD in (τ, ϵ) plane for chaotic Rössler systems on a random network, p=0.5, $m = 50$, N=100 and b) Fraction of realisations for transition to AD with p in chaotic Rössler systems for m=30(red), 40(green), 50(blue), 60(magenta), 70(cyan), 80(black), $\tau = 0.35$, $\epsilon = 0.012$

4.2 Random network of slow and fast chaotic systems

In this section we consider nodal dynamics that is chaotic for which chaotic systems such as Rössler and Lorenz systems are considered. For Rössler systems the intrinsic equation is used as eqn.(4.1) with the parameter values a=0.2,b=0.2 and c=5.7, where out of N nodes m are slow with the parameter τ. In this case the qualitative results such as AD, frequency synchronization and reverse period doubling bifurcation are re-established. For moderate number of slow systems we find the region of amplitude death in parameter plane (τ, ϵ). To see the transition in terms of probability of connections we take a suitable τ, ϵ from parameter plane of AD and for those parameters, calculate the fraction of realizations for amplitude death as described in the previous sections (Fig. 4.12).

We do similar analysis where each node of random network has the dynamics of Lorenz system with an intrinsic dynamics as eqn(4.2)

$$\begin{aligned} \dot{x}_i &= \tau_i a(y_i - x_i) + \tau_i \epsilon \sum_{j=1}^{N} A_{ij}(x_j - x_i) \\ \dot{y}_i &= \tau_i(x_i(b - z_i) - y_i) \\ \dot{z}_i &= \tau_i(x_i y_i - c z_i) \end{aligned} \tag{4.2}$$

with parameter values a=10,b=28 and c=8/3, where out of N nodes m are slow. In this case also AD is obtained for moderate m and p and for a range of (τ, ϵ). The region for AD in (τ, ϵ) plane is isolated for p=0.5 and $m = 50$ and is shown in Fig. 4.13a. Keeping a (τ, ϵ) values for AD to occur, we can similarly show the probability of transitions to AD with p for different m values as shown in Fig. 4.13b.

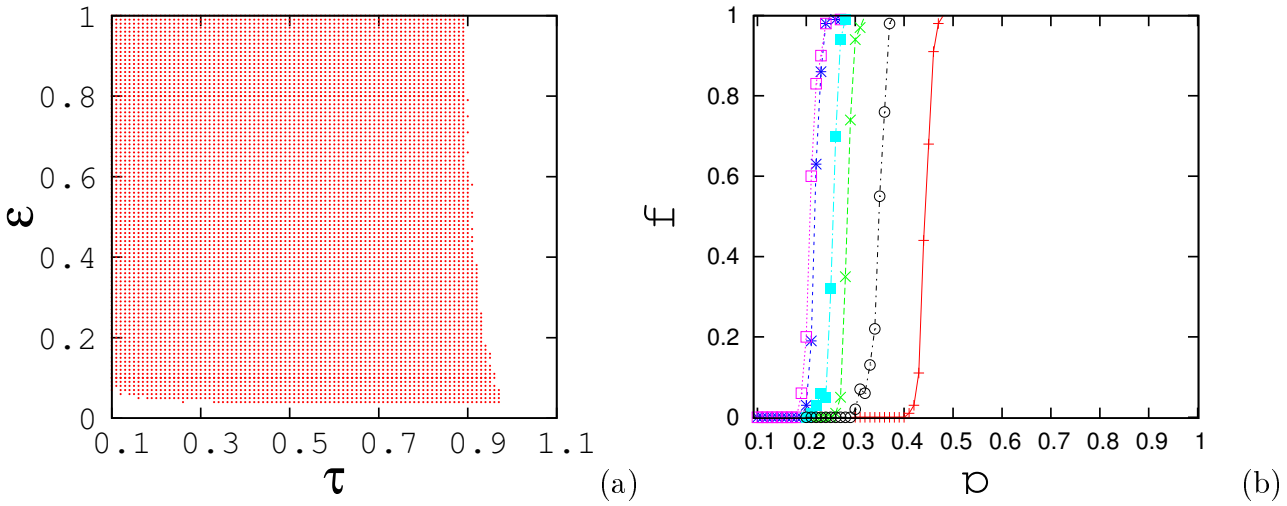

Figure 4.13: (colour online)Region of AD for random network of Lorenz systems in (τ, ϵ) plane for $m = 50$, p=0.5. b) Transition to AD, variation of fraction of realizations with p for m=20(red), 30(green), 40(blue), 50(magenta), 60(cyan), 70(black) , $\tau = 0.5$ and $\epsilon = 0.1$

4.3 Summary

In this chapter we have shown that when slow and fast nonlinear dynamical systems interact with each other on a randomly connected network, amplitude death occurs on the whole network for a range of values the parameters involved. The parameters of relevance here are the number of slow systems, probability of connections, time scale of slow systems and the coupling strength between systems. The occurrence of AD is established both for periodic and chaotic systems as nodal dynamics taking standard systems like Landau Stuart, Rössler and Lorenz. In addition we observe frequency synchronization, clustering and crossover in amplitudes and frequencies for large m. The transition curves and probability of transitions are identified and characterized. In summary, the study throws light on the role of time scales and complexity of interactions on the collective dynamics of the whole system.

Chapter 5

Multi scale dynamics on Scale free networks

5.1 Introduction

In this chapter we will discuss the results of interactions among slow and fast dynamical systems on a scale free network. We generate a scale free network using Barabási-Albert algorithm [43]. Typically the degree distribution of a scale free network follows a power law, which means there are large number of nodes with comparatively small values for degree and small number of nodes with comparatively high degrees. The nodes with high degrees are called hubs and can be found in the tail of the degree distribution. For Barabási-Albert algorithm the scaling index of the power law distribution is $\gamma = -3$. The degree distribution for 100 nodes is shown in the Fig. 5.1.

5.2 Scale free network of periodic systems

For our calculations, we generate several realizations of such a scale free network. We assume on each node of the network, the dynamics of periodic Rössler systems following eqn(5.1).

$$\begin{aligned} \dot{x}_i &= \tau_i(-y_i - z_i) + \tau_i \epsilon \sum_{j=1}^{N} A_{ij}(x_j - x_i) \\ \dot{y}_i &= \tau_i(x_i + a y_i) \\ \dot{z}_i &= \tau_i(b + z_i(x_i - c)) \end{aligned} \tag{5.1}$$

Where A_{ij} is taken as per scale free network topology using Barabási-Albert algorithm. Out of 100 nodes of the network, m nodes are taken to evolve at a slower time scale. Since in a scale free network, hubs play the role of control nodes, we mostly concentrate on cases where hubs follow slower dynamics.

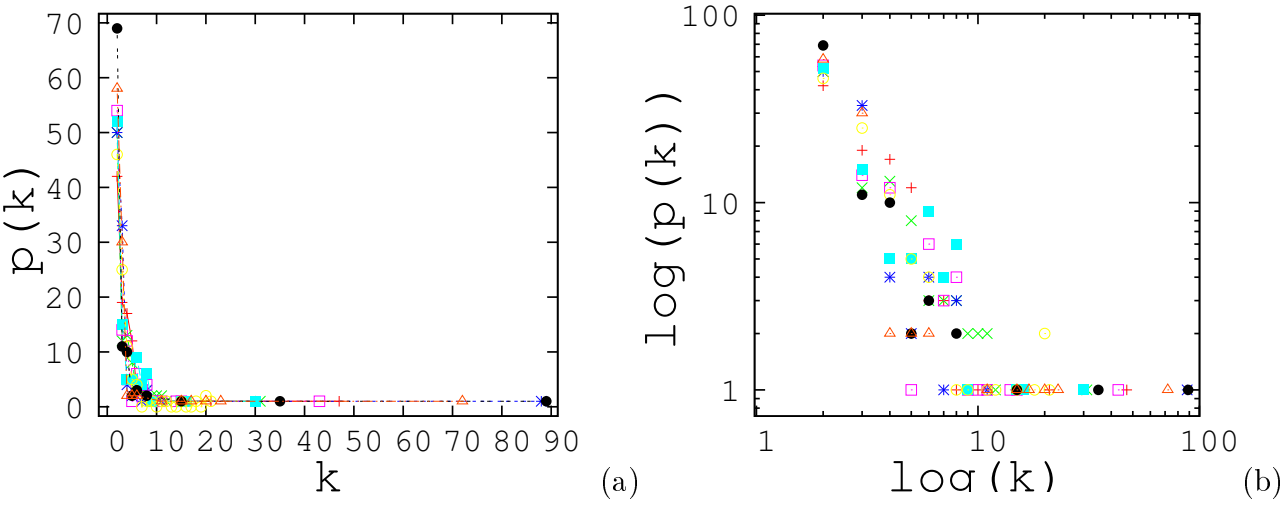

Figure 5.1: a) Degree distribution of scale free network for 100 nodes for different realizations (shown in different colors) b) Degree distribution in log scale for 100 nodes for different realizations (shown in different colors).

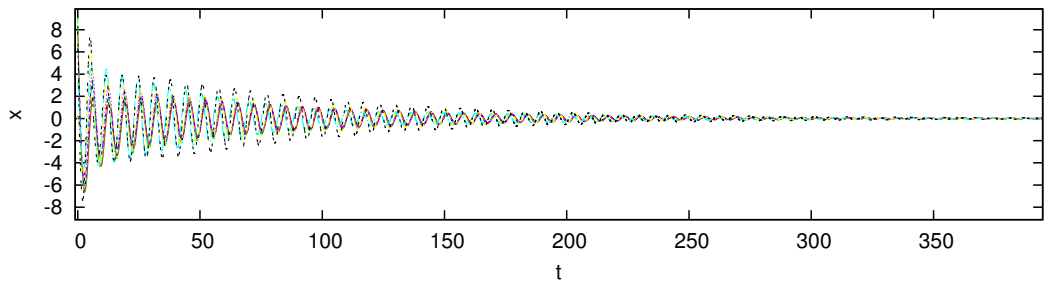

Figure 5.2: Time series of x-variable showing amplitude death in a scale free network of periodic Rössler systems for $\tau = 0.3$, $\epsilon = 0.2$ and m=8

5.2.1 Amplitude death on scale free network due to slow hubs

In this section, we display the occurrence of amplitude death, on a scale free network of 100 systems in which eight of the higher degree nodes are made to follow a dynamics with time scale mismatch of τ. For sufficient number of slow hubs in the network, we observe that for a part of (τ, ϵ) plane all the systems show amplitude death behavior. We isolate the region of AD by identifying the difference between the global maxima and global minima of all the oscillators to be zero in (τ, ϵ) plane. This is shown in Fig. 5.3 coloured as red.

Starting with the highest degree as slow and increasing the number one by one, we calculate the threshold or minimum number of number of slow hubs required for AD to happen. For each case, the average amplitude of all the oscillators is calculated. The plot of this averaged amplitude ($< A_{diff} >$) with the number of slow hubs m gives this threshold as the value of m at which ($< A_{diff} >$) becomes zero. This is repeated for different realizations and shown in Fig.5.4. Here the values of τ and ϵ are chosen from the amplitude death region.

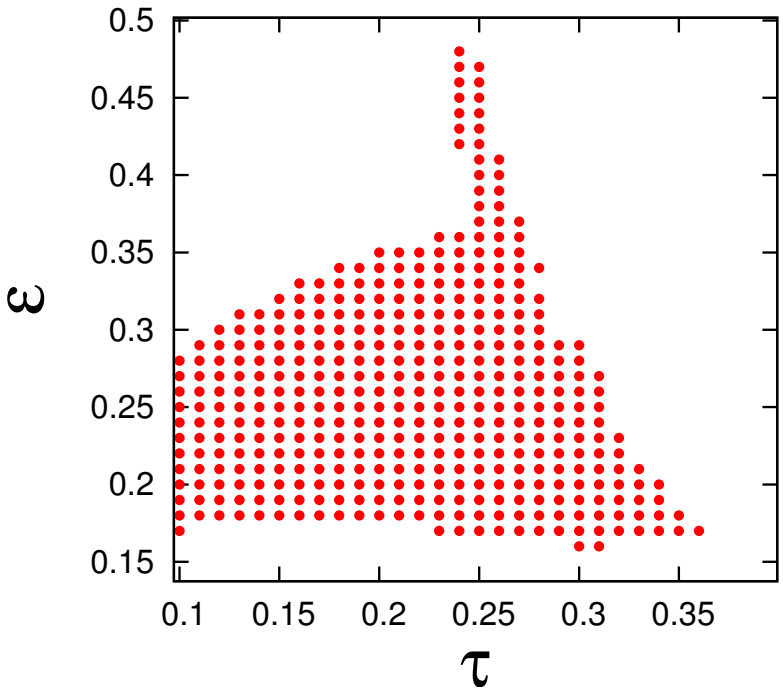

Figure 5.3: AD region in (τ, ϵ) plane for 100 periodic Rössler systems coupled on a typical realization of scale free network for m=8. Slow nodes are taken from the high degree end.

5.2.2 Frequency synchronization outside the region of AD

In the region outside AD, oscillators show frequency synchronization with a common frequency, which is less than the fast intrinsic and greater than slow intrinsic frequencies. However, in this case, unlike fully connected network, no cluster formation is observed.

When the number of slow hubs are small we see oscillatory behavior, with frequency synchronization throughout the (τ, ϵ) plane. This common frequency depends on τ similar to the cases of two coupled, fully connected network and random networks reported earlier. However we do not find synchronized clusters but the slow hubs show coherence among themselves.

5.2.3 Spread of slowness on scale free networks due to one slow node

In a scale free network of oscillators, with no time scale mismatch, all the systems on its nodes can be completely synchronized with a sufficiently strong coupling strength. Taking such a system, after giving sufficient time so that all the oscillators are synchronized, we make one of the nodes slow, called a source node. Then the slowness of that node will spread over the whole network and disrupt the dynamics of all other nodes so that they move away from the state of complete synchronization.

Due to the heterogeneity of connections in a scale free network, the time taken by each oscillator to move away from synchronization is not same. We analyze this scenario in terms of

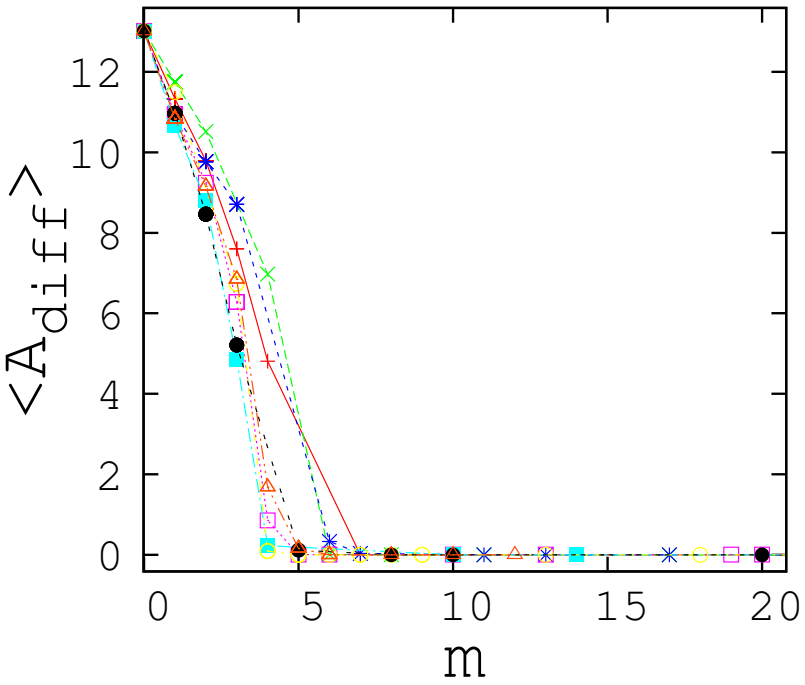

Figure 5.4: A_{diff} vs m showing he threshold value for number of slow hubs for AD to occur for periodic Rössler systems on a scale free network. Different colors correspond to different realizations.

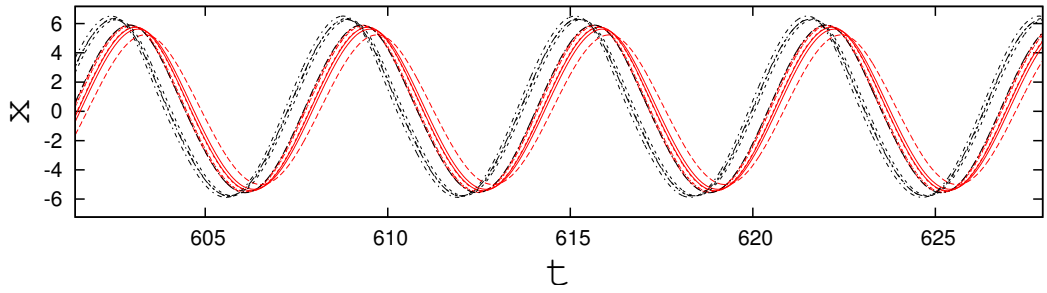

Figure 5.5: Frequency synchronization for large number of slow hubs, for $\tau = 0.6$, $\epsilon = 0.2$ $m = 8$ (8 top hubs) for periodic Rössler systems on scale free network. Here slow hubs are colored in red and fast oscillators are coloured in black.

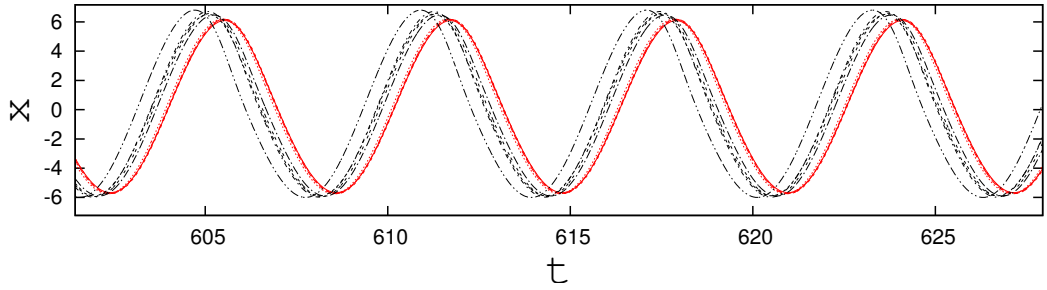

Figure 5.6: Frequency synchronization for small number of slow hubs for $\tau = 0.6$, $\epsilon = 0.2$ $m = 4$ (4 top hubs) for periodic Rössler systems on scale free network. Here slow hubs are colored in red and fast oscillators are coloured in black.

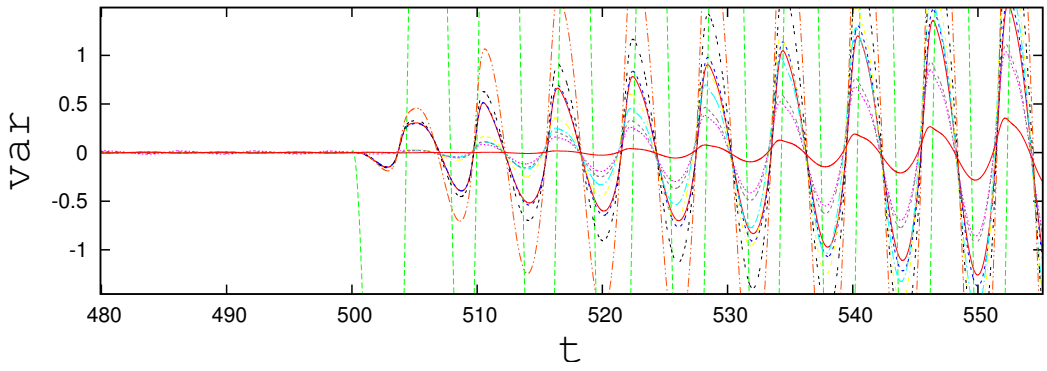

Figure 5.7: Variance of periodic Rössler oscillators with time to show that each oscillator takes different time to fall apart from the synchronized state. $\tau = 0.3$, $\epsilon = 0.03$

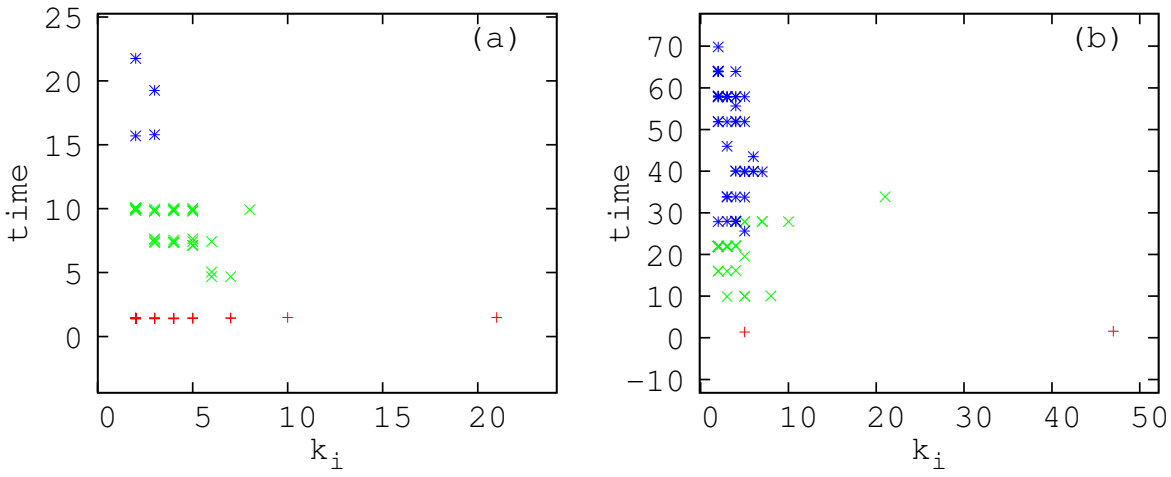

Figure 5.8: The time taken for each oscillator to fall apart is plotted with their degree for 1 source node being slow. This is shown for a particular realisation of the network of 100 systems where in a) the highest hub is made slow with degree 47 and in b) the lowest degree node is made slow with 2 degree. Different colors here represent different shortest path length from the source node with shortest path 1(red), 2(green), 3(blue). Here τ is 0.3 for the source node and ϵ is 0.03.

degree of the nodes and shortest path from the source node, in following ways. We study the change in the variance of all oscillators in time. When they are completely synchronized, the variance would be zero as shown in Fig. 5.7. When one node is made the slow, we calculate the variation of each oscillator from the mean of anticipated synchronized oscillations(the synchronized oscillation they would have followed if this node was not made slow), which is nonzero indicating desynchronization. From the Fig. 5.7 it is evident that for each oscillator the time taken for the variance to go to a non zero value is different. For example the oscillator which is made slow takes the least time. We get the time taken for each oscillator to go to a specific cut off value (typically -0.01 or 0.01) for its variation and plot as a function of the degree of the nodes. It is easy to see that this time increases as the shortest path of that node from the source node increases. We repeat this for several nodes as source, including hubs and low degree nodes. Fig. 5.8 shows this plot of time taken vs degree of nodes for the case of hub being the source node and a low degree node being the source node for a typical realization. In the case where a hub is source of slowness, we see most of the nodes fall apart quickly since the shortest path from the source node is small. However in the case where a low degree node is made slow, they take more time.

We repeat the study for different realizations of the network and calculate the number of systems that fall apart in a given time range starting from the time one node is made slow, averaged over the realizations of network taken. Fig. 5.9 shows the distribution of the number of systems that fall apart in a given time range with time, typically when a hub was the source and when a low degree node was source of slowness. It is interesting to see the maximum time taken for all the systems to fall apart from each other for each source node and its variation with the degree of source node. Fig. 5.10 shows a typical realization of network showing this

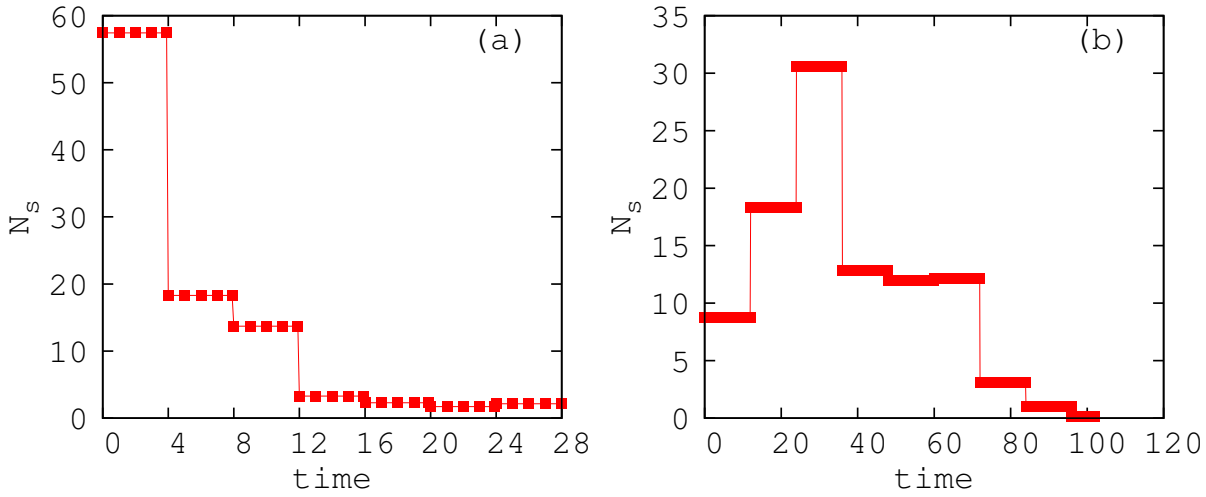

Figure 5.9: The number of systems that move away from synchrony(N_s) in a range of time is plotted with time averaging over several realisations. Here a) corresponds to the highest hub being slow as source node for each realisation and b) corresponds to one lowest degree node being slow as a source node. Here τ is 0.3 for the source node and ϵ 0.03.

behavior where it is evident that as the degree of source node increases the total time taken for all the systems to fall apart decreases in a curve that follows a power law. We fit the curve with function $f(x) = (a/x) + b$ and get a=180, b=18.

Self organization of the network to frequency synchronized state

In this process of de-synchronization due to slowness of one node, given sufficient time, all the oscillators are found to settle to a frequency synchronized state(Fig. 5.11). This is an interesting and novel phenomenon of **self-organization**, where the network goes from a collective behavior of complete synchronization to another less orderly but coherent emergent state of frequency synchronization re-adjusting the dynamics of all the nodes after the network was perturbed by making one node slow. We calculate the frequency of each oscillator and plot them with the index of each zero crossing time which shows the synchronized frequencies before one node was made slow, the de-synchronized frequencies just after the node was made slow and finally the re-adjusted frequency (lower than before) after self organization (Fig. 5.12). Also in this case the time taken for self organization is also an interesting characteristic feature, called self organization time. This time averaged over several realizations (t_{so}) for different τ ranging over $0.2 - 0.8$ for a particular ϵ=0.1 is shown in (Fig.5.12). We observe that the self organization time increases with the decrease in the time scale of the slow node.

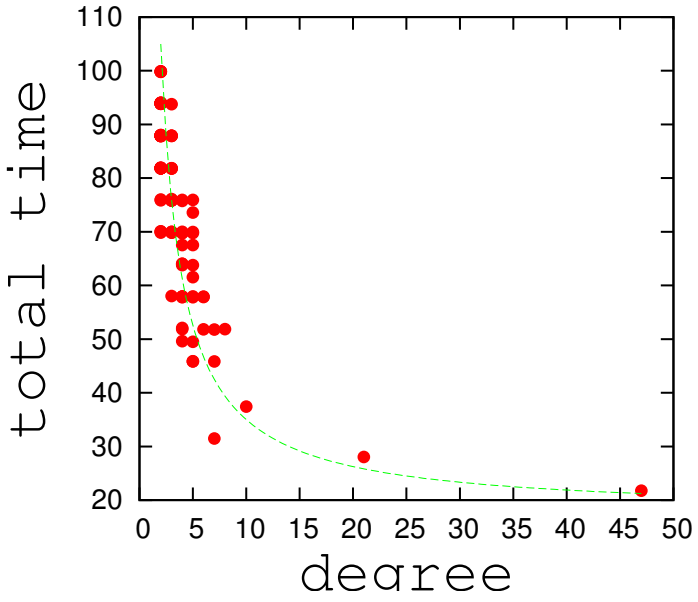

Figure 5.10: Time taken for all nodes to fall apart with the degree of source node for periodic Rössler systems on scale free network. The source node has time scale as $\tau = 0.3$ and here, $\epsilon = 0.03$

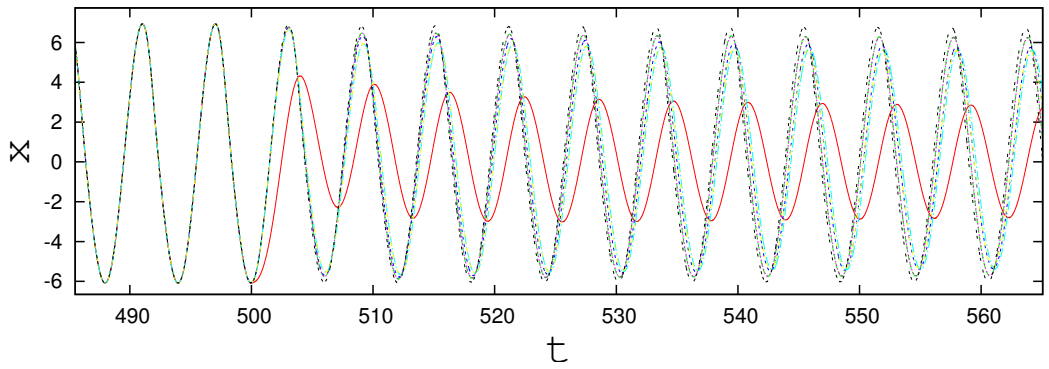

Figure 5.11: Time series of x-variables of periodic Rössler systems are plotted to show the frequency synchronized state after one node was made slow from the state of complete synchronization. Here $\tau = 0.3$ for the slow node and $\epsilon = 0.1$

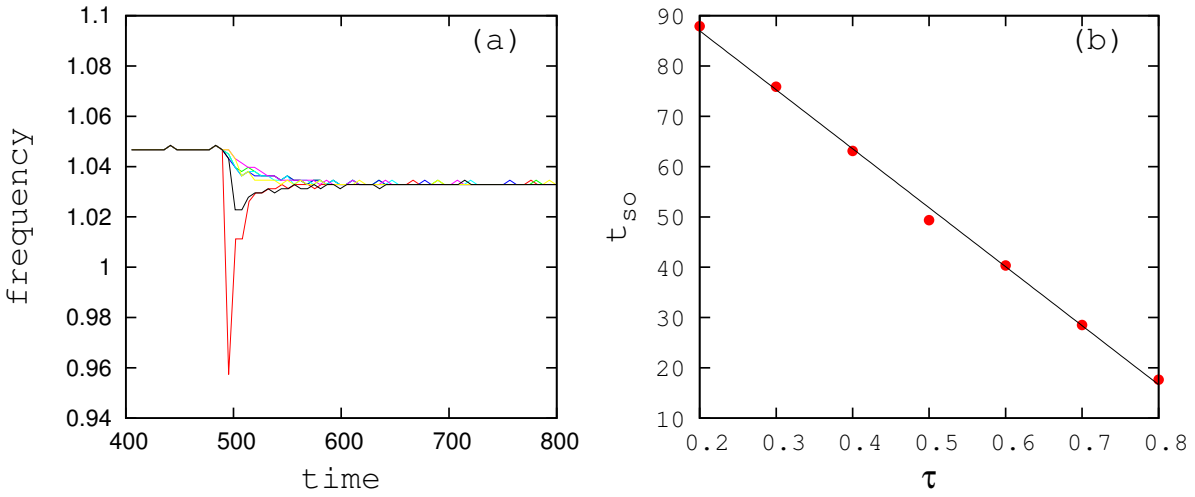

Figure 5.12: a) Self organization of frequencies for a typical realization of scale free network after one hub was made slow for periodic Rössler systems. O On the x axis the time and on y axis the corresponding frequency. b) the time taken to self organize averaged over realizations is plotted with τ for $\epsilon = 0.1$.

5.2.4 Scale free network with a distribution of time scales for nodal dynamics

In this section we study the collective dynamics of nonlinear systems on scale free network where time scale of each node varies with its degree following the relation

$$\tau_i = 2/k_i \tag{5.2}$$

This is chosen such that the node with highest degree will have the slowest time scale and vice versa. (Since in our network the lowest degree of a node is 2, for convenience the factor 2 in the numerator is taken to make the time scale of lowest degree node to be 1). In such a network we observe the phenomena of AD and find that after a threshold coupling strength all the systems reach AD. To observe the onset of AD, the averaged difference of global maxima to global minima over all oscillators, $< A_{diff} >$, is plotted for different values of ϵ. This is shown in Fig. 5.13. for different system size such as N=100,500,1000.

In this case for lower values of ϵ, we see oscillations with different amplitudes such that high degree nodes with lower time scales have much smaller amplitude than the low degree nodes with faster time scale. We estimate the distribution of amplitudes present in the network by calculating the number of oscillators(N_a) that show a certain amplitude. We also estimate the distribution of time scales by taking the number of oscillators(N_τ) in a a particular time scale (Fig.5.14). This distribution is taken for several realizations of the network with size N=1000. Clearly oscillators with large $\tau = 1$ and large amplitudes are much larger in number which corresponds to the larger number of low degree nodes and oscillators with the lowest τ and smallest amplitudes are much lower in number.

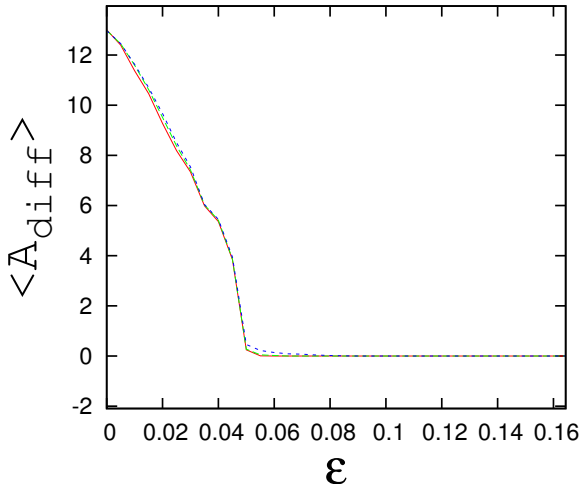

Figure 5.13: $< A_{diff} >$ vs ϵ in a scale free network for periodic Rössler systems with $\tau_i = 2/k_i$ for N=100(red), 500(green), 1000(blue) of Rössler systems, to show onset of AD with distribution of time scales.

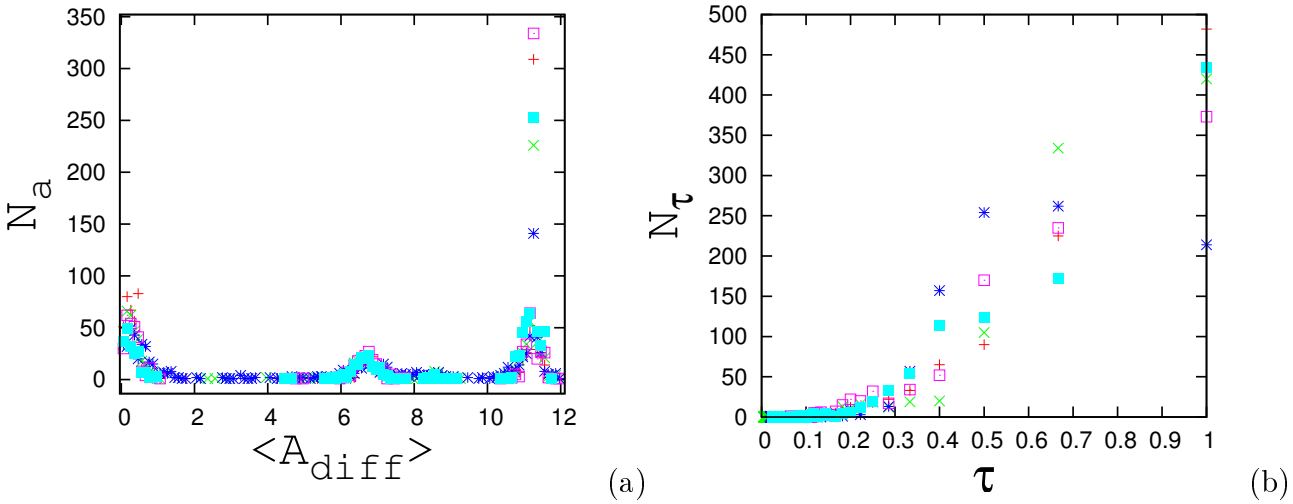

Figure 5.14: Amplitude distribution and time scale distribution for 1000 periodic Rössler systems on a scale free network for $\epsilon = 0.03$ when time scales distributed as eqn. 5.2

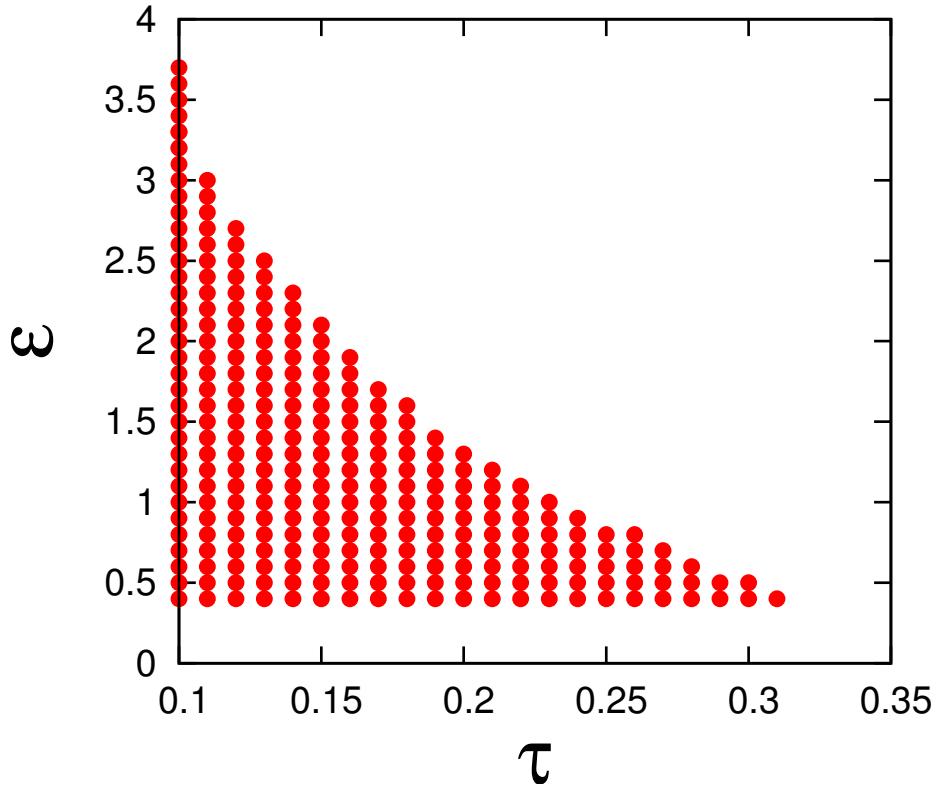

Figure 5.15: a) Region of AD for Landau-Stuart oscillators on scale free network in (τ, ϵ) plane for threshold degree 8.

5.2.5 Scale free network of Landau-Stuart oscillators

We repeat the above study using another periodic system, Landau-Stuart oscillator as nodal dynamics. We follow the eqn(. 5.3) for i^{th} node as

$$\begin{aligned} \dot{x}_i &= \tau_i((a - {x_i}^2 - {y_i}^2)x - \omega y_i) + \tau_i \epsilon \sum_{j=1}^{N} A_{ij}(x_j - x_i) \\ \dot{y}_i &= \tau_i((a - {x_i}^2 - {y_i}^2)y + \omega x_i) \end{aligned} \tag{5.3}$$

using intrinsic parameter a=0.1, where A_{ij} is the adjacency matrix of the generated scale free network. We find qualitatively similar results for this case also with amplitude death state and frequency synchronization. For a typical realization of the network when 8 systems are slow which is achieved by taking nodes having degree greater than 8 as slow, we show the region of amplitude death in τ, ϵ plane in Fig. 5.15

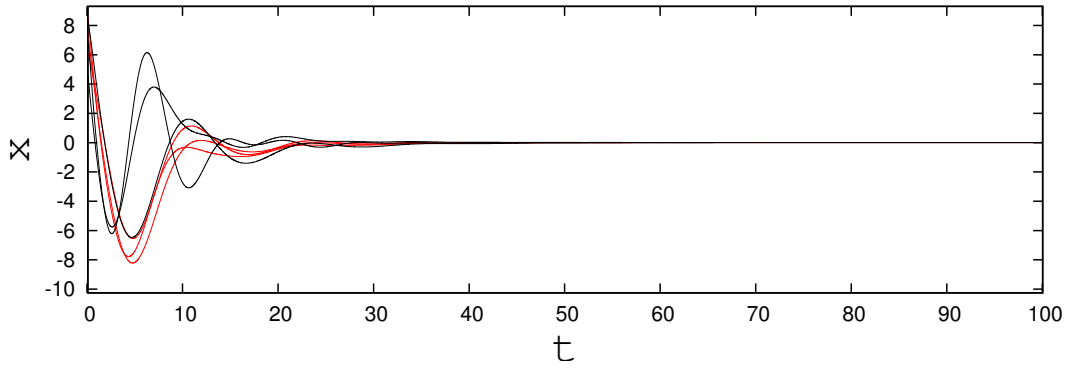

Figure 5.16: a) Time series for 18 slow nodes as nodes that have degree greater than 3 is made slow for $\tau = 0.1$ $\epsilon = 1$ in a scale free network of chaotic Rössler systems. Here 3 slow nodes (red) and 3 fast nodes (black) are plotted

5.3 Scale free network of chaotic oscillators with differing time scales

In this section we present the results of our study on the collective behaviour of slow and fast chaotic oscillators on a scale free network. In this case chaotic Rössler system and Lorenz system are taken as the dynamics on the nodes.

5.3.1 Slow and fast chaotic Rössler systems on scale free network

With chaotic Rössler systems on each node of the scale free network following eqn(5.4) with parameters a=0.2,b=0.2,c=5.7. The coupling function for each node is taken as diffusive with the nearest neighbours and normalized by degree of each node such that we get a mean field approximation. The equation for each node as per this coupling is given by

$$\dot{X}_i = \tau_i F(X_i) + \frac{G\epsilon\tau_i}{k_i} \sum_{j=1}^{N} A_{ij}(X_j - X_i) \tag{5.4}$$

where $F(X_i)$ denotes the intrinsic dynamics of i^{th} node. $\tau_i = \tau$ if i^{th} node is taken as slow, $\tau_i = 1$ otherwise. G is an n x n matrix as G = diag(1, 0, 0 ..). k_i denotes the degree of i^{th} node which divides the coupling function for each node.

In such a set up, chaotic Rössler systems are completely synchronized for strong coupling strength with no time scale mismatch. The network settles to a state of AD when sufficient the number of slow nodes taken from high degree end, with large time scale mismatch and high ϵ. Typically in one realization of scale free network, where 18 nodes are slow from the high degree end, which includes nodes with degree greater than 4, AD occurs as shown in Fig. 5.17 for $\tau = 0.3$ and $\epsilon = 1.5$. This is plotted by taking the region where $A_{diff} = 0$ for all oscillators is in (τ, ϵ) plane. When the time scale mismatch is lower but with a high value of τ, all the systems go to a frequency synchronized periodic state with a common frequency lower than the intrinsic fast frequency and higher than the intrinsic slow frequency for that τ. Unlike the case

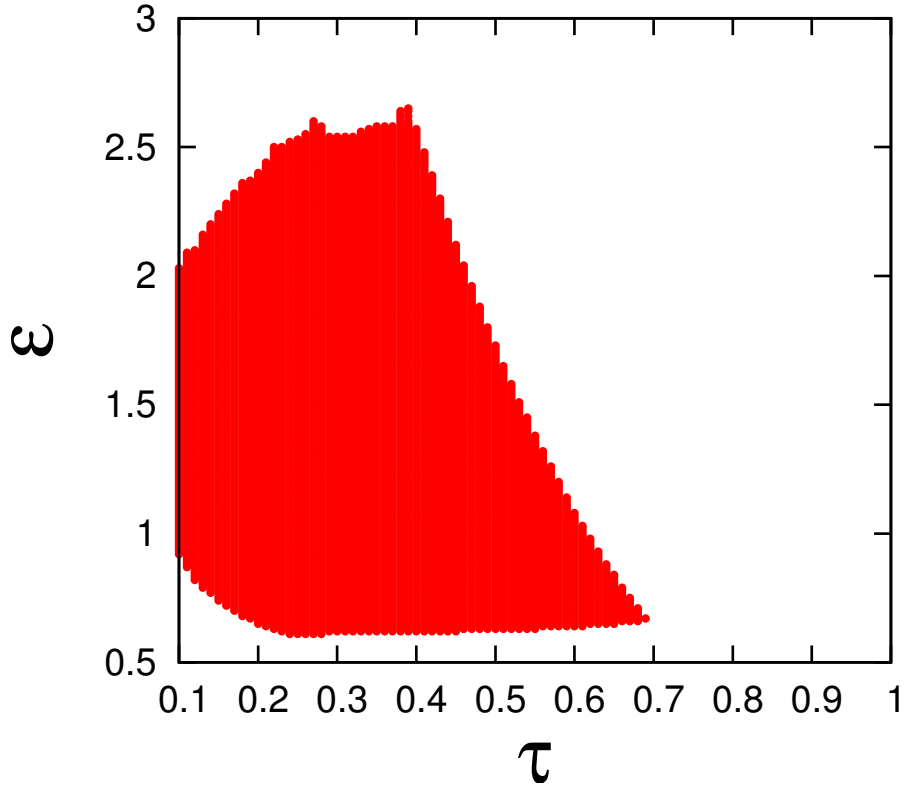

Figure 5.17: Region of AD for chaotic Rössler systems on scale free network in τ, ϵ plane for threshold degree 3.

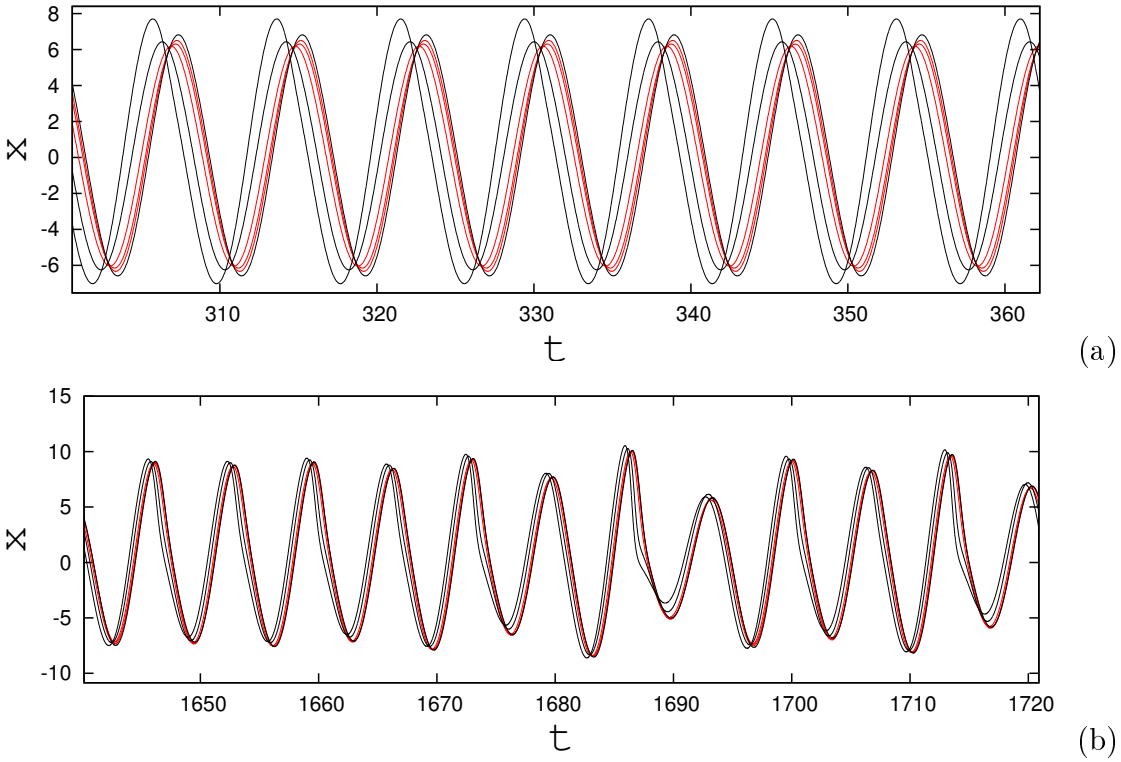

Figure 5.18: a) Time series for 18 slow nodes as nodes that have degree greater than 4 is made slow. a) $\tau = 0.6$ $\epsilon = 1.5$ b)$\tau = 0.8$ $\epsilon = 1.5$ showing periodic and chaotic trajectories of 3 typical slow (red) and 3 typical fast nodes (black) for chaotic Rössler systems on scale free network.

of fully connected network (Chapter 3) clustering is not observed here. On increasing τ, we see period doubling bifurcations until it reaches synchronized chaos for $\tau = 1$. In the chaotic state of the period doubling bifurcation we observed oscillators are phase shifted with a small phase while the wave pattern remains same for all the oscillators with different amplitudes. Fig. 5.18 shows frequency synchronized periodic states with phase shifts between oscillators for $\tau = 0.6$ and $\epsilon = 1.5$ and chaotic states for $\tau = 0.8$ and $\epsilon = 1.5$, for 18 slow nodes taken from high degree end. When number of slow systems are not sufficient, systems do not show AD but go to a periodic frequency synchronized state for large time scale mismatch.

In this case also, crossover phenomena in amplitude and frequencies happen with increasing m. Thus for small m, slow systems have smaller amplitude than fast systems. For large m this gets reversed. Similarly, synchronized frequency in frequency synchronized region, decreases with increase of m.

5.3.2 Slow and fast Lorenz systems on scale free network

We consider Lorenz systems with chaotic trajectories on each node of the scale free network. Here the intrinsic dynamics of each node follows equation(1.1) with parameter a=10, b=50,

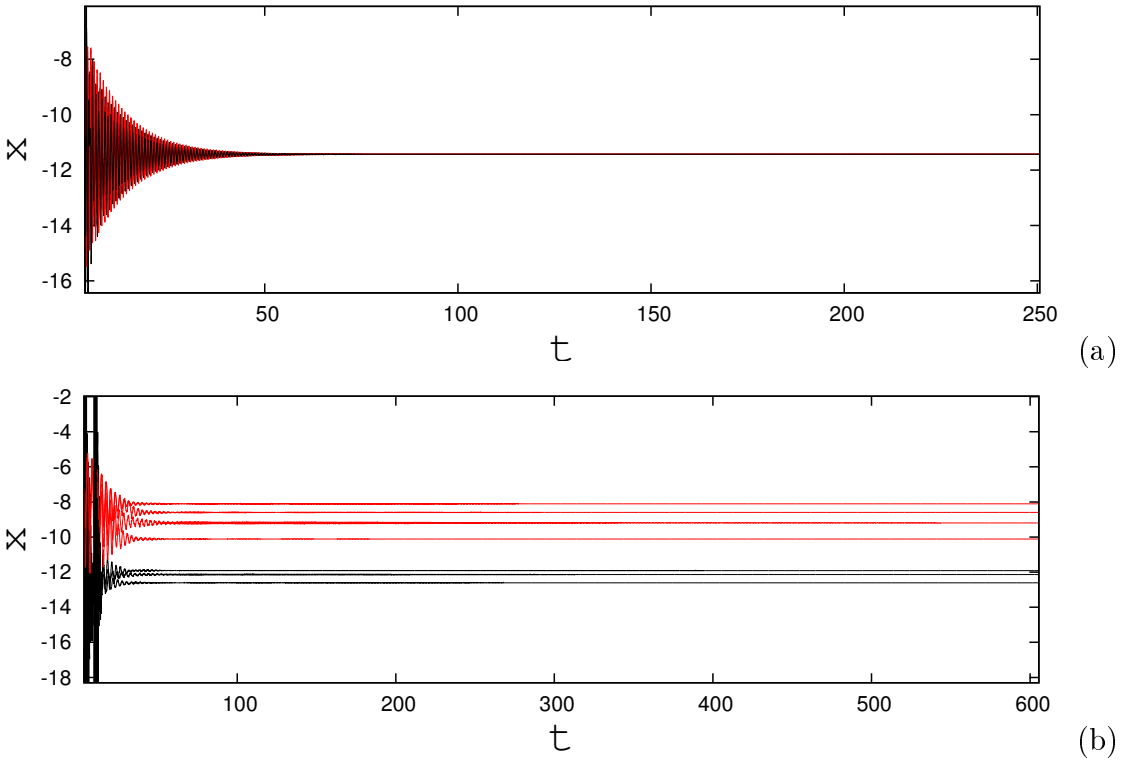

Figure 5.19: Time series of x-variable for Lorenz systems on a scale free network showing AD a) $\tau = 0.6$ $\epsilon = 20$ b)$\tau = 0.2$ $\epsilon = 20$ for $m = 29$ slow systems whose degree is greater than 3. Here 3 slow systems(red) and 3 fast systems(black) are plotted.

c=8/3 with τ_i as their time scale. The coupling function for each node is set as diffusive with the nearest neighbours and normalized by degree of each node to get a mean field approximation as for chaotic Rössler systems in the previous section. Typically for one realization on a scale free network we observe that with no time scale mismatch for a higher coupling strength, the systems show generalized synchronization ($\tau = 1$, $\epsilon = 20$) [68]. In this scenario if time scale mismatch is introduced in the network by making m number of nodes slow from the higher degree end, we see the oscillators go to AD with time scale mismatch $\tau = 0.8$. However, increasing the time scale mismatch further would lead the systems to oscillation death (OD) at $\tau = 0.2$. Fig. 5.19 shows AD and OD states for $m = 18$ with slow nodes taken as those with degree > 4 and for $\tau = 0.6$ and $\tau = 0.2$ successively and $\epsilon = 20$.

The regions of AD and OD are isolated in τ, ϵ plane by calculating the difference between global maxima and global minima. The parameter values that give this difference for each oscillator as zero ensures that either AD or OD occurs for those parameter values. Among these, AD corresponds to the case where the variance of x variable of all oscillators would become zero as they are going to a common fixed point. But for OD states since systems go to different fixed points the variance would show non zero values. Thus the AD and OD region is identified and marked in the (τ, ϵ) plane shown in Fig. 5.20

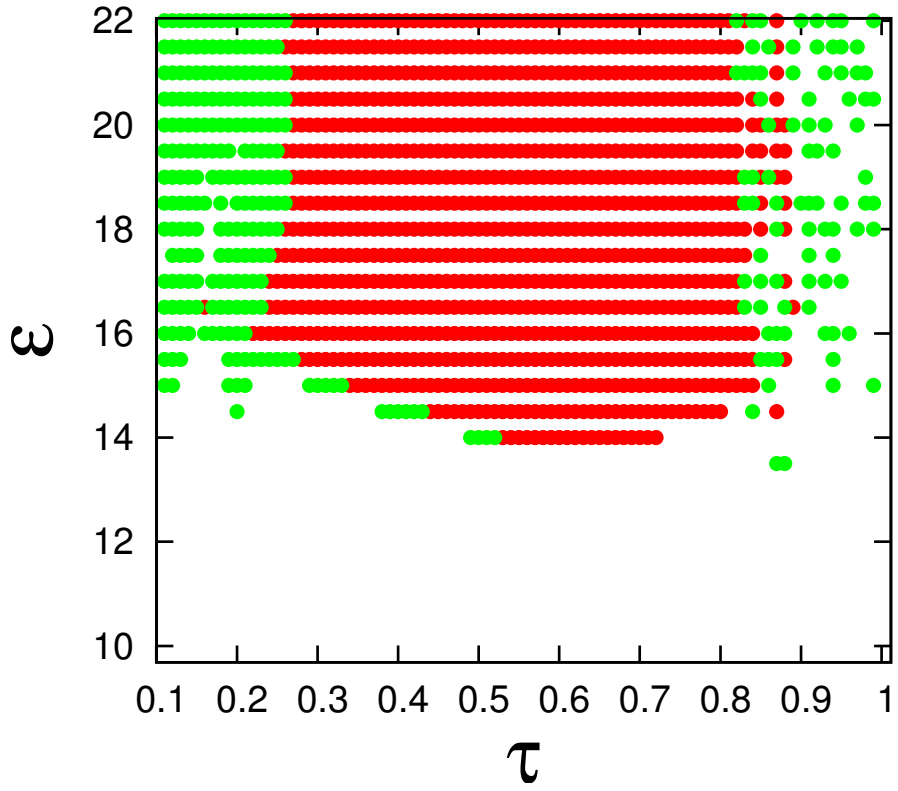

Figure 5.20: Regions of AD (red) and OD (green) for Lorenz systems on scale free network plotted in (τ, ϵ) plane where nodes with degrees above 3 are made slow.

5.4 Summary

We study the roles heterogeneous time scales play on the collective dynamics of non linear systems evolving on a scale free network. Since scale free networks have a hierarchical structure, we specifically address the effect of hubs or high degree nodes being slow in dynamics. As a main result we present and characterize the transitions of suppression of dynamics due to the presence of a threshold number of slow nodes taken from high degree end. We characterize and discuss the other types of oscillation that can happen for different parameter values of τ, ϵ and m. We study the spread of slowness due to one particular node being slow in the network after the network had achieved complete synchronization in periodic systems. In this case we show the results for one hub and one low degree node as the source of the slowness and compare their results. We also study the behavior when systems have a time scale distribution inversely proportional to their degree for periodic systems. We find AD for strong coupling strength and state of clustered amplitude distribution in the lower coupling strength range. We characterize suppression of dynamics and other oscillations for chaotic slow and fast systems on scale free network with mean field coupling.

Chapter 6

Conclusion

Multiple-timescale phenomena occur frequently in real world systems and their in-depth understanding brings in several novel challenges. Although there have been isolated studies addressing its various aspects, there are still many interesting questions that demand multidisciplinary approaches. Modeling frameworks have proposed methods to understand multiple time scale phenomena in single systems, like dynamical model for neuronal dynamics. However studies on collective behavior of connected systems that differ in their intrinsic time scales, are very minimal with many open questions. In this context the study reported in this thesis is highly relevant and has resulted in many novel phenomena and promising approaches.

We study the effect of heterogeneity in the natural frequencies on the emergent dynamics by considering systems with different dynamical time scales. The study is exhaustive with at least three standard nonlinear systems, periodic and chaotic states as intrinsic dynamics and all to fully connected, random and scale free topologies for connections or interactions on the networks with diffusive and mean field coupling. By considering two types of complex networks, we study the effect of heterogeneity in link structure on the dynamical properties and their critical behavior. Our study uses standard periodic oscillators of Rössler and Landau-Stuart type and chaotic Rössler and Lorenz dynamics so that it brings out the amplitude variations and their crossover behaviors as slowness factor increases.

The main contributions from the study are the observation of onset of emergent phenomena like amplitude death, oscillation death, frequency synchronization, cluster synchronization and their characterizations.

Several types of synchronization phenomena like complete, phase and generalized, have been studied in various contexts. However, frequency synchronization is of recent interest and has relevance in many realistic situations ranging from neuronal systems to power grids, where the individual oscillators can have non-identical natural frequencies. Similarly suppression of oscillations or amplitude death is another emergent phenomenon that we observe that has interesting implications.

We find the difference in time scales and the heterogeneity in connectivity together can drive the whole network to frequency synchronized clusters. Increasing the heterogeneity in time scales by increasing the number of slow systems or the mismatch in time scales, the whole network settles to a state of no oscillations. The transitions to that state as well as recovery to slower oscillations with cross over in amplitudes are some of the interesting results of the study.

We also address the question of what happens if part or even one node of a network of

systems suddenly slows down and how does it affect the performance of the whole network. In this case, the robustness of the network to such changes is studied in terms of the time taken for each node to escape from the synchronized state leading the whole network to desynchronized dynamics. We find this phenomenon of loss of synchrony settles in a time that decreases with he degree of the node that becomes slow first. Consequent to this, the whole network reorganizes to a frequency synchronized state and this self-organization time is characteristic of the difference in time scales.

The major contributions from the study presented in the thesis are

- Suppression of dynamics, frequency synchronization and two frequency states are observed in two coupled slow and fast nonlinear systems. This is applied to coupled ocean-atmospheric model where oscillation death and multistable periodic states are studied.
- Amplitude death, frequency synchronization cluster synchronization and frequency and amplitude crossover is studied for fully connected regular network, when each node is evolving with slow or fast dynamics. Motifs or minimal networks of slow and fast systems are studied to carry out analytical understanding for such dynamical behaviour.
- On a random network we study the interaction between slow and fast systems. Along with the study of amplitude death and frequency synchronized state, we find optimum number of slow system for sparse most network configuration for reaching AD. We carry out these studies for uniform as well as non uniform probabilities of connection.
- Spread of slowness on a scale free network is studied for one node being slow in a complete synchronized network condition. In this case the phenomena of self organization is studied in detailed. Amplitude death and distribution of clustered amplitudes are studied for a distribution of dynamical time scales on this hierarchical structure of scale free networks.

Future trends

- The study presented here gives an overview about the effect of differing time scales on interacting non linear systems on different level of connecting structures. This can serve as a basic model for understanding complex multicomponent and multi scale systems. This basic study opens up future research possibilities in various directions.
- One can apply the methods and analysis in the thesis to understand real networks like social networks, where slowness can be related to the performance of the component systems.
- The effect of noise and its robustness in the presence of noise and external perturbations can be studied as a direct extension of the present study.
- Introducing delay in connections, which is natural, will ad one more time scale to the problem and therefore will be interesting to pursue for possible emergent behavior.
- The present study can be helpful to understand time series coming form system shaving dynamics on different time scales.

- The study can be further extended to understand possible control mechanisms where emergent dynamics can be controlled by changing the time scales of suitably chosen component systems.

In conclusion, we present our work as a basic and fundamental approach for understanding the interplay of time scales and the results serve also as control mechanism for chaotic dynamics. While this work gives a new direction to study the role of time scales involved in complex systems, the stability and predictability of chaos also gets a new direction through it. We are hopeful that this research will benefit and inspire the future research in similar dircetions.

Bibliography

[1] Paul Fieguth. An introduction to complex systems. *Springer*, 2017.

[2] John S. Mattick. The hidden genetic program of complex organisms. *Scientific American, Vol. 291, No. 4, pp. 60-67*, 2004.

[3] John Guckenheimer. Organisms as complex systems. `http://www.mathaware.org`, 2011.

[4] IC Baianu. Complex systems biology of organisms. 2012.

[5] Ed Bullmore and Olaf Sporns. Complex brain networks: graph theoretical analysis of structural and functional systems. *Nature Reviews Neuroscience*, 10(3):186, 2009.

[6] Xi-Nian Zuo, Adriana Di Martino, Clare Kelly, Zarrar E Shehzad, Dylan G Gee, Donald F Klein, F Xavier Castellanos, Bharat B Biswal, and Michael P Milham. The oscillating brain: complex and reliable. *Neuroimage*, 49(2):1432–1445, 2010.

[7] Mikail Rubinov and Olaf Sporns. Complex network measures of brain connectivity: uses and interpretations. *Neuroimage*, 52(3):1059–1069, 2010.

[8] Denis Noble. Modeling the heart–from genes to cells to the whole organ. *Science*, 295(5560):1678–1682, 2002.

[9] Robert Plomin, Michael J Owen, and Peter McGuffin. The genetic basis of complex human behaviors. *Science*, 264(5166):1733–1739, 1994.

[10] Gregory S Barsh. The genetics of pigmentation: from fancy genes to complex traits. *Trends in Genetics*, 12(8):299–305, 1996.

[11] Herbert A Simon. The organization of complex systems. In *Models of discovery*, pages 245–261. Springer, 1977.

[12] Madalena D Costa, Chung-Kang Peng, and Ary L Goldberger. Multiscale analysis of heart rate dynamics: entropy and time irreversibility measures. *Cardiovascular Engineering*, 8(2):88–93, 2008.

[13] Irun R Cohen and David Harel. Explaining a complex living system: dynamics, multi-scaling and emergence. *Journal of the royal society interface*, 4(13):175–182, 2007.

[14] David Rind. Complexity and climate. *science*, 284(5411):105–107, 1999.

[15] Jonathan F Donges, Yong Zou, Norbert Marwan, and Jürgen Kurths. Complex networks in climate dynamics. *The European Physical Journal Special Topics*, 174(1):157–179, 2009.

[16] José A Rial, Roger A Pielke, Martin Beniston, Martin Claussen, JOsep Canadell, Peter Cox, Hermann Held, Nathalie De Noblet-Ducoudré, Ronald Prinn, James F Reynolds, et al. Nonlinearities, feedbacks and critical thresholds within the earth's climate system. *Climatic change*, 65(1-2):11–38, 2004.

[17] Simon A Levin. Ecosystems and the biosphere as complex adaptive systems. *Ecosystems*, 1(5):431–436, 1998.

[18] Jon Norberg. Biodiversity and ecosystem functioning: a complex adaptive systems approach. *Limnology and Oceanography*, 49(4part2):1269–1277, 2004.

[19] Walter Buckley and Walter Frederick Buckley. *Society–a Complex Adaptive System: Essays in Social Theory*, volume 9. Taylor & Francis, 1998.

[20] R Keith Sawyer. *Social emergence: Societies as complex systems*. Cambridge University Press, 2005.

[21] Fei-Yue Wang. Parallel control and management for intelligent transportation systems: Concepts, architectures, and applications. *IEEE Transactions on Intelligent Transportation Systems*, 11(3):630–638, 2010.

[22] Vittoria Colizza, Alain Barrat, Marc Barthélemy, and Alessandro Vespignani. The role of the airline transportation network in the prediction and predictability of global epidemics. *Proceedings of the National Academy of Sciences of the United States of America*, 103(7):2015–2020, 2006.

[23] W Brian Arthur. *The economy as an evolving complex system II*. CRC Press, 2018.

[24] Didier Sornette. *Why stock markets crash: critical events in complex financial systems*. Princeton University Press, 2017.

[25] Takashi Kimoto, Kazuo Asakawa, Morio Yoda, and Masakazu Takeoka. Stock market prediction system with modular neural networks. In *Neural Networks, 1990., 1990 IJCNN International Joint Conference on*, pages 1–6. IEEE, 1990.

[26] Edward N Lorenz. Deterministic nonperiodic flow. *Journal of the atmospheric sciences*, 20(2):130–141, 1963.

[27] Colin Sparrow. *The Lorenz equations: bifurcations, chaos, and strange attractors*, volume 41. Springer Science & Business Media, 2012.

[28] Morris W Hirsch, Stephen Smale, and Robert L Devaney. *Differential equations, dynamical systems, and an introduction to chaos*. Academic press, 2012.

[29] Geoff Boeing. Visual analysis of nonlinear dynamical systems: Chaos, fractals, self-similarity and the limits of prediction. *Systems*, 4(4):37, 2016.

[30] Otto E Rössler. An equation for continuous chaos. *Physics Letters A*, 57(5):397–398, 1976.

[31] OE Rossler. An equation for hyperchaos. *Physics Letters A*, 71(2-3):155–157, 1979.

[32] Heinz-Otto Peitgen, Hartmut Jürgens, and Dietmar Saupe. *Chaos and fractals: new frontiers of science*. Springer Science & Business Media, 2006.

[33] John Trevor Stuart. On the non-linear mechanics of hydrodynamic stability. *Journal of Fluid Mechanics*, 4(1):1–21, 1958.

[34] Steven H Strogatz. *Nonlinear dynamics and chaos: with applications to physics, biology, chemistry, and engineering*. CRC Press, 2018.

[35] Robert C Hilborn. *Chaos and nonlinear dynamics: an introduction for scientists and engineers*. Oxford University Press on Demand, 2000.

[36] Muthusamy Lakshmanan and Shanmuganathan Rajaseekar. *Nonlinear dynamics: integrability, chaos and patterns*. Springer Science & Business Media, 2012.

[37] Rajarshi Roy, TW Murphy Jr, TD Maier, Z Gills, and ER Hunt. Dynamical control of a chaotic laser: Experimental stabilization of a globally coupled system. *Physical Review Letters*, 68(9):1259, 1992.

[38] Tilmann Heil, Ingo Fischer, Wolfgang Elsässer, Josep Mulet, and Claudio R Mirasso. Chaos synchronization and spontaneous symmetry-breaking in symmetrically delay-coupled semiconductor lasers. *Physical Review Letters*, 86(5):795, 2001.

[39] L Cavaleri, B Fox-Kemper, and M Hemer. Wind waves in the coupled climate system. *Bulletin of the American Meteorological Society*, 93(11):1651–1661, 2012.

[40] Aiguo Dai. Precipitation characteristics in eighteen coupled climate models. *Journal of Climate*, 19(18):4605–4630, 2006.

[41] Mark Newman, Albert-Laszlo Barabasi, and Duncan J Watts. *The structure and dynamics of networks*. Princeton University Press, 2011.

[42] Mark EJ Newman, Steven H Strogatz, and Duncan J Watts. Random graphs with arbitrary degree distributions and their applications. *Physical review E*, 64(2):026118, 2001.

[43] Réka Albert and Albert-László Barabási. Statistical mechanics of complex networks. *Reviews of modern physics*, 74(1):47, 2002.

[44] Alex Arenas, Albert Díaz-Guilera, Jurgen Kurths, Yamir Moreno, and Changsong Zhou. Synchronization in complex networks. *Physics reports*, 469(3):93–153, 2008.

[45] Jinhu Lü, Xinghuo Yu, and Guanrong Chen. Chaos synchronization of general complex dynamical networks. *Physica A: Statistical Mechanics and its Applications*, 334(1-2):281–302, 2004.

[46] Soon-Hyung Yook and Hildegard Meyer-Ortmanns. Synchronization of rössler oscillators on scale-free topologies. *Physica A: Statistical Mechanics and its Applications*, 371(2):781–789, 2006.

[47] Stefano Boccaletti, Jürgen Kurths, Grigory Osipov, DL Valladares, and CS Zhou. The synchronization of chaotic systems. *Physics reports*, 366(1-2):1–101, 2002.

[48] Meng Zhan, Xingang Wang, Xiaofeng Gong, GW Wei, and C-H Lai. Complete synchronization and generalized synchronization of one-way coupled time-delay systems. *Physical Review E*, 68(3):036208, 2003.

[49] Jianquan Lu and Jinde Cao. Adaptive complete synchronization of two identical or different chaotic (hyperchaotic) systems with fully unknown parameters. *Chaos: An Interdisciplinary Journal of Nonlinear Science*, 15(4):043901, 2005.

[50] Adilson E Motter, Changsong Zhou, and Jürgen Kurths. Network synchronization, diffusion, and the paradox of heterogeneity. *Physical Review E*, 71(1):016116, 2005.

[51] Chil-Min Kim, Sunghwan Rim, Won-Ho Kye, Jung-Wan Ryu, and Young-Jai Park. Anti-synchronization of chaotic oscillators. *Physics Letters A*, 320(1):39–46, 2003.

[52] CAS Batista, AM Batista, JAC De Pontes, RL Viana, and SR Lopes. Chaotic phase synchronization in scale-free networks of bursting neurons. *Physical Review E*, 76(1):016218, 2007.

[53] Michael G Rosenblum, Arkady S Pikovsky, and Jürgen Kurths. Phase synchronization of chaotic oscillators. *Physical review letters*, 76(11):1804, 1996.

[54] Michael G Rosenblum, Arkady S Pikovsky, and Jürgen Kurths. From phase to lag synchronization in coupled chaotic oscillators. *Physical Review Letters*, 78(22):4193, 1997.

[55] Jun-nosuke Teramae and Dan Tanaka. Robustness of the noise-induced phase synchronization in a general class of limit cycle oscillators. *Physical review letters*, 93(20):204103, 2004.

[56] Arkady S Pikovsky, Michael G Rosenblum, Grigory V Osipov, and Jürgen Kurths. Phase synchronization of chaotic oscillators by external driving. *Physica D: Nonlinear Phenomena*, 104(3-4):219–238, 1997.

[57] Ming-Chung Ho, Yao-Chen Hung, and Chien-Ho Chou. Phase and anti-phase synchronization of two chaotic systems by using active control. *Physics letters A*, 296(1):43–48, 2002.

[58] Jian-bo Liu, Chun-fei Ye, Shu-jing Zhang, and Wen-tao Song. Anti-phase synchronization in coupled map lattices. *Physics Letters A*, 274(1-2):27–29, 2000.

[59] Weiqing Liu, Jinghua Xiao, Xiaolan Qian, and Junzhong Yang. Antiphase synchronization in coupled chaotic oscillators. *Physical Review E*, 73(5):057203, 2006.

[60] Ye Wu, Nianchuang Wang, Lixiang Li, and Jinghua Xiao. Anti-phase synchronization of two coupled mechanical metronomes. *Chaos: An Interdisciplinary Journal of Nonlinear Science*, 22(2):023146, 2012.

[61] EM Shahverdiev, S Sivaprakasam, and KA Shore. Lag synchronization in time-delayed systems. *Physics Letters A*, 292(6):320–324, 2002.

[62] Chuandong Li, Xiaofeng Liao, and Kwok-wo Wong. Chaotic lag synchronization of coupled time-delayed systems and its applications in secure communication. *Physica D: Nonlinear Phenomena*, 194(3-4):187–202, 2004.

[63] S Boccaletti and DL Valladares. Characterization of intermittent lag synchronization. *Physical Review E*, 62(5):7497, 2000.

[64] Nikolai F Rulkov, Mikhail M Sushchik, Lev S Tsimring, and Henry DI Abarbanel. Generalized synchronization of chaos in directionally coupled chaotic systems. *Physical Review E*, 51(2):980, 1995.

[65] Lj Kocarev and U Parlitz. Generalized synchronization, predictability, and equivalence of unidirectionally coupled dynamical systems. *Physical review letters*, 76(11):1816, 1996.

[66] Henry DI Abarbanel, Nikolai F Rulkov, and Mikhail M Sushchik. Generalized synchronization of chaos: The auxiliary system approach. *Physical Review E*, 53(5):4528, 1996.

[67] Hui Liu, Juan Chen, Jun-an Lu, and Ming Cao. Generalized synchronization in complex dynamical networks via adaptive couplings. *Physica A: Statistical Mechanics and its Applications*, 389(8):1759–1770, 2010.

[68] Yao-Chen Hung, Yu-Ting Huang, Ming-Chung Ho, and Chin-Kun Hu. Paths to globally generalized synchronization in scale-free networks. *Physical Review E*, 77(1):016202, 2008.

[69] Suman Acharyya and RE Amritkar. Generalized synchronization of coupled chaotic systems. *The European Physical Journal Special Topics*, 222(3-4):939–952, 2013.

[70] Renato E Mirollo and Steven H Strogatz. Amplitude death in an array of limit-cycle oscillators. *Journal of Statistical Physics*, 60(1-2):245–262, 1990.

[71] Garima Saxena, Awadhesh Prasad, and Ram Ramaswamy. Amplitude death: The emergence of stationarity in coupled nonlinear systems. *Physics Reports*, 521(5):205–228, 2012.

[72] Wei Zou, Xin-gang Wang, Qi Zhao, and Meng Zhan. Oscillation death in coupled oscillators. *Frontiers of Physics in China*, 4(1):97, 2009.

[73] A Zakharova, I Schneider, YN Kyrychko, KB Blyuss, Aneta Koseska, B Fiedler, and E Schöll. Time delay control of symmetry-breaking primary and secondary oscillation death. *EPL (Europhysics Letters)*, 104(5):50004, 2013.

[74] Awadhesh Prasad, Mukeshwar Dhamala, Bhim Mani Adhikari, and Ramakrishna Ramaswamy. Amplitude death in nonlinear oscillators with nonlinear coupling. *Physical Review E*, 81(2):027201, 2010.

[75] DV Ramana Reddy, Abhijit Sen, and George L Johnston. Time delay induced death in coupled limit cycle oscillators. *Physical Review Letters*, 80(23):5109, 1998.

[76] Rajat Karnatak, Ram Ramaswamy, and Awadhesh Prasad. Amplitude death in the absence of time delays in identical coupled oscillators. *Physical Review E*, 76(3):035201, 2007.

[77] V Resmi, G Ambika, and RE Amritkar. General mechanism for amplitude death in coupled systems. *Physical Review E*, 84(4):046212, 2011.

[78] V Resmi, G Ambika, RE Amritkar, and G Rangarajan. Amplitude death in complex networks induced by environment. *Physical Review E*, 85(4):046211, 2012.

[79] A Koseska, E Volkov, and J Kurths. Parameter mismatches and oscillation death in coupled oscillators. *Chaos: An Interdisciplinary Journal of Nonlinear Science*, 20(2):023132, 2010.

[80] AN Pisarchik. Oscillation death in coupled nonautonomous systems with parametrical modulation. *Physics Letters A*, 318(1-2):65–70, 2003.

[81] Tanmoy Banerjee and Debarati Ghosh. Transition from amplitude to oscillation death under mean-field diffusive coupling. *Physical Review E*, 89(5):052912, 2014.

[82] CR Hens, Olasunkanmi I Olusola, Pinaki Pal, and Syamal K Dana. Oscillation death in diffusively coupled oscillators by local repulsive link. *Physical Review E*, 88(3):034902, 2013.

[83] Aneta Koseska, Evgenii Volkov, and Jürgen Kurths. Transition from amplitude to oscillation death via turing bifurcation. *Physical review letters*, 111(2):024103, 2013.

[84] Yoshiki Kuramoto. *Chemical oscillations, waves, and turbulence*, volume 19. Springer Science & Business Media, 2012.

[85] Yoshiki Kuramoto. Self-entrainment of a population of coupled non-linear oscillators. In *International symposium on mathematical problems in theoretical physics*, pages 420–422. Springer, 1975.

[86] Steven H Strogatz. From kuramoto to crawford: exploring the onset of synchronization in populations of coupled oscillators. *Physica D: Nonlinear Phenomena*, 143(1-4):1–20, 2000.

[87] Yamir Moreno and Amalio F Pacheco. Synchronization of kuramoto oscillators in scale-free networks. *EPL (Europhysics Letters)*, 68(4):603, 2004.

[88] Grigory V Osipov, Jürgen Kurths, and Changsong Zhou. *Ensembles of Phase Oscillators*. Springer, 2007.

[89] Wei Wu, Wenjuan Zhou, and Tianping Chen. Cluster synchronization of linearly coupled complex networks under pinning control. *IEEE Transactions on Circuits and Systems I: Regular Papers*, 56(4):829–839, 2009.

[90] Vladimir N Belykh, Igor V Belykh, and Erik Mosekilde. Cluster synchronization modes in an ensemble of coupled chaotic oscillators. *Physical Review E*, 63(3):036216, 2001.

[91] Daniel M Abrams and Steven H Strogatz. Chimera states for coupled oscillators. *Physical review letters*, 93(17):174102, 2004.

[92] Mark R Tinsley, Simbarashe Nkomo, and Kenneth Showalter. Chimera and phase-cluster states in populations of coupled chemical oscillators. *Nature Physics*, 8(9):662, 2012.

[93] Mark J Panaggio and Daniel M Abrams. Chimera states: coexistence of coherence and incoherence in networks of coupled oscillators. *Nonlinearity*, 28(3):R67, 2015.

[94] Daniel M Abrams and Steven H Strogatz. Chimera states in a ring of nonlocally coupled oscillators. *International Journal of Bifurcation and Chaos*, 16(01):21–37, 2006.

[95] Arthur T Winfree. *The geometry of biological time*, volume 12. Springer Science & Business Media, 2001.

[96] Paul Johnson and Alexander Sutin. Slow dynamics and anomalous nonlinear fast dynamics in diverse solids. *The Journal of the Acoustical Society of America*, 117(1):124–130, 2005.

[97] MR Hansen, X Feng, Volker Macho, Klaus Müllen, Hans Wolfgang Spiess, and G Floudas. Fast and slow dynamics in a discotic liquid crystal with regions of columnar order and disorder. *Physical review letters*, 107(25):257801, 2011.

[98] Katherine A Henzler-Wildman, Ming Lei, Vu Thai, S Jordan Kerns, Martin Karplus, and Dorothee Kern. A hierarchy of timescales in protein dynamics is linked to enzyme catalysis. *Nature*, 450(7171):913, 2007.

[99] Stefan J Kiebel, Jean Daunizeau, and Karl J Friston. A hierarchy of time-scales and the brain. *PLoS computational biology*, 4(11):e1000209, 2008.

[100] Michael Breakspear and Cornelis J Stam. Dynamics of a neural system with a multiscale architecture. *Philosophical Transactions of the Royal Society of London B: Biological Sciences*, 360(1457):1051–1074, 2005.

[101] Anne-Sophie Crépin, Jon Norberg, and Karl-Göran Mäler. Coupled economic-ecological systems with slow and fast dynamicsâĂŤmodelling and analysis method. *Ecological Economics*, 70(8):1448–1458, 2011.

[102] D Das and DS Ray. Multiple time scale based reduction scheme for nonlinear chemical dynamics. *The European Physical Journal Special Topics*, 222(3-4):785–798, 2013.

[103] Miguel C Soriano, Luciano Zunino, Osvaldo A Rosso, Ingo Fischer, and Claudio R Mirasso. Time scales of a chaotic semiconductor laser with optical feedback under the lens of a permutation information analysis. *IEEE Journal of Quantum Electronics*, 47(2):252–261, 2011.

[104] GD Mitsis, R Zhang, BD Levine, and VZ Marmarelis. Modeling of nonlinear physiological systems with fast and slow dynamics. ii. application to cerebral autoregulation. *Annals of biomedical engineering*, 30(4):555–565, 2002.

[105] Leslie M Kay. A challenge to chaotic itinerancy from brain dynamics. *Chaos: An Interdisciplinary Journal of Nonlinear Science*, 13(3):1057–1066, 2003.

[106] J David Neelin. The slow sea surface temperature mode and the fast-wave limit: Analytic theory for tropical interannual oscillations and experiments in a hybrid coupled model. *Journal of the atmospheric sciences*, 48(4):584–606, 1991.

[107] Benjamin R Lintner and J David Neelin. Time scales and spatial patterns of passive ocean–atmosphere decay modes. *Journal of Climate*, 21(10):2187–2203, 2008.

[108] Zvi Artstein. Analysis and control of coupled slow and fast systems: a review. In *9th Brazilian conference on dynamics, control and their applications*, 2010.

[109] M Peña and E Kalnay. Separating fast and slow modes in coupled chaotic systems. *Nonlinear Processes in Geophysics*, 11(3):319–327, 2004.

[110] RE O'Malley Jr. Averaging methods in nonlinear dynamical systems.(ja sanders and f. verhulst), 1987.

[111] William H Press, Saul A Teukolsky, William T Vetterling, and Brian P Flannery. *Numerical recipes in C*, volume 2. Cambridge university press Cambridge, 1996.

[112] DV Ramana Reddy, Abhijit Sen, and George L Johnston. Experimental evidence of time-delay-induced death in coupled limit-cycle oscillators. *Physical Review Letters*, 85(16):3381, 2000.

[113] Ernst Niebur, Heinz G Schuster, and Daniel M Kammen. Collective frequencies and metastability in networks of limit-cycle oscillators with time delay. *Physical review letters*, 67(20):2753, 1991.

[114] L Siqueira and B Kirtman. Predictability of a low-order interactive ensemble. *Nonlinear Processes in Geophysics*, 19(2):273–282, 2012.

[115] SERGEI Soldatenko and DENIS Chichkine. Basic properties of slow-fast nonlinear dynamical system in the atmosphere-ocean aggregate modeling. *WSEAS Transactions on Systems*, 13:757–766, 2014.

[116] Kajari Gupta and G. Ambika. Suppression of dynamics and frequency synchronization in coupled slow and fast dynamical systems. *The European Physical Journal B*, 89(6):1, 2016.

[117] Ron Milo, Shai Shen-Orr, Shalev Itzkovitz, Nadav Kashtan, Dmitri Chklovskii, and Uri Alon. Network motifs: simple building blocks of complex networks. *Science*, 298(5594):824–827, 2002.

[118] Chung-Yuan Huang, Chuen-Tsai Sun, Chia-Ying Cheng, and Ji-Lung Hsieh. Bridge and brick motifs in complex networks. *Physica A: Statistical Mechanics and its Applications*, 377(1):340–350, 2007.

[119] Mostafa Salehi, Hamid R Rabiee, and Mahdi Jalili. Motif structure and cooperation in real-world complex networks. *Physica A: Statistical Mechanics and its Applications*, 389(23):5521–5529, 2010.